

# Clinical implementation of adaptive intensity-modulated proton therapy (aIMPT) for locally advanced cervical cancer (LACC)



Master's thesis  
by Anouk Corbeau



# **Clinical implementation of adaptive intensity-modulated proton therapy (aIMPT) for locally advanced cervical cancer (LACC)**

Anouk Corbeau

Student number: 4374096

4th of June 2021

Thesis in partial fulfilment of the requirements for the joint degree of Master of Science in

*Technical Medicine*

Leiden University | Delft University of Technology | Erasmus University Rotterdam

*Master thesis project (TM30004 | 35 ECTS)*

Radiotherapy department, Erasmus MC

September 2020 – June 2021

*Supervisors:*

dr. ir. J. Schiphof-Godart

drs. J.W.M. Mens

prof. dr. R.A. Nout

prof. dr. M.S. Hoogeman

*Thesis committee members:*

dr. ir. J. Schiphof-Godart

drs. J.W.M. Mens

prof. dr. R.A. Nout (chair)

prof. dr. M.S. Hoogeman

prof. dr. ir. J. Harlaar

An electronic version of this thesis is available at <http://repository.tudelft.nl/>.



# Preface

Throughout my bachelor's programme Clinical Technology and the subsequent master's programme Technical Medicine, I have become increasingly fascinated by ionizing radiation. Even though ionizing radiation seems incomprehensible as it cannot be felt or seen, it has a wide array of applications in the medical field. An internship at the Radiotherapy department in LUMC showed me that radiotherapy provides the interesting combination of state-of-the-art technologies regarding ionizing radiation and patient care. Technicians and radiation oncologists work closely together in a very dynamic research field that has advanced considerably over the last decades. I also enjoy the extensive patient contact. As a whole treatment course may take several weeks, patients spend a lot of time at the department which facilitates a solid physician-patient relationship.

The radiotherapy courses I have followed gave me a good impression of the Radiotherapy department in Erasmus MC and motivated me to conduct my master's thesis research here. I was lucky that the PROTECT-project was initiated around the time that I had to start my graduation internship. The project offered me the challenge to investigate the implementation of proton therapy for locally advanced cervical cancer. In this way, one of the first clinical studies in this field could be initiated. In my opinion, such an implementation project is an excellent fit for technical physicians. Technical physicians can work with the medical and technical aspects of medicine and thus connect all stakeholders. Besides, I am happy to contribute to any improvements in cervical cancer treatment because the majority of women suffer treatment-related morbidities. I am therefore looking forward to continuing with this contribution during a PhD research project at LUMC.

Lastly, this graduate internship enabled me to develop myself both professionally and personally. I am thankful for the support and enthusiasm from my supervisors Jeremy, Jan Willem, Mischa, and Remi and the great collaboration with Sander while working on the same project. I would also like to thank my family and friends for their support during my years as a student.

*Anouk Corbeau  
Rotterdam, May 2021*



# Summary

Each year, more than 800 women in the Netherlands are diagnosed with cervical cancer, of which approximately half have locally advanced disease. The standard treatment for locally advanced cervical cancer (LACC) is external beam radiotherapy (EBRT) with concurrent chemotherapy followed by brachytherapy. The combination of these treatment modalities has proven to be effective for locoregional tumor control but many patients experience some degree of toxicity, mainly concerning the bowel, urinary tract, or vagina. Another important morbidity is hematologic toxicity (HT) due to bone marrow suppression, which might negatively impact the efficacy of adjuvant therapies. Since the majority of patients are diagnosed in the early decades of life, treatment-related morbidity has a profound impact on their quality of life. Proton therapy allows a reduction in the integral dose to the patient and easier sparing of organs at risk (OARs), which might result in a decrease of treatment-related morbidities. One initiative to reduce treatment morbidities for LACC-patients was proposed in a collaborative project between Erasmus Medical Center (EMC), Leiden University Medical Center (LUMC), and Holland Proton Therapy Center (HollandPTC): the PROTECT-project. A clinical pilot study will be conducted to determine differences in dose to OARs and in morbidity outcomes when comparing state-of-the-art photon therapy with adaptive intensity-modulated proton therapy (aIMPT) for patients with LACC. Additionally, bone marrow sparing capabilities of both delivery techniques will be evaluated. The focus of this thesis is on the clinical implementation of aIMPT to facilitate the pilot-study and consists of three parts.

The thesis started with a systematic review of the literature about the relationship between bone marrow dose and HT in LACC-patients treated with primary chemoradiation. The review has been submitted for publication. A systematic search identified 1346 articles of which seventeen studies were included. There was a scarcity of studies investigating the relationship between bone marrow dose and HT and clinically useful prediction models were not available yet. The majority of the studies defining bone marrow as the whole pelvic bone found a significant association between bone marrow and HT, in contrast to studies evaluating lower density marrow spaces or active bone marrow. Future studies may use whole pelvic bone contouring to develop normal tissue complication probability models.

Secondly, the development and implementation of the treatment planning strategy for LACC-patients in HollandPTC were proposed. Uncertainties arising from proton therapy delivery were identified and strategies to address these uncertainties were determined. The proposed aIMPT-strategy for LACC-treatment consisted of a plan-of-the-day-approach with margins and robust planning. Further work includes establishing the balance between robustness settings and margins and optimizing the clinical implementation of the plan-of-the-day-strategy.

Lastly, the workflow for LACC-patients in Erasmus MC was translated into the HollandPTC environment. The current workflow was used to generate requirements for the new workflow with input from both the investigator and a risk evaluation with the users. A workflow was designed and translated into HollandPTC's situation. Secondly, the implementation of the plan-of-the-day-strategy in the treatment management process of the oncology information system ARIA was investigated. Recommendations were made to finalize and validate the implementation of the workflows.

This thesis provides a base for the clinical implementation of aIMPT for LACC in HollandPTC. The systematic review gives guidance on bone marrow contouring methods and clinical utilization of detected relationships, which can be used for bone marrow sparing techniques in Erasmus MC and HollandPTC. Additionally, a combination of a plan-of-the-day-approach with margins and robust planning was identified as the most optimal treatment planning strategy. Lastly, an implementation strategy for the clinical workflow and treatment management process in HollandPTC was determined. Further work should focus on finalizing and validating the clinical implementation so that PROTECT's clinical pilot study in HollandPTC can be initiated.





# Contents

<b>Preface</b>	<b>v</b>
<b>Summary</b>	<b>vii</b>
<b>1 Introduction to cervical cancer</b>	<b>1</b>
1.1 Cervical cancer, epidemiology and risk factors . . . . .	1
1.2 Pathology . . . . .	1
1.3 Vaccine program and population screening. . . . .	2
1.4 Diagnosis at the gynecologist . . . . .	2
1.4.1 CIN . . . . .	2
1.4.2 Invasive carcinoma . . . . .	3
1.5 Treatment of cervical cancer . . . . .	4
1.5.1 Early stage cervical cancer . . . . .	4
1.5.2 Locally advanced cervical cancer (LACC) . . . . .	4
<b>2 Radiation therapy</b>	<b>7</b>
2.1 External beam radiation therapy . . . . .	7
2.1.1 Treatment planning . . . . .	8
2.1.2 Treatment delivery. . . . .	10
2.1.3 Evaluation of the plan-of-the-day-strategy. . . . .	10
2.1.4 Toxicities after radiation therapy. . . . .	10
2.1.5 Proton therapy. . . . .	11
2.2 Brachytherapy . . . . .	11
<b>3 Online adaptive proton therapy for cervical cancer to reduce the impact on morbidity and the immune system (PROTECT)</b>	<b>13</b>
3.1 PROTECT-project . . . . .	13
3.2 Thesis overview. . . . .	14
<b>4 Correlations between bone marrow radiation dose and hematologic toxicity in locally advanced cervical cancer patients receiving chemoradiation with cisplatin: a systematic review</b>	<b>15</b>
4.1 Abstract. . . . .	15
4.2 Introduction . . . . .	15
4.3 Method . . . . .	16
4.3.1 Search Strategy. . . . .	16
4.3.2 Data Extraction and Quality Assessment. . . . .	16
4.4 Results . . . . .	18
4.4.1 Eligible studies. . . . .	18
4.4.2 Whole pelvic bone contour (PB) . . . . .	21
4.4.3 Lower density marrow spaces (PBM). . . . .	23
4.4.4 Active bone marrow (ABM) . . . . .	23
4.4.5 Other predictors . . . . .	25
4.5 Discussion . . . . .	25
<b>5 Implementing treatment planning for LACC in HollandPTC</b>	<b>29</b>
5.1 Introduction . . . . .	29
5.2 Methods . . . . .	29
5.3 Identified uncertainties for proton therapy and related approaches. . . . .	29
5.3.1 Range uncertainties for proton therapy . . . . .	29
5.3.2 Strategies to address uncertainties in proton therapy . . . . .	31

5.4	Proposed strategy for aIMPT of LACC . . . . .	34
5.4.1	Range calculation in the treatment planning system . . . . .	34
5.4.2	Setup uncertainties . . . . .	34
5.4.3	Organ motion . . . . .	36
5.4.4	Clinical implementation of aIMPT . . . . .	39
5.5	Discussion . . . . .	41
<b>6</b>	<b>Translating the current workflow for LACC-patients in Erasmus MC into the HollandPTC environment</b>	<b>43</b>
6.1	Introduction . . . . .	43
6.2	Map the current workflow in Erasmus MC . . . . .	43
6.2.1	Methods . . . . .	43
6.2.2	Results . . . . .	43
6.3	Generating requirements for the workflow . . . . .	45
6.3.1	Input from the investigator . . . . .	45
6.3.2	Input from a risk evaluation of the current workflow . . . . .	45
6.3.3	Results . . . . .	47
6.4	Implement the workflow in HollandPTC . . . . .	51
6.4.1	Introduction . . . . .	51
6.4.2	Methods . . . . .	52
6.4.3	Results . . . . .	52
6.5	Discussion . . . . .	60
<b>7</b>	<b>Conclusion</b>	<b>63</b>
	<b>Bibliography</b>	<b>65</b>
	<b>Appendices</b>	<b>77</b>
<b>A</b>	<b>Search term</b>	<b>79</b>
<b>B</b>	<b>Selected items from TRIPOD-statement</b>	<b>81</b>
<b>C</b>	<b>TRIPOD-score per included article</b>	<b>83</b>
<b>D</b>	<b>Pugh's checklist</b>	<b>85</b>
<b>E</b>	<b>Requirements from the Pugh's checklist</b>	<b>87</b>
<b>F</b>	<b>Identified risks</b>	<b>91</b>

# Introduction to cervical cancer

## 1.1. Cervical cancer, epidemiology and risk factors

Cervical cancer originates from the cervix, which is a cylinder-shaped lower part of the uterus and therefore part of the female reproductive system (see Figure 1.1a). Each year, more than 800 women in the Netherlands are diagnosed with cervical cancer and more than 200 women die from this type of gynecological cancer [1]. The two peaks in the incidence of cervical cancer for women are at the age of 30 and 60 years. Persistent infections with high-risk types of the Human Papillomavirus (hrHPV) are the main causative events in the development of cervical cancer. Most women and men will be infected with any type of HPV at least once in their lives, mainly due to sexual activity, but the infection is very likely to be transient [2, 3]. However, HPV16/18 are high-risk types and most commonly associated to the majority of cervical cancers and non-cervical HPV-related cancers. 70% of cancers of the vagina and anus and 30 to 40% of the cancers of the vulva, penis, and oropharynx are also caused by HPV [4]. In total, fifteen HPV-types are classified as high-risk and six types are identified as potential high-risk [5]. It is estimated that between 70 and 80% of the cervical mucosal hrHPV-infections give no clinical abnormalities and resolve spontaneously [2]. Risk factors are related to persistent hrHPV-infections, including a suppressed immune system, smoking, high parity, and multiple hrHPV-infections, mainly caused by sexual activity starting at a young age and a high total number of sexual partners [6–8]. Women with early cervical cancer often do not experience any symptoms, whereas locally advanced disease could cause symptoms including abnormal vaginal bleeding, pelvic pain, vaginal discharge, and dyspareunia [9, 10].

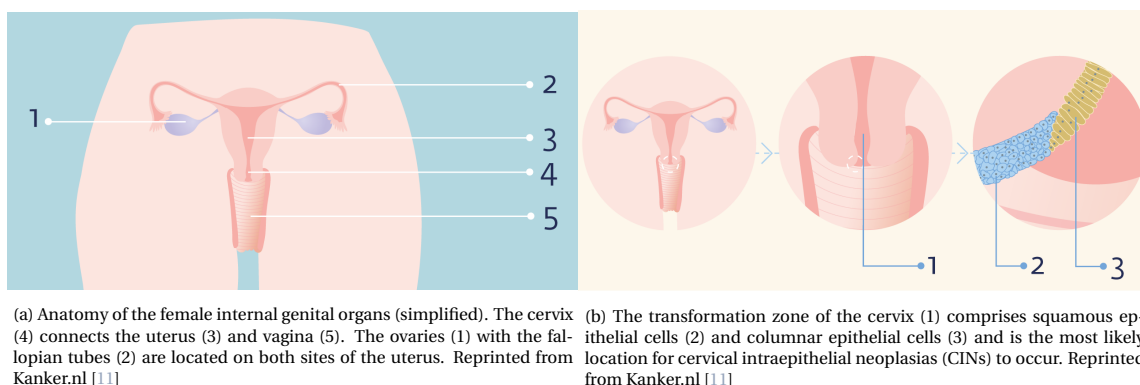


Figure 1.1: Anatomy of female internal genital organs and transformation zone of the cervix.

## 1.2. Pathology

The cervix consists of the ectocervix, which is the part of the cervix that can be seen during a gynecologic examination, and the endocervix, which is the tunnel through the cervix. The ectocervix is made up of squamous epithelial cells and the endocervix of columnar epithelial cells, as shown in Figure 1.1b. The outer and inner part of the cervix meet in the so called transformation zone. Most of the cervical cancers originate from

this transformation zone. The majority of the women with cervical cancer have a squamous cell carcinoma [9]. Adenocarcinomas, starting in the columnar epithelial cells, comprise 20-25% of the cervical cancers [12]. Other uncommon types of cervical cancers include adenosquamous cancers and small-cell (neuroendocrine) carcinomas [8]. When starting in the squamous epithelial cells, a persistent infection with hrHPV can give rise to cervical intraepithelial neoplasias (CINs). CINs are categorized in CIN1, CIN2, and CIN3, defined as respectively low, moderate, and high-grade dysplasia [13]. Only two to five percent of the women with a cervical mucosal hrHPV-infection will develop a high-grade CIN-lesion and less than one percent will develop cervical cancer [14].

### 1.3. Vaccine program and population screening

A vaccine program for preadolescent girls, targeting hrHPV16/18-types with a vaccine, was introduced in the Netherlands in 2009. From 2021, both girls and boys will be vaccinated at the age of nine [15]. The vaccine is most effective when administered before the first sexual activity and has demonstrated a high protection against HPV-infection, CIN2, and CIN3 in young women [16]. The vaccine program has to be complemented with screening since not all women choose to participate in the vaccination program and the vaccine prevents 70% of the cervical cancer cases [17]. Currently, women between 30 and 60 years of age are invited for cervical cytology with five year intervals [15]. With the use of a smear test, the presence of HPV is assessed. If a HPV-infection is demonstrated, the smear test will be analyzed for abnormal cells and examined with a cytology test. The outcomes are classified according to Papanicolaou (PAP) (see Table 1.1). For a PAP-score of 2 (low-grade lesions) and above, the patient is referred to the gynecologist for an examination of the cervix for any CINs [15]. The referral strategy is similar when a general practitioner takes a cervical smear for examination because of a patient's complaints.

Table 1.1: Definitions of Papanicolaou (PAP) smear test results and next steps [15] *hrHPV = high risk Humano Papillomavirus*

hrHPV-positive and	Definition	Next step
PAP 0	Not assessable	Repeat smear test after six weeks
PAP 1	Normal	Repeat smear test after six weeks
PAP 2-3a1	Low-grade lesions	Refer to the gynecologist
PAP >3a2	High-grade lesions or carcinoma in situ	Refer to the gynecologist

### 1.4. Diagnosis at the gynecologist

At the gynecologist, patients will have a colposcopy and biopsies may also be taken. In some cases, the gynecologist removes the lesion immediately. A pathologist examines the samples and classifies the lesion as normal, CIN, or invasive cancer. The corresponding appearance of the cervix is visualized in Figure 1.2.

#### 1.4.1. CIN

CIN1 is mostly not treated because the chance on spontaneous regression is high [19]. CIN2 can be treated when the risk of progression is considered to outweigh the chance on complications [20]. Factors including age, type of HPV-infection, location, and size of the lesion need to be considered. The observation of untreated CIN1 and CIN2 consists of follow-up cytology and colposcopy. CIN3 is a precursor to invasive cervical cancer and has to be treated. The first choice of treatment is a loop excision of the transformation zone (LETZ), involving removal of the abnormal cells using a thin wire loop that is heated with an electric current. Conization is a surgical procedure reserved for more severe CIN and is defined as the excision of a cone-shaped wedge from the cervix. It increases the risk of preterm birth. To decrease the chances on recurrence, it is important to remove the entire transformation zone and to have clear resection margins, meaning that there is no tumor at the margin. After treatment, follow-up takes place in the form of smear tests.

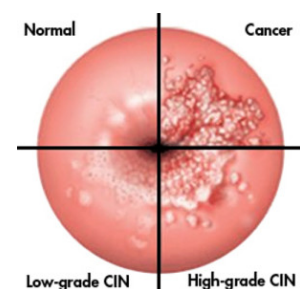


Figure 1.2: View of the cervix for different stages [18]

Table 1.2: Staging of cervical carcinoma according to the International Federation of Gynecology and Obstetrics (FIGO) and TNM-classification [10, 23]

TNM	FIGO	Description
<b>T1</b>	<b>I</b>	Strictly confined to the cervix
T1a	IA	Invasive carcinoma that can be diagnosed only by microscopy, with maximum depth of invasion <5 mm
T1b	IB	Invasive carcinoma with measured deepest invasion >5 mm, lesion limited to the cervix
T1b1	IB1	Invasive carcinoma >5 mm depth of stromal invasion, and ≤ 2 cm in greatest dimension
T1b2	IB2	Invasive carcinoma >2 cm and ≥ 4 cm in greatest dimension
T1b3	IB3	Invasive carcinoma > 4 cm in greatest dimension
<b>T2</b>	<b>II</b>	The carcinoma invades beyond the uterus, but not onto the lower third of the vagina or to the pelvic wall
T2a	IIA	Involvement limited to the upper two-thirds of the vagina without parametrial involvement
T2b	IIB	With parametrial involvement but not up to the pelvic wall
<b>T3</b>	<b>III</b>	The carcinoma involves the lower third of the vagina and/or extends to the pelvic wall and/or causes hydronephrosis or nonfunctioning kidney and/or involves pelvic and/or para-aortic lymph nodes
T3a	IIIA	The carcinoma involves the lower third of the vagina, with no extension to the pelvic wall
T3b	IIIB	Extension to the pelvic wall and/or hydronephrosis or nonfunctioning kidney (unless known to be due to another cause)
T3c	IIIC	Involvement of pelvic and/or para-aortic lymph nodes (including micrometastases), irrespective of tumor size and extent
	<b>IV</b>	The carcinoma has extended beyond the true pelvis or has involved (biopsy proven) the mucosa of the bladder or rectum
<b>T4</b>	<b>IVA</b>	Spread to adjacent pelvic organs
N1		Regional metastases
M1	<b>IVB</b>	Spread to distant organs

#### 1.4.2. Invasive carcinoma

If a tissue diagnosis of invasive carcinoma has been established, staging is performed following the International Federation of Gynecology and Obstetrics (FIGO) cervical cancer staging system. This staging system can be linked to the TNM-Classification of Malignant Tumors (TNM), which terms each individual aspect of the staging as a category [22]:

- T describes the primary tumor site
- N describes the regional lymph node involvement
- M describes the presence or otherwise of distant metastatic spread

Table 1.2 provides an overview of both staging systems. For smaller lesions (stage IA and IB1), staging can be based on the measurement of the depth of tumor invasion with a cone biopsy, physical examination to assess tumor size clinically, or both [8]. These tumors are confined to the cervix and have a maximum size of 4 cm. For more advanced tumors, physical examination can be complemented with magnetic resonance imaging (MRI) for visualization of the primary tumor. For evaluation of nodal involvement and metastases, (a combination of) MRI, computed tomography (CT), and positron-emission tomography (PET) could be used [10]. Nodal involvement at diagnosis increases with increasing stage of disease [24]. Nodal spread starts in

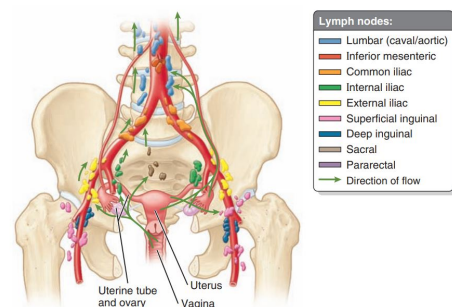


Figure 1.3: Lymphatic drainage of female pelvis. Reprinted from Moore et al. [21]

the lymphatics coursing through the parametria. The parametrium is a connective tissue, extending from the lateral uterus to the pelvic sidewalls. The fallopian tubes are situated superior of the parametria [25]. From there, lymphatic channels draining the cervix can follow three routes [26]. The anatomy of the lymphatic drainage is visualized in Figure 1.3. The lateral route is to the external iliac nodes, the hypogastric route is to the internal iliac nodes, and the posterior route is along the uterosacral ligaments to the lateral sacral and sacral promontory nodes. All pathways lead to the common iliac nodes followed by the para-aortic nodes. Nodal spread to the para-aortic region is still treated with curative intent, but beyond the para-aortic region, including mediastinal, supraclavicular, and inguinal regions, the metastases are considered distant [24]. In a high stage of cervical cancer, metastases could spread to the lungs, liver, or bones.

## 1.5. Treatment of cervical cancer

In general, the treatment of cervical cancer with curative intention consists of surgery, radiotherapy, or a combination of radiotherapy and chemotherapy [10]. Tumors confined to the cervix are commonly treated with surgery, while tumors extending beyond the cervix are primarily treated with radiotherapy, optionally complemented with chemotherapy. Patients diagnosed with metastatic disease to distant organs (stage IVB) could be offered chemoradiotherapy for palliation.

### 1.5.1. Early stage cervical cancer

For patients with stage IA who want to preserve fertility, cervical conisation is a reasonable treatment option. If the patient has completed childbearing, the first choice of treatment is removal of the uterus or hysterectomy [8, 10]. For stage IB1 and IIA1, a radical hysterectomy with pelvic and para-aortic lymphadenectomy or radiotherapy are treatments of choice [10]. Advantages of hysterectomy over radiotherapy include a shorter duration of treatment, preservation of the ovarian function in younger patients, avoidance of vaginal stenosis, and reassurance that there will be no future recurrence in the uterus or the cervix [8]. However, if patients are not eligible for surgery, because of comorbidity or age, radiotherapy is a reasonable treatment option.

### 1.5.2. Locally advanced cervical cancer (LACC)

Stage IB3 to IVA cancers, often referred to as locally advanced cervical cancer (LACC), have substantially worse survival when compared early-stage disease because of the more frequent occurrences of pelvic and para-aortic lymph-node metastasis and the larger size of the tumor [8, 28]. Therefore, it is advised to treat patients with LACC with concomitant chemotherapy and radiotherapy. With respect to this treatment, Erasmus Medical Center (Erasmus MC) participates in the International Study on MRI-Based Brachytherapy in Cervical Cancer (EMBRACE), initiated by the gynecological working group of the uniting of the Groupe Européen de Curiethérapie and the European Society for Radiotherapy and Oncology (GEC-ESTRO), and follows the corresponding study protocol [29]. According to this protocol, radiochemotherapy includes external beam radiotherapy, delivered in 25 fractions, with weekly concurrent chemotherapy, followed by three or four sessions of brachytherapy. Possible treatment schedules are visualized in Figure 1.4. Several studies demonstrated the overall treatment time (OTT) of LACC to be a significant prognostic factor in the treatment outcomes [30, 31]. Therefore, EMBRACE aims that 80% of the patients will adhere to the <50 days threshold [27, 32].

#### 1.5.2.1. Chemotherapy or hyperthermia

Chemotherapy is usually administered with single-agent cisplatin (40 mg/m<sup>2</sup>) and consists of five weekly cycles concurrent with radiation therapy [27]. The improvement in overall survival in women with LACC when

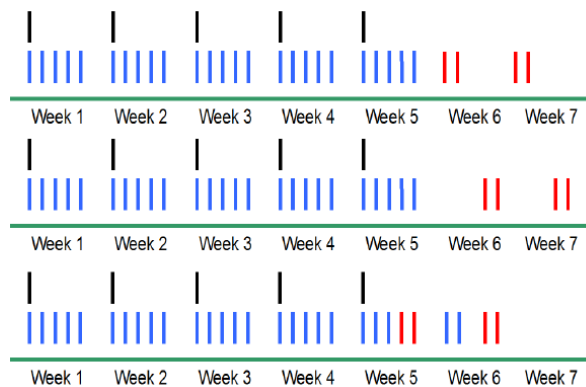


Figure 1.4: Three possible schedules for locally advanced cervical cancer treatment according to EMBRACE. External beam radiation therapy (blue bars) consist of 25 fractions with five courses of concurrent cisplatin (black bars) followed by four (or three) fractions of brachytherapy (red bars). An overall treatment time of 50 days is important for local control. Adjusted from Pötter et al. [27]

combining radiotherapy with chemotherapy might be because of the chemotherapy acting synergistically with radiotherapy or the direct cytotoxic effect of chemotherapy [33]. However, cisplatin is associated with toxicities, including the risks of long-standing neuropathy, ototoxicity, bone marrow depression, and potentially chronic renal insufficiency [12]. Therefore, chemotherapy might be contraindicated in patients with renal impairments, bone marrow depression, and hearing loss [34]. Hyperthermia treatment is an alternative treatment option [35, 36]. Deep hyperthermia is an intended artificial increase of temperature by interstitial and intracavitary delivery of heat using electromagnetic waves [35]. During five weekly sessions concurrent with radiotherapy, which is similar to the schedule of chemotherapy, hyperthermia aims at heating the tumor to a temperature of 39-43°C. As a result, perfusion, apoptosis, and reoxidation are induced and the repair of sublethal and potentially lethal damage caused by radiotherapy is inhibited [37]. In this way, the cytotoxic effect of radiotherapy is reinforced. Even though its results are promising, hyperthermia is not a widely acknowledged treatment as the technique has challenging problems [36]. Challenges consider homogeneous heating, temperature monitoring, defining the thermal dose goals, quality assurance, and standardisation. In the Netherlands, deep hyperthermia for LACC-patients is only offered in Erasmus MC and Academic Medical Center (AMC) in Amsterdam.

#### **1.5.2.2. Radiation therapy**

Radiation therapy applied for LACC can be categorized in external beam radiation therapy (EBRT) and brachytherapy. EBRT is delivered from outside the body by aiming high-energy photons to the location of the tumor [38]. It has the primary aim to obtain regional and nodal control and will be delivered concurrent with chemotherapy [27]. EBRT and chemotherapy are followed by brachytherapy. Brachytherapy is a radiotherapy modality where the source of radiation therapy is placed inside and around the cervix to give a higher dose locally. Radiation therapy will be discussed into detail in the next chapter.





# 2

## Radiation therapy

Along with surgery and chemotherapy, radiation therapy is an important modality applied in cancer treatment. The ionizing radiation used can eject electrons from molecules within the cells. The ejected electrons can disrupt the structure of macromolecules such as DNA and lead to biological damage to cells. This can be due to direct action, when the electron directly ionizes the atom, or indirect action, when the electron interacts with other atoms or molecules, particularly water, to produce free radicals, which can break chemical bonds [39]. Ionizing radiation can therefore be used to kill or genetically change cancer cells resulting in cancer cell death [38]. About two-thirds of the biologic damage by photons is caused by indirect action. The unit of radiation dose delivered to tissue is expressed in gray (Gy). 1 Gy is equal to 1 Joule/kilogram. Radiobiological characteristics of the cells determine the amount of dose required for cell death. Since tumor and normal cells are unavoidably included within a treatment plan and exposed to radiation, radiation damages both [39]. The goal of radiation therapy is to maximize radiation dose to abnormal cancer cells while minimizing exposure to normal cells [38]. This goal can be obtained through, for instance, optimization of the radiobiological response of tumors and normal tissues. Normal cells can repair themselves faster than tumor cells. To allow repairing time for normal cells and reduce the final damage to normal tissues, the total amount of prescribed dose is split into a number of treatments called fractions. For LACC-treatment, the patient is treated with multiple fractions of EBRT and brachytherapy. The application of these two techniques will be further introduced in this chapter.

### 2.1. External beam radiation therapy

For LACC-patients, EBRT will be delivered in 25 fractions with a total dose of 45 Gy to the target volume i.e. the tumor and surrounding node regions. Thus, a patient is irradiated 25 times with 1.8 Gy per fraction. Involved lymph nodes are given a simultaneous integrated boost (SIB) of 55 - 57.5 Gy. With this SIB treatment schedule, lymph nodes receive a higher dose during each of the 25 fractions of the whole treatment course.

Large and complex day-to-day anatomical variations within the pelvic area make accurate dose delivery difficult. Variations in bladder-filling can have a large impact on the shape and position of the cervix and uterus [40–42]. The uterus can move up to 15 mm and the cervix up to 6 mm in the upward direction due to bladder-filling [42]. Since the cervix and the uterus are the target volumes for radiation therapy, such large motion could lead to underdosage of the tumor. Increasing the irradiated volume might be a solution. However, even though this strategy decreases the risk of missing the target volume, the larger amount of healthy tissue within the irradiated volume increases morbidity.

Ahmad et al. established a patient-specific linear correlation between bladder volume changes and the position of the uterus [43]. Based on these bladder volume changes, a model to predict the shape of the uterus at any given position during a treatment course was generated. Clinical application of this model facilitated the introduction of the plan-of-the-day (PotD) approach into Erasmus MC in 2011 [44]. In short, the PotD-strategy uses a patient-specific model that predicts the uterus shape and position to make a plan library containing treatment plans linked to a certain bladder volume range. Each treatment fraction, a cone-beam CT (CBCT) is generated and the plan that fits the anatomy of that day is selected for treatment.

The process of EBRT-treatment consists of two steps, i.e. treatment planning and treatment delivery, and will be discussed with a focus on the PotD-strategy for LACC as implemented in Erasmus MC.

### 2.1.1. Treatment planning

A simplified overview of the treatment planning process is shown in Figure 2.1.

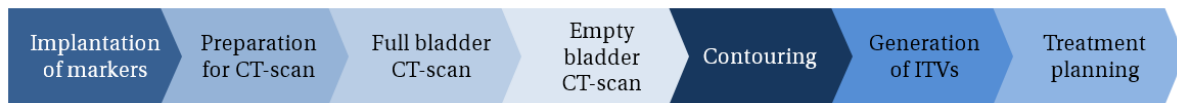


Figure 2.1: Process of treatment planning for cervical cancer with a plan-of-the-day strategy. *CT* = computed tomography, *ITV* = internal target volume

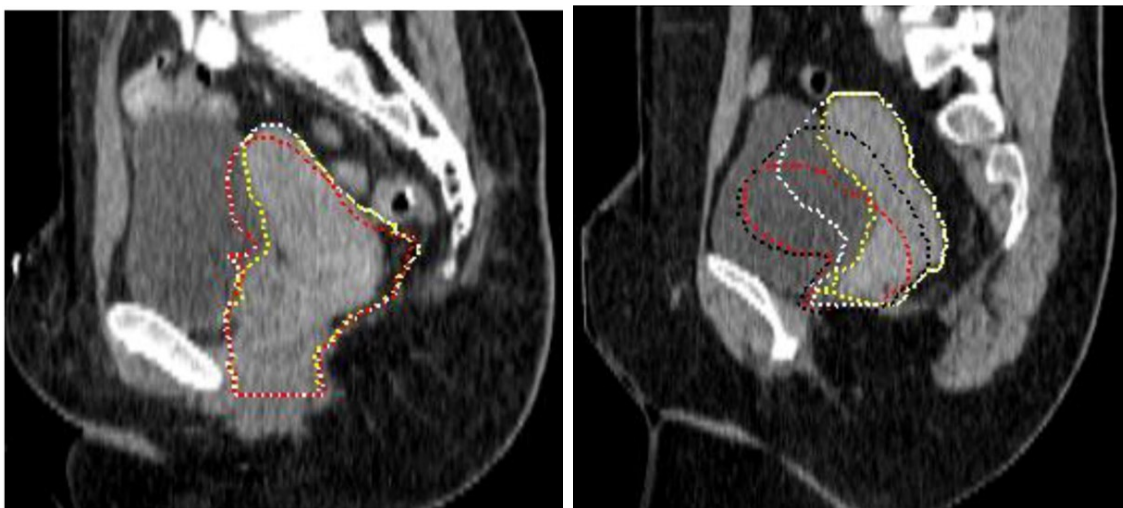
#### 2.1.1.1. Preparations for treatment planning

The radiation oncologist places three or four polymer-based markers in the unaffected vaginal fornices of the patient. These markers can be detected on a CT-scan and will be used for the localization of the cervix and therefore the tumor. The patient is instructed to drink contrast material for a better visualization of the bowel, use rectum laxation in the form of a suppository to empty the rectum, and follow drinking instructions for the bladder filling [45]. Then, two planning CT-scans are acquired. First, a full-bladder CT-scan is made with the patient in the treatment position (supine). Before the acquisition of the empty-bladder CT, the patient is asked to go to the toilet and empty her bladder. These two planning CT-scans and an earlier acquired diagnostic MR-scan are then aligned by a radiation therapist.

#### 2.1.1.2. Contouring and generating planning structures

The planning CT-scans are used for contouring of the structures and treatment planning while the diagnostic MR-scan aids in the identification of structures, especially of the tumor. The gross tumor volume (GTV-T) is delineated on both the full-bladder and empty-bladder CT-scan and a margin for suspected microscopic tumor extension is added to create the clinical target volume (CTV-T). The CTV-T can be subdivided into initial high risk (CTV-HR), containing the GTV-T and the whole cervix, and initial low risk (CTV-LR), including the CTV-HR with an additional margin of 20 mm towards the vagina, the whole uterus, and a 5 mm border towards the bladder and rectum. The deformation of the CTV-LR between a full and empty bladder is quantified with a nonrigid registration algorithm and a CTV-LR-shape model that specifies the CTV-LR for each possible bladder volume is generated [46, 47].

The shape model is used to derive a prespecified number of internal target volumes (ITV-T). These ITV-Ts compensate for internal motion. Firstly, the patient is identified as a mover or non-mover. This depends on whether the fundus of the uterus has moved more or less than 2.5 cm when comparing the full-bladder



(a) Patient with a small cervix-uterus motion (non-mover). One ITV-T (the *zITV*) (white) containing the full range of the cervix-uterus motion is created.

(b) Patient with a large cervix-uterus motion (mover). ITV-Ts containing the empty-to-half-full (ITV-empty-T) (black) and the half-full-to-full (ITV-full-T) (white) bladder range of motion are created.

Figure 2.2: Full bladder CT-scans (sagittal view) of two locally advanced cervical cancer patients. The cervix-uterus is delineated on the full bladder CT-scan (yellow) and empty bladder CT-scan (red). Figure 2.2a visualizes a non-mover and Figure 2.2b a mover. Adjusted from Heijkoop et al. [47]

and empty-bladder CT-scan (see Figure 2.2) [47]. For non-movers, one ITV-T containing the full range of the cervix-uterus motion is created. This ITV-T is first named 'zITV' and a medical physicist expands the zITV with a margin of 5 mm, except for the caudal direction, to create the ITV-T. For movers, two ITV-Ts, one containing the empty-to-half-full bladder range of motion (ITV-empty-T) and the other containing the half-full-to-full bladder range of motion (ITV-full-T), are created. Each ITV-T will be expanded using an additional set-up margin of 5 mm to generate its own planning target volume (PTV-T). Additionally, both movers and non-movers will have an ITV-BU-T. For non-movers, this contains the same structure as the ITV-T does. On the contrary, the ITV-BU-T of movers consists of a newly-generated ITV containing all cervix-uterus model shapes for empty-to-full bladders. Both ITV-BU-Ts are expanded with a 1.5 cm margin, 1 cm in the caudal direction, to create the PTV-BU-T. The PTV-BU-T is created as a motion robust target volume that can be used to ensure target coverage if the daily uterus shape is not represented by the shape model or in case of poor CBCT-image quality.

Per pathologic lymph node identified on the planning CT-scan or diagnostic MRI, the GTV-N and CTV-N are contoured on the planning CT-scan. Additionally, it depends on the (risk of) nodal pathology whether a LACC-patient is irradiated on the small pelvis, large pelvis, or large pelvis + para-aortic region [27]. For the large pelvis EBRT, the common iliac node region is additionally included in the irradiation field and for the large pelvis + para-aortic EBRT, the para-aortic region is included in the dose scheme. The included region is delineated and defined as the elective nodal CTV. The CTV-E includes both the elective nodal CTV and the pathologic lymph node(s) (CTV-N). The CTV-E with an isotropic margin of 5 mm and (one of the) PTV-T together form the PTV-45. As a result, non-movers will have a PTV-45 and PTV-45-BU and movers a PTV-45-full, PTV-45-empty, and PTV-45-BU. These structures will receive 45 Gy during the EBRT-course. Next, each individual CTV-N will have an individual PTV-N by applying a 5 mm margin. The treatment planning aim for the PTV-N is 55 - 57.5 Gy by using a SIB.

For LACC, the organs at risk (OARs) include the bladder, rectum, sigmoid, bowel, femoral heads, and, when para-aortic irradiation is applied, kidneys, and spinal cord [27]. These OARs are delineated on the full bladder planning CT-scan and the delineation method and dose constraints for these organs are defined in the EMBRACE-protocol [27].

Lastly, help structures for position verification are created around the implanted polymer markers' position. The markers' positions are marked on the empty-bladder and full-bladder CT-scan. The range of the marker motion is represented by a vector from the start to the end of the motion, which will be expanded with an 8 mm isotropic margin to create a tubular structure. These tubes will be used to verify the position of the markers during daily plan selection.

### 2.1.1.3. Treatment planning

The goal of treatment planning is to design an optimized and deliverable radiation distribution. A radiation therapist uses a treatment planning system to configure the beams to determine how the system will deliver radiation when planning goals for target and OARs have to be met. Non-movers will have two and movers will have three treatment plans. The planning aims are defined in the form of constraints and/or objectives. For instance, the aim for the PTV-45 is 45 Gy. This is translated into two dose constraints. The first constraint is that 95% of the PTV-45 volume has to receive more than 95% of the prescribed dose ( $V_{95\%} > 95\%$ ). However, the dose should not be too high, which means that the maximum dose should be below 107% of the prescribed dose ( $D_{\max} < 107\%$ ). The delineated planning CT-scan together with a list of constraints and/or objectives are the input for the treatment planning system. The treatment planning system calculates the weight of each radiation beam, which corresponds to the dose delivery, aiming for the constraints and objectives. The radiation therapist checks whether the planning goals are met. If not, constraints and/or objectives are adjusted and the treatment plan is recalculated. Treatment planning is therefore an iterative process. When the radiation oncologist has reviewed and approved the treatment plan, the radiation therapist generates per PTV-45 an isodose contour that shows where 95% of 45 Gy is delivered (the iso45-contour). This contour will be used for plan selection during treatment delivery.

### 2.1.2. Treatment delivery

A simplified overview of the treatment delivery process is shown in Figure 2.3.



Figure 2.3: Process of treatment delivery for locally advanced cervical cancer with a plan-of-the-day strategy. *CBCT = cone beam computed tomography*

Before each of the 25 treatment fractions, the patient has to follow the drinking instructions. A full bladder is favorable as it limits the bowel dose by 'pushing' the bowel outside the treatment field [48]. Then, the patient is positioned supine and a CBCT is acquired and rigidly aligned to the full bladder planning CT-scan. The registration clip box is defined around the pelvic bones. Consequently, the rotation and translation of the pelvic and vertebral bones are compared between the CBCT and planning CT-scan. The table can be moved to correct for translation, but the patient will be repositioned if the rotational deviation is too large. Then, the library plan that best fits the observed anatomy is selected based on the bladder filling (for movers), the position of the markers, and the coverage of the uterus with the iso45-contour [49]. If more than 10% of the uterus volume is outside the boundaries of the empty or full iso45-contour, the backup plan will be selected. However, since the bowel and rectum receive a higher dose with the backup plan when compared to the other plans [47], it is protocolized that the radiation oncologist should be informed when the backup plan is used more than three times during the whole treatment course. The radiation oncologist will decide whether a new treatment plan is required.

The medical linear accelerator (LINAC) is the device most commonly used for EBRT and delivers the high-energy photon beams to the patient. Advanced treatment delivery techniques for photon therapy include intensity-modulated radiation therapy (IMRT) and volumetric-modulated arc therapy (VMAT). In IMRT, the irradiation field shape and beam intensity are modulated according to the target and OARs. In this way, the intensity of the beam passing through the OARs can be modulated, and set lower, and the intensity of the beam going primarily through the target can be increased [50]. VMAT is based on IMRT but with the addition of overlapping arcs, variable gantry rotation speeds, and dose rates. It can be described as rotational IMRT delivered in a single arc [51]. VMAT reduces delivery times when compared to IMRT. Both IMRT and VMAT are considered to be the standard radiation therapy techniques used for cervical cancer [27].

### 2.1.3. Evaluation of the plan-of-the-day-strategy

Bondar et al. designed and evaluated the shape model for predicting the cervix-uterus shape and position before the implementation of the PotD-approach in Erasmus MC [44]. The shape model provided adequate coverage and better sparing of OARs than population-based margins [52]. The average PTV-volume could be reduced by 48% and bladder and rectal volumes within the PTV by respectively 5-45% and 26-74%. In the article of Heijkoop et al., the first experiences with this strategy in Erasmus MC were reported [47]. The PotD-strategy was able to manage target motion in the treatment of LACC and required limited extra treatment time. van de Schoot et al. found significant improvements in target coverage and significant reductions in bowel and rectum dose when comparing a daily plan selection strategy similar to the method used by Heijkoop et al. to non-adaptive radiotherapy treatment in LACC-patients [53]. Unfortunately, PotD-strategies are not widely implemented since the workflow is labor-intensive and sub-optimal CBCT-quality makes plan selection sometimes difficult [54]. Instead, a full-motion range ITV-T or an ITV-T from one planning CT-scan is expanded with a population-based margin to use for one treatment plan [54, 55].

### 2.1.4. Toxicities after radiation therapy

During the last decades, several improvements have been introduced to obtain a high tumor control rate and decrease dose to OARs [27]. However, 70.3% of patients with LACC undergoing treatment experience some degree of toxicity [56]. During the first weeks of treatment, patients can experience bowel cramps, dysuria, an irritated vagina, and fatigue [9, 10]. These toxicities have a profound impact on patient's quality of life and affect functioning during the treatment course [57]. For instance, even though treatment with a full bladder is favorable and patients have drinking instructions, as discussed in section 2.1.2, bladder volumes reduce significantly during the course of treatment [40]. This might be the result of treatment side effects, including acute cystitis [42]. Additionally, patients report on diarrhea, nausea, appetite loss, fecal leakage,

difficulties voiding, menopausal symptoms, and pain [57]. The majority of the symptoms reach a maximum of severity at the end of EBRT and are recovered three months after treatment. However, several symptoms remain increased during further follow-up, up to one year after treatment. Studies indicate that there is a link between early and long-term treatment-related symptoms because some symptoms persist [57, 58].

Another important morbidity for LACC-patients is hematologic toxicity (HT) due to bone marrow suppression. HT is defined as a lack of cell types present in the blood, including lymphopenia, neutropenia, and anemia. 69.5% of the cervical cancer patients treated with chemoradiation experience HT grade 2 or higher [59] and severe HT might lead to postponing or stopping chemotherapy and hospitalizations or blood transfusions, which may negatively impact the efficacy of chemotherapy treatment and other adjuvant therapies [60, 61]. Radiotherapy of the pelvic region contributes significantly to the development of HT. Bone marrow is important for hematopoiesis, the process of generation of all the cell types present in blood, and is sensitive to radiation damage [39, 62]. The pelvic bones, including the bone marrow, are included in the treatment volume of pelvic radiotherapy, which results in bone marrow suppression [63]. Continuous improvements in radiotherapy techniques have to be made to further spare OARs and reduce the occurrence and severity of toxicities.

### 2.1.5. Proton therapy

During the past few years, interest in proton therapy arose due to its superior spatial dose distribution in the patient when compared to currently used photon therapy (see Figure 2.4) [65]. Protons have the property to increase the deposition of energy as the particle reaches the end of its range. The absorbed dose suddenly rises to a peak which is known as the Bragg peak. Bragg peaks have important characteristics including a low dose proximal to the target volume, a uniform energy deposition, and a sharp distal dose fall-off, when compared to the dose deposition with photons [66, 67]. These favorable characteristics allow a reduction in integral dose to the patient and easy sparing of OARs that are located a few centimeters distal from the target [67].

The proton beam delivery method that is considered in this research is pencil beam scanning. This technique uses magnetic fields to deflect the path of each proton beam towards the planned position in the target volume [66, 68]. The beam "paints" the treatment volume in successive layers. The energy of the beam, and therefore the range of the protons, can be varied. By painting the dose non-uniformly on a field-by-field basis, the overall uniform target dose can be yield. Pencil beam scanning is ideally suited for intensity-modulated proton therapy (IMPT), which is one of several pencil-beam delivery optimization strategies [69, 70]. With IMPT, each field is allowed to have an inhomogeneous proton fluence distribution so that when all the fields are combined, a homogeneous dose is delivered to the target volume [70, 71]. This is illustrated in Figure 2.5. IMPT, when compared to standard proton therapy, offers the advantage for further dose conformality and further sparing of OARs that are in the beam path and is considered a superior technique for reducing toxicities [67].

## 2.2. Brachytherapy

EBRT with concurrent chemotherapy is followed by brachytherapy (BT). EBRT with concurrent chemotherapy to a reduction in central tumor bulk and permits more effective dosimetry in BT-application [8]. BT may be initiated already during the radiochemotherapy to shorten the overall treatment time and maintain it below the threshold of 50 days [27]. The standard BT consists of high-dose-rate therapy (2 Gy/min) given with three to four fractions with weekly intervals to reach the final dose of 21 Gy to the CTV-HR [27, 72]. Before each fraction, the radiation oncologist creates a treatment plan, which tailors the dose delivery as much as possible

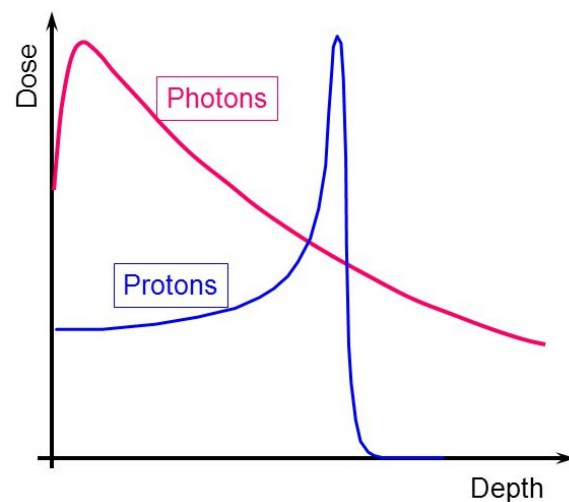


Figure 2.4: Absorbed dose as a function of depth from a Bragg peak (blue) compared to photons (red) [64]



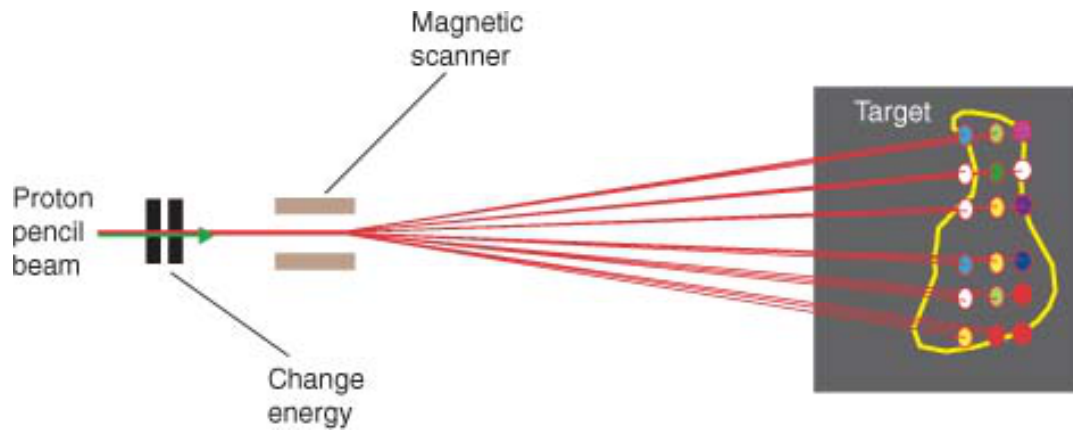


Figure 2.5: Intensity modulated proton therapy (IMPT) where the dose is delivered in successive layers. Adjusted from Khan et al. [71]

to the vaginal anatomy and the tumor. The BT-applicator used consists of an intracavitary tandem and either ovoids or a ring [73]. Needles, aiding in the dose delivery, can be inserted through holes in the ovoids or the ring. After implanting the BT-applicator, needles, and any vaginal packing in the operating room, the patient is transferred to the MRI-scanner for imaging. The target volume and OARs are delineated on the MR-scan or these contours are transferred and adjusted from an earlier planning scan. Maximum limits and planning aims are set for the bladder, rectum, recto-vaginal point, sigmoid, and bowel for treatment planning. Dose optimization concerns the implant geometry, the dwell time distribution, and the fractionation. When the treatment plan is finished and approved, the patient is brought into the treatment room for treatment. Transfer tubes from a shielded afterloader are connected to the applicator and/or needles. The radioactive sources move from the shielded afterloaders through the cables into the applicators and/or needles to deliver the treatment. The treatment time is between five and fifteen minutes. Then, the radioactive source returns into the afterloader and the BT-applicator, needles, and vaginal packing are removed. Since the focus of this research is on EBRT, BT will not be discussed further.

# 3

## Online adaptive proton therapy for cervical cancer to reduce the impact on morbidity and the immune system (PROTECT)

### 3.1. PROTECT-project

There is an increasing interest in treating LACC-patients with proton therapy. Since these patients are diagnosed at a relatively young age, toxicities have a profound impact on their lives. Proton therapy has demonstrated to reduce dose to OARs in treatment planning studies for LACC [53, 74, 75]. The biggest dose reductions are observed in low-dose regions such as the bowel and bone marrow. However, prospective studies on the beneficial effect of proton therapy for LACC are lacking. Erasmus MC, Leiden University Medical Center (LUMC), and Holland proton therapy center (HollandPTC) initiated a collaboration in this field. Erasmus MC and LUMC are two of the eight academic hospitals in the Netherlands. HollandPTC is an independent center for proton therapy and focuses on treatment, research, and education. Some of its staff is also working in Erasmus MC and LUMC. The three centers together proposed the PROTECT-project. The first aim of the PROTECT-project is to determine reductions in dose to OARs and morbidity outcomes with IMPT compared to photon therapy with IMRT/VMAT. In this way, proton therapy indication algorithms can be developed. A second goal is to evaluate the bone marrow sparing capability of proton therapy when compared to IMRT/VMAT. The hypothesis is that proton therapy is clinically feasible for LACC and will provide better OAR-sparing and lower bone marrow suppression, resulting in a clinically relevant reduction of morbidities, when compared to IMRT/VMAT. The PROTECT-project consists of two work packages (WP) (Figure 3.1). LUMC is responsible for WP1 and will address the development of an indication algorithm for proton therapy and the assessment of the impact of proton therapy on morbidity and the immune system. Erasmus MC is responsible for WP2 and will focus on the clinical implementation of adaptive intensity-modulated proton therapy (aIMPT) to prepare a clinical pilot-study. The clinical pilot-study will be a multicentre, prospective, non-randomised trial. Eligible LACC-patients from LUMC or Erasmus MC will be treated with either IMRT/VMAT or aIMPT and dosimetric and clinical outcomes will be compared.

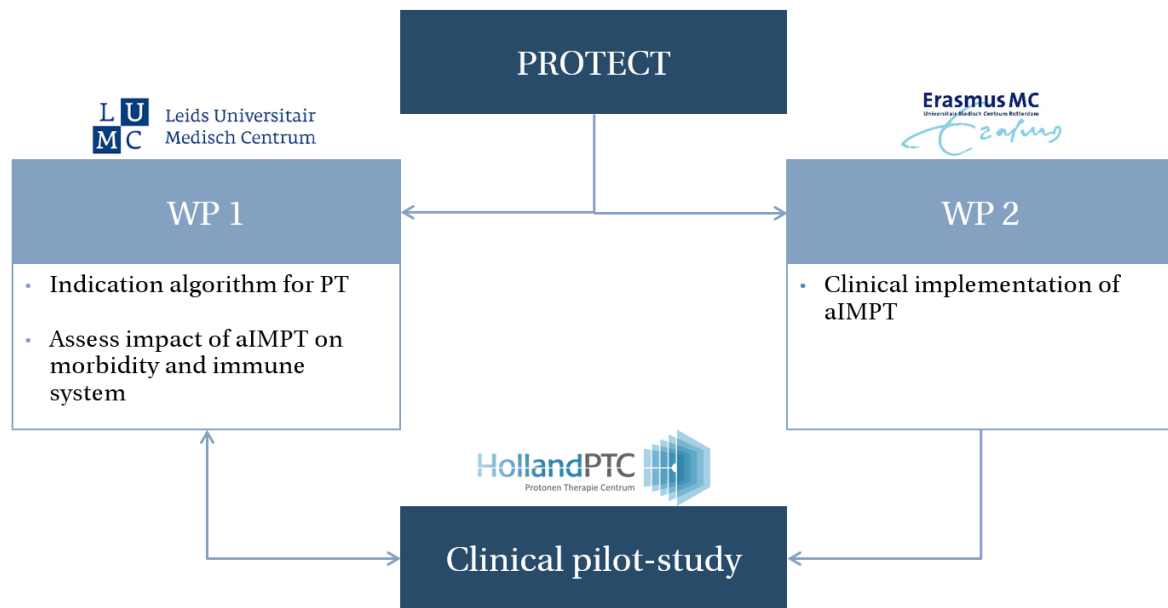


Figure 3.1: The PROTECT-project consists of two work packages (WP) in Erasmus MC and LUMC and a clinical pilot-study in HollandPTC. *PT* = proton therapy, *aIMPT* = adaptive intensity modulated proton therapy

### 3.2. Thesis overview

This master's thesis will focus on WP 2 in Erasmus MC. More knowledge on the relationship between dose and bone marrow suppression is required as one of PROTECT's aims is to study bone marrow sparing. Since LACC currently is not treated in HollandPTC, treatment planning for aIMPT needs to be investigated, optimized, and implemented. Lastly, the workflow and PotD-strategy in Erasmus MC have to be translated into and implemented in the HollandPTC environment to facilitate aIMPT. This thesis will therefore have three goals:

- Analyzing the correlation between dose received by the bone marrow and occurrence of hematologic toxicity (HT) for patients with LACC
- Implementing treatment planning for LACC in HollandPTC
- Translating the current workflow for LACC-patients in Erasmus MC into the HollandPTC environment

This thesis started with the conduction of a systematic review. This review provides an overview of medical literature evaluating the relationship between bone marrow dose and HT in LACC-patients treated with primary chemoradiation. Bone marrow contouring methods and the clinical utilization of detected relationships were also discussed. The systematic review has been submitted for publication and is presented in Chapter 4. Chapter 5 provides an overview of the implementation of treatment planning for LACC in HollandPTC. Uncertainties arising from proton therapy were taken into account for developing the proton therapy strategy for LACC-patients. Next, the current workflow for patients in Erasmus MC was examined. Requirements for the workflow were generated in HollandPTC with input from the investigator and a risk evaluation to design and investigate clinical implementation of the workflow. This process will be discussed in Chapter 6. Lastly, Chapter 7 concludes the three goals of this thesis.



# 4

## Correlations between bone marrow radiation dose and hematologic toxicity in locally advanced cervical cancer patients receiving chemoradiation with cisplatin: a systematic review

### 4.1. Abstract

**BACKGROUND** Patients with locally advanced cervical cancer (LACC) often experience hematologic toxicity (HT) up to several months after treatment, as chemoradiation can induce bone marrow (BM) suppression. However, developing BM-sparing (BMS) radiotherapeutic techniques is challenging because knowledge on the location of BM and the degree of required sparing is limited. Studies on the relationship between BM dosimetric parameters and clinically significant HT might provide relevant indices for BMS. The aim of this systematic review is to provide an overview of the literature on the relationship between the bone marrow dose and HT in LACC-patients treated with primary chemoradiation. **METHODS** A systematic search was conducted in Embase, Medline, and Web of Science. Studies were eligible when the treatment for LACC-patients was chemoradiation with cisplatin and when HT or complete blood cell count (CBC) was reported as an outcome. To determine the applicability of prediction models, the included articles were scored according to a selection of the TRIPOD-criteria and analyzed qualitatively. **RESULTS** The search identified 1346 papers of which seventeen studies were included. Most of the included studies had a retrospective design and a low applicability with a mean TRIPOD-score of 12.1 (SD 3.3) out of 29. Three out of fourteen, six out of fourteen, and four out of eleven studies defining BM as the whole pelvic bone contour (PB) detected significant associations with respectively V10, V20, and V40. Recommended cut-off values were V10>95-75%, V20>80-65%, and V40>37-28%. The studies using lower density marrow spaces (PBM) or active bone marrow (ABM) as a proxy for BM only found limited associations with HT. **CONCLUSION** There is a scarcity of studies investigating the relation between bone marrow dose and HT in LACC-patients treated with primary cisplatin-based chemoradiation. Clinically useful prediction models are currently not available. The majority of the studies defining bone marrow as the whole pelvic bone found a significant association between bone marrow and HT, in contrast to studies evaluating lower density marrow spaces or active bone marrow. Future studies may use whole pelvic bone contouring to develop normal tissue complication probability models.

### 4.2. Introduction

Bone marrow (BM) is made up of the active red marrow, comprising mostly hematopoietic tissue, and inactive yellow bone marrow, containing mostly fatty tissue [76]. Most of the red marrow can be found within the axial skeleton and upper half of the limbs [77]. Within the BM, hematopoietic stem cells are important for hematopoiesis, which is the process of generation of all the cell types present in the blood [62]. While

circulating blood cells have no self-renewal ability, stem cells can undergo a self-renewing proliferation [78]. However, if the stem cells are injured, the hematopoietic system suffers long-term or permanent damage and BM-failure may occur, resulting in immunosuppression. Chemoradiation for cancer patients can damage stem cells and therefore induce hematologic toxicities (HT), including lymphopenia, neutropenia, and anemia [60, 63, 79–81]. McGuire et al. reported a dose threshold for BM-suppression of 4 Gy, with no benefit from fractionation, for pelvic cancer patients undergoing chemoradiation [82]. During external beam radiotherapy (EBRT) both BM and circulating blood cells are exposed to possibly toxic radiation doses leading to an increased risk of lymphopenia [83]. An increase in BM-toxicity was demonstrated when adding chemotherapy to the treatment in comparison to radiotherapy (RT) alone [79, 84]. The extrapelvic compensatory response was decreased with intensive chemotherapy regimens which may lead to increased HT. The BM-tolerance to chemotherapy differs between chemotherapy regimens [85–87]. Patients receiving pelvic radiotherapy with concurrent chemotherapy have a higher BM-tolerance when comparing cisplatin-based to mitomycin-C (MMC) based chemotherapy but a lower BM-tolerance when comparing cisplatin to 5-fluorouracil (5FU) [87].

The standard chemoradiation treatment for LACC-patients combines EBRT with concurrent platinum-based chemotherapy followed by brachytherapy [88]. Huang et al. showed HT grade 2 or higher in 69.5% of cervical cancer patients undergoing chemoradiation [59]. High-grade HT might lead to postponing or stopping chemotherapy and hospitalizations or blood transfusions for cancer patients [60, 61]. It was demonstrated that LACC-patients can have HT during chemoradiation until at least 3 months post-treatment [89]. The slow recovery of the immune suppression underlines the importance to decrease the incidence of HT in this patient group [81, 89].

Currently, development of effective pelvic bone marrow sparing (BMS) RT-techniques is limited. The introduction of proton therapy raises interest in the correlation between RT-dose and HT. The beneficial physical characteristics of proton therapy and its ability to achieve satisfactory target dose distributions using only a few beams enables BMS [90, 91]. Gort et al. and Dinges et al. showed significantly better BMS for proton therapy when compared to photon therapy [90, 92]. However, knowledge on the spatial location of bone marrow sparing and the required degree of sparing is essential for the development of BMS-radiotherapy techniques [93]. Assessing the relationship between BM dose-volume histogram (DVH) parameters and clinically relevant HT can provide indices for BMS, such as the  $V_{\text{dose}}$  (e.g.  $V_{20}$  and  $V_{30}$ ), defined as the percentage of organ volume receiving a dose greater than a threshold (20 and 30 Gy, respectively). The occurrence of HT might depend on multiple factors in addition to dosimetric parameters, such as chemotherapy regimen [87].

The aim of this systematic review is to provide an overview of the medical literature evaluating the relationship between the dose to (subsites of) pelvic bone marrow and HT in LACC-patients treated with primary cisplatin-based chemoradiation. Interpretation and discussion of the literature can give guidance on bone marrow contouring methods and the clinical utilization of detected relationships.

## 4.3. Method

### 4.3.1. Search Strategy

We conducted a systematic search based on Embase, Medline, and Web of Science for the period from the earliest data to February 24th, 2021. The search term consisted of three parts focusing on pelvic cancer, radiotherapy, and BM. The search term can be found in Appendix A. Firstly, the studies were screened on eligibility by title and abstract. Then, a full-text evaluation was independently performed by two reviewers. Disagreements on the inclusion of articles were discussed. The following inclusion criteria were used: 1) patients had cervical cancer, 2) received chemoradiation as primary or postoperative treatment, 3) the first choice of chemotherapeutic agent was cisplatin, another platinum-based chemotherapy was allowed in case of contraindications for cisplatin, 4) the correlation between hematologic toxicity or complete blood count (CBC) and dose-volume parameters of the BM was analyzed, 5) the study was published in English.

### 4.3.2. Data Extraction and Quality Assessment

Clinical and methodological data were extracted using prespecified data collection forms covering the reference, study design, number of patients, number of patients treated postoperatively, the chemotherapeutic agent used, radiation technique, delineation method for BM, whether BMS was applied, method for HT-scoring (following the toxicity criteria of the CTCAE (Common Terminology Criteria for Adverse Events) or the RTOG (Radiation Therapy Oncology Group)), time of follow-up and measuring HT, definition of endpoints (grade of HT or blood counts nadirs), and the (dosimetric) predictors evaluated for the risk of the

endpoints. The included papers were evaluated using a checklist depicting whether key items from the transparent reporting of a multivariable prediction model for individual prognosis or diagnosis (TRIPOD) consensus statement on model development and validation were addressed [94]. The selected key items were based on the selection as performed by [Brodin et al.](#) and highlight the variation in statistical methodology in the various models [95]. The number of items to be checked are listed in Appendix B and summed to a total score of 29. Additionally, the studies were classified according to the type of prediction model depending on whether the investigators developed or validated a model, using the classification from [Collins et al.](#) [94]:

- Type Ia defines the development of a model where the predictive performance is directly evaluated using the same data.
- Type Ib defines the development of a model where performance is evaluated on the development dataset using resampling techniques.
- Type IIa defines a model where a dataset is randomly split into two groups, one used to develop a model and the other to evaluate its predictive performance.
- Type IIb applies a more robust technique by non-random splitting of data (by location, time, etc.).
- Type III defines a model developed and evaluated on separate datasets by the model developers.
- Type IV defines an external validation of an existing prediction model.

## 4.4. Results

### 4.4.1. Eligible studies

Seventeen studies were included in this systematic review. A study flowchart diagram is visualized in Figure 4.1. Table 4.1 provides an overview of the characteristics and outcomes of the included studies. The included articles had a mean TRIPOD-adherence score of 12.1 (SD 3.3) out of 29. A detailed overview of the TRIPOD-scoring per item and study is provided in Appendix C. The paper by Rose et al. had the highest TRIPOD-adherence score (22 out of 29) and was the only IV prediction model included [96]. The majority of the included articles used all data from a single data set to develop a prediction model without validation and were therefore type IA prediction models. In total, three delineation methods for BM were identified. Seven articles only delineated the whole pelvic bone (PB), four articles used the lower density marrow spaces (PBM) as a proxy for BM and compared this with PB, and six articles contoured both the active bone marrow (ABM) and the PB for comparison. The ABM was visualized using fluorodeoxyglucose positron emission tomography (FDG-PET) or technetium-99m (99mTc) sulfur colloid single-photon emission tomography (SPET). Six articles not only recorded dosimetric parameters for the whole pelvic bone but also divided the pelvic bone into subregions and analyzed dosimetric parameters per subsite [59, 63, 97–100]. In this systematic review, the correlation between BM and HT will be described per delineation method.

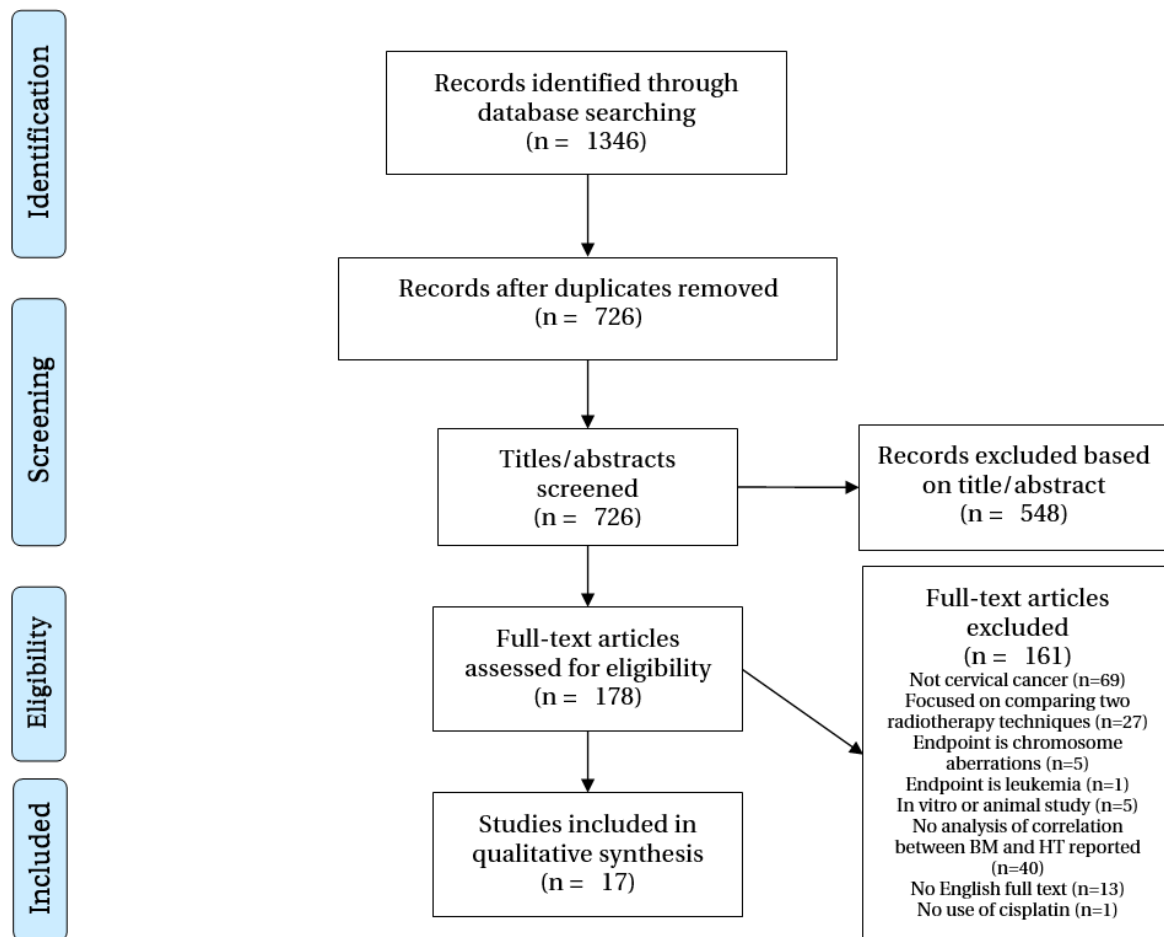


Figure 4.1: The PRISMA-flowchart [101]

Table 4.1: Characteristics of the included articles. RT = radiation therapy, CRT = chemoradiotherapy, BM = bone marrow, HT = hematologic toxicity, NTCP = normal tissue complication probability, RCT = randomized controlled trial, 3DCRT = 3D conformal radiation therapy, IMRT = intensity modulated radiation therapy, VMAT = volumetric modulated arc therapy, RTOG = Radiation Therapy Oncology Group, CTCAE = Common Terminology Criteria for Adverse Events, PB = whole pelvic bone, LSS = lumbosacral spine, LOW = lower pelvic bones, LP = lower pelvic bones, PBM = pelvic bone marrow (lower density marrow spaces), LSSM = lumbosacral spine marrow (lower density marrow spaces), ABM = active bone marrow, IBM = inactive bone marrow (PB - ABM), CT = computed tomography, FDG-PET = fluorodeoxyglucose positron emission tomography, TC-99m SPECT = technetium-99m single photon emission computed tomography, SUV = standardized uptake value.  
<sup>a</sup> = WBC, <sup>b</sup> = ANC, <sup>c</sup> = HB, <sup>d</sup> = PLT (platelets), <sup>e</sup> = HT2+, <sup>f</sup> = HT3+, <sup>g</sup> = HT1+

TRIPOD-score	Author	Study design	No of patients	No of patients treated postoperatively	Chemotherapeutic regimen	RT-technique	BM definition	BM optimization	HT-scoring scale	Timing of measuring endpoints	Endpoint	Dosimetric predictors
22	Rose, B.S. et al	Validate NTCP on retrospective data	81	0 (0%)	Cisplatin 40 mg/m2	IMRT	CT based PB contour [Mell]	No	RTOG	Weekly during CRT	WBC <sup>a</sup> ANC <sup>b</sup> HB <sup>c</sup> HT3+ <sup>f</sup>	PB-V10 <sup>a,b,f</sup> , V20 <sup>a,b,c,f</sup> , V30 <sup>a,b</sup> , Dmean <sup>a,b</sup> PB-V10>95% <sup>f</sup> PB-V20>76% <sup>f</sup>
17	Huang J. et al	Prospective RCT	164	0 (0%)	Cisplatin 40 mg/m2	IMRT	CT based PB contour and low-density marrow spaces (PBM)	Yes, using PB and LSS	RTOG	Weekly to end of CRT	HT2+ <sup>e</sup>	PB-V40 <sup>e</sup> PB-V40>28% <sup>e</sup> LSS-V10 >87% <sup>e</sup> LSS-D <sub>mean</sub> >39Gy <sup>e</sup> PBM-V40 <sup>e</sup> LSSM-mean <sup>e</sup> , V10 <sup>e</sup> , V20 <sup>e</sup> , V40 <sup>e</sup> PB-V20 <sup>a,b,f</sup> , V40 <sup>e,f</sup>
15	Chang, Y. et al	Retrospective case series, officially cohort	100	0 (0%)	Cisplatin 25 mg/m2	3DCRT, IMRT, RapidARC	CT based PB contour [Mell]	No	Unknown	Weekly during treatment	WBC <sup>a</sup> ANC <sup>b</sup> HB <sup>c</sup> PLT <sup>d</sup> HT2+ <sup>e</sup> HT3+ <sup>f</sup>	
13	Klopp, A.H.	Retrospective case series	43	43 (100%)	Cisplatin 40 mg/m2	IMRT	CT based PB contour	No	CTCAEv3	<90 days from start RT	HT2+ <sup>e</sup>	PB-V40>37% <sup>e</sup> PB-D <sub>median</sub> >34.1 Gy <sup>e</sup>
12	Kumar, T. et al	Retrospective case series	114	0 (0%)	Cisplatin 40 mg/m2	3DCRT, IMRT	CT based PB contour [Mell] and low-density marrow spaces (PBM)	No	CTCAEv4	Weekly during CRT prior to brachytherapy implantation	HT4+ <sup>g</sup>	LP-PB-V5>95% <sup>g</sup> LP-PB-V20>45% <sup>g</sup> Iliac crests-PB-Dmean>31 Gy <sup>g</sup> PB-V20>65% <sup>g</sup>
12	Rose, B.S. et al.	Retrospective case series	26	5 (19%)	Cisplatin 40 mg/m2	IMRT	CT based PB contour FDG-PET (> SUVmean PB) based ABM inactive BM (IBM) = PB - ABM	No	RTOG	CBC: weekly during CRT	WBC <sup>a</sup> ANC <sup>b</sup> HB <sup>c</sup> PLT <sup>d</sup> HT3+ <sup>f</sup>	ABM-D <sub>mean</sub> <sup>a,b,c,d</sup> , V10 <sup>a</sup> , V20 <sup>a</sup> , V30 <sup>a</sup> PB-V10 <sup>a</sup> ABM-D <sub>mean</sub> <26.8Gy <sup>f</sup> No correlation with IBM
12	Wang, S.B. et al	Prospective clinical trial	39	0 (0%)	Cisplatin 30-40 mg/m2	(39, 100%)	CT based PB contour Tc-99m SPECT (> SUVmean TB) based ABM	No	CTCAEv3	Weekly to two weeks after CRT	HT3+ <sup>f</sup>	ABM-volume > 387.5 cm <sup>3</sup> ABM-V30 > 46.5% <sup>f</sup> ABM-V40 > 23.5% <sup>f</sup>
12	Zhu, H. et al	Retrospective multicenter cohort	102	Unknown	Cisplatin 40 mg/m2	IMRT, 3DCRT	CT based PB contour [Mell]	According to the discretion of the treating oncologist	/	Weekly during CRT	WBC <sup>a</sup> ANC <sup>b</sup> HB <sup>c</sup> PLT <sup>d</sup>	PB-D <sub>mean</sub> <sup>a,b</sup> , V20 <sup>a,b</sup> , V30 <sup>a,b</sup> , V40 <sup>a,b</sup> LSS-V10 <sup>a,b</sup> , V40 <sup>a,b</sup> LOW-V20 <sup>a,b</sup> , V30 <sup>a,b</sup>
11	Lewis, S. et al	Retrospective case series	75	75 (100%)	Cisplatin 40 mg/m2	IMRT, 3DCRT	CT based PB contour [Mell] and low-density marrow spaces (PBM)	No	CTCAEv3	Weekly during CRT	HT2+ <sup>e</sup>	Ilium PB-V20 >90% <sup>e</sup>

TRIPOD-score	Author	Study design	No of patients	No of patients treated postoperatively	Chemotherapeutic regimen	RT-technique	BM definition	BM optimization	HT-scoring scale	Timing of measuring endpoints	Endpoint	Dosimetric predictors
11	Albuquerque, M.D. et al	Retrospective case series	40	0 (0%)	Cisplatin 40 mg/m2 (40, 100%)	3DCRT	CT based PB contour [Mell]	No	CTCAEv3	During RT	HT2+ <sup>e</sup>	PB-V20 >80% <sup>e</sup>
11	Khullar K. et al	Retrospective case series	21	0 (0%)	Cisplatin (21, 100%)	3DCRT, IMRT	FDG-PET (> SUVmean TB) based ABM	No	CTCAEv4	Weekly to 6 weeks after end of CRT	HT3+ <sup>f</sup>	ABM-volume <1201 ml <sup>f</sup> ABM-V40 <sup>f</sup>
10	Elicin, O. et al.	Retrospective case series	17	0 (0%)	Cisplatin 40 mg/m2 (17, 100%)	IMRT	CT based PB contour FDG-PET (> SUVmean PB) based ABM	No	RTOG	FDG-PET: Pre- and 3 months post-treatment CBC: 1 week before, weekly during, 3 months after, and at last follow-up after treatment	WBC <sup>a</sup> ANC <sup>b</sup> HB <sup>c</sup> PLT <sup>d</sup>	3m post-treatment: ABM-SUV <sup>a</sup> , PB-D <sub>mean</sub> <sup>a</sup> , V10 <sup>a</sup> , V20 <sup>a</sup> , V30 <sup>a</sup> , V40 <sup>a</sup> , ABM-V40 <sup>a</sup> Late follow-up: PB-D <sub>mean</sub> <sup>a</sup> , V10 <sup>a</sup> , V20 <sup>a</sup> , V30 <sup>a</sup> , V40 <sup>a</sup> , ABM-V20 <sup>a</sup> , V30 <sup>a</sup> , V40 <sup>a</sup>
10	Mell, L.K. et al	Retrospective case series	37	3 (8.1%)	Cisplatin 40 mg/m2 (37, 100%)	IMRT	CT based PB contour	No	RTOG	Weekly during CRT	WBC <sup>a</sup> ANC <sup>b</sup> HB <sup>c</sup> PLT <sup>d</sup> HT2+ <sup>e</sup> HT1+ <sup>g</sup>	PB-V10 <sup>a,g</sup> , V20 <sup>a,g</sup> LSS-V10 <sup>a,b</sup> , V20 <sup>a,g</sup> LP-V10 <sup>a,g</sup> , V20 <sup>a,g</sup> PB-V10 > 90% <sup>a,g</sup> , V20 > 75% <sup>a,g</sup> LSS-V10 > 90% <sup>b</sup> LP-V10 > 90% <sup>c</sup>
10	Yan, K. et al	Retrospective case series	38	0	Cisplatin 40 mg/m2 (38, 100%)	3DCRT, IMRT	CT based PB contour FDG-PET (> SUVmean PB) based ABM	No	CTCAEv4	Weekly to end treatment	HT3+ <sup>f</sup>	PB-V20 > 78.6% <sup>f</sup> , V30 > 47.1% <sup>f</sup> , V45 > 20.4% <sup>f</sup> , D <sub>mean</sub> > 30.3 Gy <sup>f</sup> ABM-V10 > 95.5% <sup>f</sup> , V20 > 80.5% <sup>f</sup> , V30 > 59.6% <sup>f</sup> , V45 > 31.7% <sup>f</sup> , D <sub>mean</sub> > 32.4 Gy <sup>f</sup>
9	Mahantshetty, U. et al	Retrospective case series	47	0	Cisplatin 40 mg/m2 (47, 100%)	IMRT	CT based PB contour and low-density marrow spaces (PBM)	No	RTOG	Weekly during CRT	WBC <sup>a</sup> ANC <sup>b</sup> HB <sup>c</sup> PLT <sup>d</sup> HT2+ <sup>e</sup>	Baseline HB and PLT <sup>c,d</sup> PBM-V40 > 40% <sup>e</sup>
9	Gupta, M. et al	Retrospective case series	43 (16 excluded for this review (neo-adjuvant chemotherapv))	4 out of 43 (8%)	Cisplatin 40 mg/m2 (37, 97%)	IMRT	CT based PB contour	No	CTCAEv4	Weekly during CRT and 6 weeks after treatment	WBC <sup>a</sup> ANC <sup>b</sup> HB <sup>c</sup> PLT <sup>d</sup> HT2+ <sup>e</sup> HT3+ <sup>f</sup>	PB-V10 > 75% <sup>e</sup>
9	Zhou, Y.M. et al	Retrospective case series	31	0	Cisplatin 40 mg/m2 (31, 100%)	IMRT, 3DCRT	CT based PB contour FDG-PET (> SUVmean TB) based ABM	No	CTCAEv4	Weekly and one week after treatment	WBC <sup>a</sup> ANC <sup>b</sup> HB <sup>c</sup> PLT <sup>d</sup> HT3+ <sup>f</sup>	Volume spared of PB: 10 Gy < 230 cc <sup>f</sup> of ABM: V10 < 179 cc <sup>f</sup> OR V20 < 186 cc <sup>f</sup> OR V40 < 738 cc <sup>f</sup>

#### 4.4.2. Whole pelvic bone contour (PB)

##### 4.4.2.1. Delineation method specified

In total, sixteen out of the seventeen included articles reported correlations between BM, approximated by the CT-based whole bone contour (PB), and the development of HT. The majority of these articles, including the studies by Rose et al., Zhu et al., Lewis et al., Kumar et al., Chang et al. and Albuquerque et al., based their contouring method on the strategy as proposed by Mell et al. [63]. Mell et al. delineated the external contour of all bones within the pelvis, extending from L5 to the inferior border of the ischial tuberosities, as a proxy for the BM in order to ensure reproducibility. Other methods applied specified CT-window settings or anatomical landmarks of the vertebrae, ischium, and/or femora.

##### 4.4.2.2. Whole pelvic bone

Table 4.2 describes that three out of fourteen articles found a significant correlation between V10 of the whole bone and grade 2 or higher HT [63, 96, 104]. Six out of fourteen articles demonstrated a significant relationship between V20 and HT [63, 96, 99, 102, 103, 105]. Furthermore, four out of eleven articles showed that V40 is a significant predictor for HT2+ or HT3+ [59, 84, 100, 102]. An overview of the cut-off values for dosimetric parameters as recommended by the included studies is provided in Figure 4.2. The recommended cut-off values for HT2+ and HT3+ for the whole pelvic bone were similar. V10 <75-95% [63, 96, 104], V20 <65-80% [96, 99, 103, 105], and V40 <28-37% [59, 84] were recommended to reduce HT. Some other significant relationships were reported, including the V30 and V45 of the whole pelvic bone. Additionally, one article investigated the volume of the whole pelvic bone spared 10, 20, and 40 Gy and found the volume of whole pelvic bone spared 10 Gy <230cc to be associated with HT2+ (not visualized in Figure 4.2) [106]. Lastly, the mean or median dose to the whole pelvic bone was found to be associated with HT by two out of eight articles [84, 105]. These studies recommended to keep the  $D_{\text{mean}}$  and  $D_{\text{median}}$  below respectively 30.3 Gy and 34.1 Gy (not visualized in Figure 4.2) [84, 105].

Table 4.2: Number and percentage of the included studies demonstrating a significant relationship between various dosimetric parameters of the whole pelvic bone contour (PB) and hematologic toxicity (HT). *CT = computed tomography*

Contouring method	Dosimetric parameter	Number of studies including dosimetric parameter	Number of studies finding significant results / number of studies including dosimetric parameter	HT2+	HT3+	HT4+
CT based PB contour – whole bone	V5	2	0/2 (0%)	0/1	0/1	0/1
	V10	14	3/14 (21%)	2/8	1/7	0/1
	V15	1	0/1 (0%)	-	-	0/1
	V20	14	6/14 (43%)	3/8	2/7	1/1
	V30	10	1/10 (10%)	0/7	1/4	0/1
	V40	11	4/11 (36%)	4/7	1/5	0/1
	V45	2	1/2 (50%)	0/1	1/1	-
	$D_{\text{mean}}/D_{\text{median}}$	8	2/8 (25%)	1/4	1/3	0/1
	Spared 10 Gy	1	1/1 (100%)	-	1/1	-
	Spared 20 Gy	1	0/1 (0%)	-	0/1	-
	Spared 40 Gy	1	0/1 (0%)	-	0/1	-



4. Correlations between bone marrow radiation dose and hematologic toxicity in locally advanced cervical cancer patients receiving chemoradiation with cisplatin: a systematic review

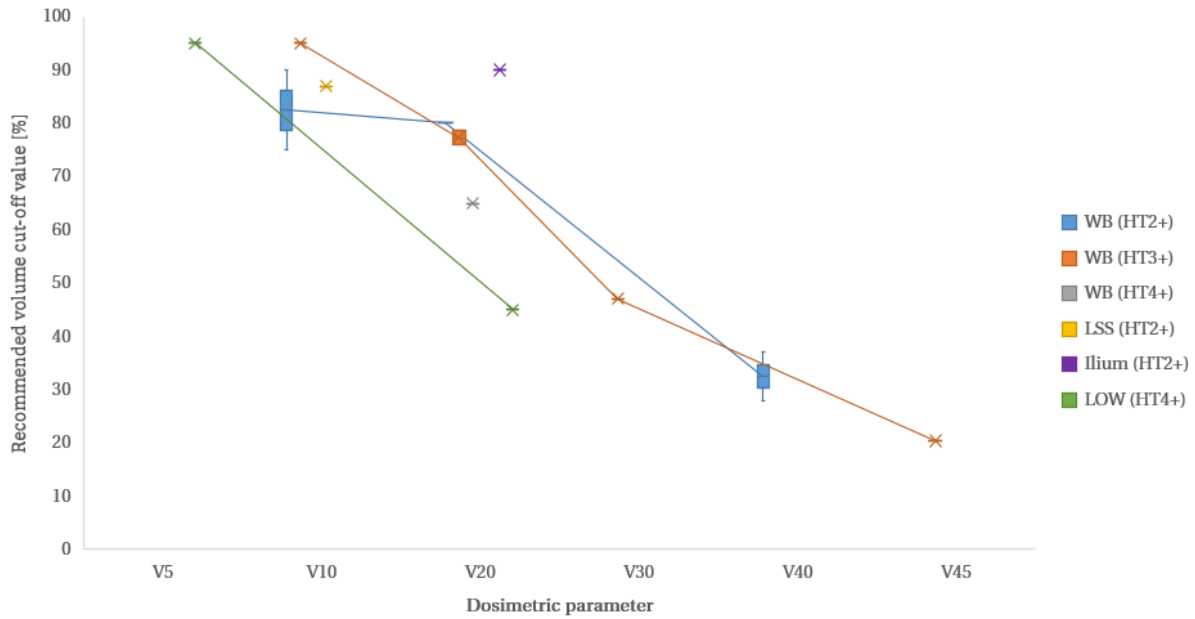


Figure 4.2: Cut-off values for dosimetric parameters of the whole pelvic bone contour (PB) which are correlated with hematologic toxicity (HT) as recommended by the included studies. *HT* = hematologic toxicity, *WB* = whole bone, *LSS* = lumbosacral spine, *LOW* = lower pelvic bones

4.4.2.3. Subsites of the pelvic bone

Six articles analyzed the correlation between three subsites of the pelvic bone and HT but the studies detected different relationships, as can be concluded from Table 4.3 [59, 63, 98–100, 103]. An overview of the corresponding cut-off values can be found in Figure 4.2. The lumbosacral spine (LSS) includes the lumbar vertebrae and the entire sacrum, the lower pelvis (LOW) consists of the pubes, ischia, acetabula, and femoral heads, and the ilium extends from the iliac crests to the superior border of the femoral heads. For LSS, the V10 [59],  $D_{mean}$  [59], and V20 [63] were each found significant by one article.  $D_{mean}$  was recommended to be <39 Gy (not visualized in Figure 4.2) and  $V10 < 87\%$  [59]. Although significant LSS-sparing might be difficult due to its proximity to the target volume, efforts to constrict the dose of the LSS and whole pelvic bone simultaneously were expected to result in a more homogeneous dose distribution of the pelvic region [59, 63]. The V5 [99], V10 [63], and V20 [63, 99] of LOW were reported to be predictive of HT.  $V5 < 95\%$  and  $V20 < 45\%$  to decrease HT4+ [99]. Only two dosimetric parameters of the ilium, the  $D_{mean}$  [99] and V20 [98], were demonstrated to be correlated to HT and it was recommended that  $D_{mean} < 31$  Gy [99] (not visualized in Figure 4.2) and  $V20 < 90\%$  [98]. One study additionally analyzed the hip bone (HIP), which was defined as the total area of LOW and ilium, but did not find any dosimetric parameters that were associated with HT (results not visualized in Table 4.3) [59].

Table 4.3: Number and percentage of studies demonstrating a significant relationship between various dosimetric parameters of subsites of the whole pelvic bone contour (PB) and hematologic toxicity (HT). *CT* = computed tomography, *LSS* = lumbosacral spine, *LOW* = lower pelvic bones

Dosimetric parameter	Number of studies finding significant results number of studies including dosimetric parameter		
	LSS	LOW	Ilium
V5	0/1 (0%)	1/1 (100%)	0/1 (0%)
V10	1/6 (17%)	1/5 (20%)	0/5 (0%)
V15	0/1 (0%)	0/1 (0%)	0/1 (0%)
V20	1/5 (20%)	2/5 (40%)	1/5 (20%)
V30	0/5 (0%)	0/5 (0%)	0/5 (0%)
V40	0/4 (0%)	0/4 (0%)	0/4 (0%)
V45	0/1 (0%)	0/1 (0%)	0/1 (0%)
$D_{mean}$	1/2 (50%)	0/1 (0%)	1/1 (100%)



#### 4.4.2.4. Relationship with blood cell nadirs

Lastly, some articles demonstrated a significant relationship between the dose received by PB and nadirs of blood cells, including white blood cells (WBC), absolute neutrophil count (ANC), hemoglobin (Hgb), and platelets (PLT). An overview is provided in Table 4.4. However, the reported dose cut-offs for HT vary widely. Several studies detected a correlation between V10 [63, 89, 96, 107], V20 [89, 96, 97, 102], V30 [89, 96, 97],  $D_{\text{mean}}$  [89, 96, 97] and WBC nadirs. Elicin et al. noted that the V10, V20, V30, and V40 even have an effect on the WBC-count three months after treatment and during late follow-up [89]. Similar dosimetric findings were reported for ANC nadirs, besides that a lower number of studies demonstrated V10 to be a significant predictor. Only the dosimetric parameters V10 [63] and V20 [63, 96] were significantly correlated with HB nadirs. None of the dosimetric parameters analyzed had any statistically significant association with PLT nadirs. Only three articles evaluated the dosimetric parameters of pelvic bone subsites and the consequences for nadirs of blood cells (results not visualized in this article) [63, 97, 100]. Dosimetric parameters of the LOW and LSS were found to be significantly related to nadirs in ANC, WBC, and Hgb [63, 97]. For the ilium, V20 was predictive for Hgb [63]. None of the dose-volume parameters influenced the PLT-count.

Table 4.4: Number and percentage of studies demonstrating a significant relationship between various dosimetric parameters of the whole pelvic bone contour (PB) and nadirs of blood cells *CT = computed tomography, ANC = absolute neutrophil count, WBC = white blood cells, Hgb = hemoglobin, PLT = platelets*

Contouring method	Subsite	Dosimetric parameter	Number of studies finding significant results / number of studies including dosimetric parameter	ANC	WBC	Hgb	PLT
CT based PB contour	Whole bone	V10	4/8 (50%)	1/7 (14%)	4/8 (50%)	1/6 (17%)	0/5 (0%)
		V20	5/8 (63%)	3/7 (43%)	4/8 (50%)	2/6 (33%)	0/5 (0%)
		V30	3/7 (43%)	2/6 (33%)	3/7 (43%)	0/6 (0%)	0/5 (0%)
		V40	2/8 (25%)	1/7 (14%)	2/8 (25%)	0/6 (0%)	0/5 (0%)
		$D_{\text{mean}}$	3/6 (50%)	2/5 (40%)	3/6 (50%)	0/4 (0%)	0/3 (0%)

#### 4.4.3. Lower density marrow spaces (PBM)

Four articles included the marrow cavity (PBM) as a surrogate for BM in their analyses [59, 98–100]. Table 4.5 shows that only the V40 is found to be associated with HT by two out of four papers [59, 100]. A  $V40 < 40\%$  might decrease the risk of HT2+ [100] (visualized in Figure 4.3). Two other studies did not demonstrate any associations of the PBM with HT [98, 99]. All authors noted that other contouring methods might be more suitable for BM-definition.

#### 4.4.4. Active bone marrow (ABM)

##### 4.4.4.1. Delineation method specified

Six of the included studies examined the correlation between radiation dose to the active bone marrow (ABM) and the development of HT [89, 105–109]. 18F-FDG-PET-CT was used by five studies and the technetium-99m (Tc-99m) sulfur colloid SPET was used by one study to quantify standardized uptake values (SUVs). Two methods for identifying ABM were applied: defining ABM as  $>SUV_{\text{mean}}$  of the total body or as  $>SUV_{\text{mean}}$  of the total pelvic bone.

##### 4.4.4.2. $>SUV_{\text{mean}}$ of the total body

ABM was defined as the region within the PB with an SUV greater than the  $SUV_{\text{mean}}$  of the total body using the 18F-FDG-PET-CT, applied by two authors [106, 108], or the Tc-99m sulfur colloid SPET, used by one author [109]. A volume consisting of SUVs higher than the  $SUV_{\text{mean}}$  and the total pelvic bone was defined as the ABM.

#### 4. Correlations between bone marrow radiation dose and hematologic toxicity in locally advanced cervical cancer patients receiving chemoradiation with cisplatin: a systematic review

Table 4.5: Number and percentage of studies demonstrating a significant relationship between various dosimetric parameters of the whole bone delineated as CT-based lower density marrow spaces (PBM) or active bone marrow (ABM) and hematologic toxicity (HT). *CT* = computed tomography, *SUV* = standardized uptake value, *TB* = total body, *FDG-PET* = fluorodeoxyglucose positron emission tomography, *SPECT* = single-photon emission computed tomography, *PB* = pelvic bone

Dosimetric parameter	pa-	Number of studies finding significant results / number of studies including dosimetric parameter			
		CT based PBM	ABM (>SUVmean TB FDG-PET)	ABM (>SUV mean TB SPECT)	ABM (>SUV mean PB FDG-PET)
V5		0/1 (0%)	-	-	-
V10		0/4 (0%)	0/2 (0%)	0/1 (0%)	1/1(100%)
V15		0/1 (0%)	-	-	-
V20		0/4 (0%)	0/2 (0%)	0/1 (0%)	1/1 (100%)
V30		0/3 (0%)	-	1/1 (100%)	1/1 (100%)
V40		2/4 (50%)	1/2 (50%)	1/1 (100%)	-
V45		-	-	-	1/1 (100%)
D <sub>mean</sub>		0/2 (0%)	0/2 (0%)	0/1 (0%)	1/1(100%)
Spared 10 Gy		-	1/1 (100%)	-	-
Spared 20 Gy		-	1/1 (100%)	-	-
Spared 40 Gy		-	1/1 (100%)	-	-

Similar mean PB-volumes (1553cm<sup>3</sup> (range 1117 – 1920cm<sup>3</sup>)[108] vs. 1433cm<sup>3</sup> (range 901 – 1920cm<sup>3</sup>)[106]) and ABM-volumes (1227cm<sup>3</sup> (range 793 – 1671cm<sup>3</sup>)[108] vs. 1098cm<sup>3</sup> (range 387 – 1671cm<sup>3</sup>)[106]) were reported in the articles applying 18F-FDG-PET-CT. The article focusing on Tc-99m sulfur colloid SPET showed lower volumes as the mean PB-volume was 954(±156)cm<sup>3</sup> and the mean ABM-volume was 355(±173) cm<sup>3</sup> which might be due to the different imaging modality used [109]. All three authors agreed that patients with a low pretreatment ABM-volume were more likely to develop HT3+ than patients with a larger ABM-volume before irradiation. Cut-off values of <1201 mL [108] and 387.5 cm<sup>3</sup> [109] were suggested. The V30 [109] and V40 [108, 109] were highly predictive for HT and V30>46.5% and V40>23.5% [109] were correlated with HT (see Figure 4.3). Additionally, V40 was also identified as a predictor a lymphocytes nadir [108]. Lastly, the volume of ABM spared was compared against HT and correlations were found for the volume spared 10, 20, and 40 Gy when <179cc, <186cc, and <738cc, respectively [106].

#### 4.4.4.3. >SUV<sub>mean</sub> of the total pelvic bone

A different method for determining ABM defines the SUV<sub>mean</sub> of the pelvic bones to be the threshold instead of the SUV<sub>mean</sub> of the total body. Three articles applied this method and studied the correlation between ABM and HT or nadirs of blood cells [89, 105, 107]. All three articles defined the ABM following the method as described by Rose et al. [107]. ABM was contoured by selecting the subset of the pelvic bones that had an SUV greater than or equal to the individual's SUV<sub>mean</sub> in the pelvic bones. Two authors reported similar mean values for the whole pelvic bone contour (1278.0(±224.7) cm<sup>3</sup> [107] and 1406.7 (±232.6) cm<sup>3</sup> [89]) and ABM (553.0(±133.1) cm<sup>3</sup> [107] and 651.5 (±188.4) cm<sup>3</sup> [89]). The researchers also evaluated inactive bone marrow (IBM), defined as the whole pelvic bone contour minus the ABM, and reported similar volumes for IBM (respectively 695.5(±147.0) cm<sup>3</sup> [107] and 755.2 (±144.1) cm<sup>3</sup> [89]). These two articles analyzed the correlation between dosimetric parameters and complete blood cell counts (results not visualized in this article). Most associations were identified for WBC. One article found the V10, V20, V30, and D<sub>mean</sub> to be highly predictive for WBC nadirs [107], while the other demonstrated that V20, V30, and V40 were predictors [89]. For ANC, HgB, and PLT-count, only D<sub>mean</sub> was associated [107]. Lastly, Rose et al. found no correlation between the D<sub>mean</sub> of IBM and blood cell nadirs [107]. A mean relative SUV-reduction in the whole pelvic bone and ABM of respectively 27% and 38% in comparison to the SUVs at pre-treatment was described [89]. This even occurred in parts of the ABM receiving relatively small doses (< 5Gy). These findings suggested the additional value of defining bone marrow as ABM when compared to the whole pelvic bone contour. The third article compared dosimetric parameters of ABM to HT (see Table 4.5) [105]. It showed that for para-aortic lymph node metastasis (PALN) patients, the V20, V30, and V45 of the whole pelvic bone were significant predictors for HT3+ at 78.6%, 47.1%, 20.4%, as discussed in section 4.4.2.2, and V10, V20, V30, and V45 of the ABM at 95.5%, 80.5%, 59.6% and 31.7%, visualized in Figure 4.3, respectively [105]. In addition, the D<sub>mean</sub> to PB and ABM ≥ 30.3 and 32.4Gy were associated with HT (not visualized in Figure 4.3). Due to the large irradiation

#### 4. Correlations between bone marrow radiation dose and hematologic toxicity in locally advanced cervical cancer patients receiving chemoradiation with cisplatin: a systematic review

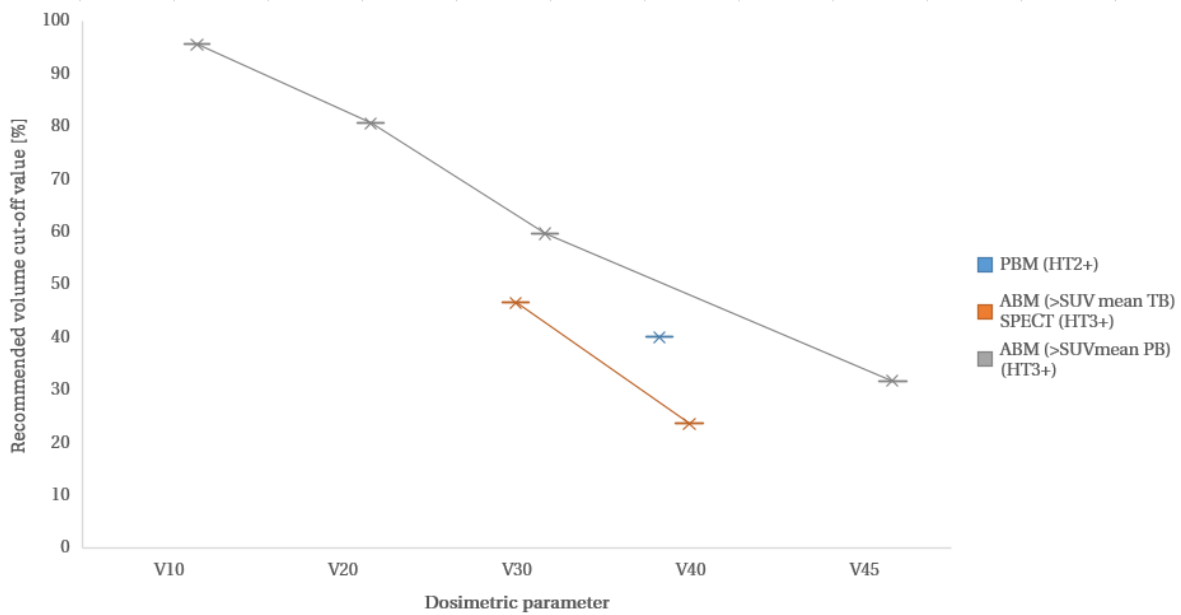


Figure 4.3: Dose cut-off values for the (subsites of) the pelvic bone delineated as CT-based lower density marrow spaces (PBM) or active bone marrow (ABM) and correlation to hematologic toxicity (HT) as recommended by included studies. *SUV* = standardized uptake value, *TB* = total body, *PB* = pelvic bone

field for PALN-patients, an additional value of ABM when compared to the whole pelvic bone could not be detected [105].

#### 4.4.5. Other predictors

All studies evaluated other predictors, besides dose volume characteristics, for HT except for four studies [98, 104, 106, 109]. The baseline WBC, ANC, HgB, and PLT were demonstrated to be predictive for their nadir values [100, 102]. The use of para-aortic irradiation was also associated with >HT3+ [89], in contrast to other findings [99]. Lastly, articles did report different outcomes for the association between body mass index (BMI) and HT. While some articles found BMI to be highly predictive for WBC nadir [96] or HT3+ [100], other articles did not show this correlation [84, 89, 97, 99, 102, 103, 107]. No associations were found between HT and race [84, 89, 96, 97, 103, 107], age [84, 89, 96, 97, 99, 100, 102, 103, 105, 107, 108], stage [89, 96, 103, 105, 107, 108], bone marrow volume [102, 103], comorbidity [96, 97, 105], PTV-volume [89, 100, 107], pre-treatment transfusions [105], positive lymph nodes [89], intensity or number of cycles of chemotherapy [89, 99, 100, 108], performance status [99], chemotherapy regimen (cisplatin vs. carboplatin) [99], and smoking history [108].

### 4.5. Discussion

To our knowledge, this systematic review is the first literature review providing an overview of articles evaluating the correlation between irradiation of the BM in patients with locally advanced cervical cancer and the development of hematologic toxicity (HT). Seventeen articles were included. Except for the article by Rose et al., all included articles used a single dataset to develop a HT-prediction model. Three BM-delineation methods were identified: contouring of the whole pelvic bone (PB), lower density marrow spaces (PBM), and nuclear imaging-based active bone marrow (ABM). Dosimetric parameters of (subsites of) the pelvic bone associated with HT or nadirs of blood cells were identified for each delineation method.

It should be noted that the majority of the included studies had a retrospective design and a limited sample size. We utilized the TRIPOD-system as a way to quantitatively analyze the prediction strength of models. Only one of the articles was dedicated to model validation. The majority of the included articles, however, did not develop a complete dose-response model but evaluated selected dosimetric parameters. For these articles, the overall adherence to the TRIPOD-statement was low. Our review demonstrated therefore scarcity of studies independently validating developed prediction models. Ideally, studies should include both the development and external validation of a complete dose-response model before implementing it as a normal

tissue complication probability (NTCP) tool in the clinic to support decision-making during treatment planning. External validation studies are important to improve a model's generalizability, validity, and clinical usefulness.

Additionally, studies reported contradicting results on dosimetric parameters correlated with HT. Some articles defining bone marrow as the whole bone contour (PB) detected a correlation between low dose-volume parameters and HT [63, 96, 104], while other articles only reported high dose parameters to be associated [59, 84]. A reason for this could be multicollinearity. It is highly likely that dose-volume parameters are correlated. Entry of multiple dose parameters in one model could lead to incorrect estimates. Likewise, multiple studies investigating ABM reported difficulties in finding a correlation between dose-volume parameters of the bone marrow and HT [84, 105, 108]. The inability to detect associations might be due to a lack of low-dose regions targeting the sensitive bone marrow resulting from characteristics of the patient cohort, radiation therapy technique used, or proximity of the bone marrow to the target volume. For instance, lumbar and pelvic bone marrow receives high doses in the irradiation of PALN-patients [105]. 3DCRT leads to a sharper gradient between moderate and low isodose levels when compared to IMRT and may therefore limit dose-volume associations [103, 108]. Lastly, the proximity of pelvic bone subsites, including the lumbosacral spine, to the target volume leads to high bone marrow dose [99].

In general, volume-based metrics might be a better predictor for HT when compared to dose-volume metrics. Included studies emphasized the importance of sparing a threshold volume and believed that bone marrow acts as a parallel organ, similar to the liver [106, 108, 109]. As long as there are enough active functional cells left, HT will not occur. The detected correlation between a low baseline bone marrow volume and HT supports the idea of sparing threshold volumes. However, further evaluation of a volume-based model is warranted.

Knowledge on the effect of bone marrow dose for LACC-patients could aid in the development of BMS-techniques. Dose constraints are important to minimize the occurrence of hematologic toxicity and can be applied during treatment planning. Studies by [Platta et al.](#) and [Mell et al.](#) were excluded in this systematic review, since their articles did not analyze the correlation between bone marrow dosimetric parameters and HT, but showed a significant decrease in dosimetric parameters with the use of BMS-techniques [110, 111]. [Platta et al.](#) applied the method proposed by [Mell et al.](#) to contour the whole pelvic bone marrow (PB) for cervical or endometrial cancer patients and created a standard and BMS IMRT-plan [110]. For the standard IMRT-plan and BMS IMRT-plan, the resulting PB-V10, V20, and V40 were respectively 94%, 74%, and 37% and 83%, 65%, and 35%. Secondly, [Mell et al.](#) demonstrated that PET-CT-based BMS-IMRT, sparing the ABM, showed significantly lower rates of HT3+ (neutropenia) when compared to CT-based BMS-IMRT, sparing the PB [111].

The effect of various dose delivery techniques on BMS has been investigated in multiple planning studies. The dose in the bone marrow could be significantly reduced without increasing the dose in the bladder, rectum, and bowels with both IMRT and VMAT compared to 3D conventional RT [112]. The developments in intensity-modulated proton therapy (IMPT) technique are promising for BMS. IMPT could not only reduce the dose directly received by the BM but also reduce the field size which is correlated to bone marrow suppression [83]. A large field size bears a higher risk of lymphopenia, as more circulating lymphocytes receive irradiation dose. A study wherein ABM identified on 18F-fluorothymidine (FLT) PET was used to delineate bone marrow in cervical cancer patients showed a significant reduction in median volume with IMPT compared to IMRT for all dose levels, with reductions from 23% to 41% [90]. The impact of such dose reductions on the risk of HT should be further evaluated and compared among radiation techniques before certain techniques can be recommended.

Studies have evaluated delineation methods different from those included in this systematic review for other pelvic cancers than LACC. 18F-fluorothymidine (FLT) PET can identify and spare ABM in patients with pelvic cancer. FLT detects chronic suppression of bone marrow by correlating FLT-uptake to complete blood cell counts. IMRT-plans sparing the FLT-identified pelvic bone marrow significantly reduced the dose to the pelvic bone marrow [113]. Additionally, fat-fraction imaging can be utilized to measure bone marrow composition changes during chemoradiation treatment in patients [114, 115]. With water-fat imaging methods, fat fraction maps can be acquired. The fat fraction in bone marrow can significantly increase during the treatment, especially in areas close to the target radiation field, and is associated with declining peripheral blood cell counts [115]. An increase in the fat fraction is the highest in regions close to the target volume, whereas chemotherapy gives more uniform changes [114]. Continued efforts should be made to identify functional pelvic bone marrow using PET-tracers, MR-imaging, or other imaging modalities. Since functional imaging is expensive and not commonly available, earlier studies proposed an atlas-based method for delineating the

ABM in patients with cervical cancer [116, 117]. Atlas-based BMS-IMRT can reduce the dose to the ABM. Future studies on delineation and sparing methods for bone marrow in LACC-patients are required to establish the most optimal sparing strategy.

This systematic review showed that only a limited number of studies have investigated the relation between bone marrow dose and HT in LACC-patients treated with primary cisplatin-based chemoradiation and that clinically useful predictions models are currently not available. The majority of the studies defining bone marrow as the whole pelvic bone found a significant association between bone marrow and HT, in contrast to studies evaluating lower density marrow spaces or active bone marrow. A significant increase in hematologic toxicity was observed for whole pelvic bone doses of  $V_{10}>95-75\%$ ,  $V_{20}>80-65\%$ , and  $V_{40}>37-28\%$ . Future studies may use whole pelvic bone contouring to develop normal tissue complication probability models.



# 5

## Implementing treatment planning for LACC in HollandPTC

### 5.1. Introduction

Implementing treatment planning for LACC in HollandPTC gives rise to various challenges. Firstly, a major difference between LACC and the cancers currently treated with aIMPT is that LACC involves complex day-to-day anatomical variation. Tumors with a standard indication for aIMPT are chordomas or chondrosarcomas, pediatric, intra-ocular, and base-of-skull tumors. Head and neck, breast, prostate, and lung tumors are conditionally eligible for proton therapy. The motion within the pelvic area makes accurate proton therapy delivery for LACC more demanding. Additionally, the effect of uncertainties is more profound for proton therapy than it is for photon therapy [67]. To make a fair comparison between IMRT/VMAT and aIMPT during PROTECT's clinical pilot-study, technical aspects of the most optimal proton therapy delivery have to be determined. As earlier discussed, LACC is currently treated with an adaptive planning strategy based on a pre-treatment library-of-plans in Erasmus MC.

In this chapter, the development and implementation of the aIMPT-planning strategy for LACC-patients in HollandPTC are proposed. Firstly, the uncertainties arising from proton therapy characteristics are identified, in addition to the already known errors related to LACC-treatment. Then, previous experiences with LACC-treatment in Erasmus MC are combined with more advanced techniques to deal with those uncertainties. Lastly, a planning strategy and a corresponding workflow are proposed.

### 5.2. Methods

Uncertainties arising from proton therapy were identified in the literature and provided in an overview. Strategies to address each uncertainty were then systematically investigated in the literature. The magnitude and impact of the detected uncertainties for LACC-treatment were quantified based on published results and an analysis of a formula and a data set available in Erasmus MC. The analysis will be discussed in section 5.4.3.2. Then, the proton delivery strategy considering the identified uncertainties was established and recommendations for future work were made.

### 5.3. Identified uncertainties for proton therapy and related approaches

#### 5.3.1. Range uncertainties for proton therapy

Several sources of uncertainty present in photon therapy also apply to proton therapy [69]. These include variation in delineation, set-up uncertainties, imaging inaccuracies, and patient motion. However, there are significant differences between protons and photons which makes proton therapy less tolerant than photon therapy to uncertainties in both treatment planning (i.e. dose calculation) and delivery [66, 118]. Protons have a well-defined range, sharp distal fall-off, and specific scattering characteristics [119]. The range of proton beams is predominantly determined by the initial energy of protons and the stopping power to protons of the medium they transverse [69]. Uncertainties in the proton's range, a dimension not present in photon therapy, raise a new challenge for proton therapy [120]. Figure 5.1 visualizes the two main sources of range uncertainty. Uncertainty in the calculation of the stopping power translates directly into uncertainty in the



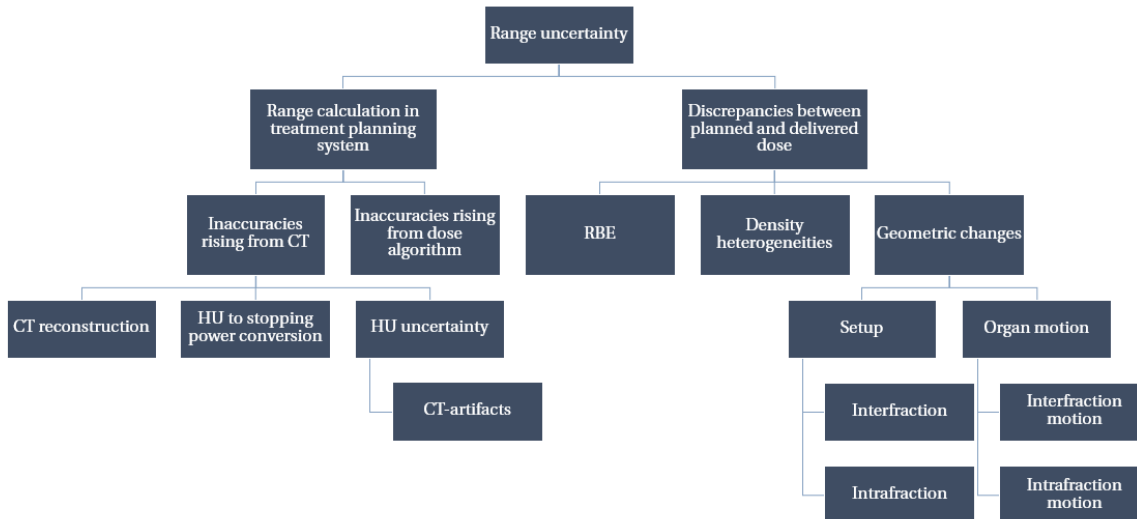


Figure 5.1: Sources of range uncertainties for proton therapy. Adjusted from McGowan et al. [69] *CT* = *computed tomography*, *HU* = *Hounsfield Unit*, *RBE* = *relative biological effectiveness*

range and depth of the distal edge of the Bragg peak and in the dose distribution that is displayed by the treatment planning system [120]. Secondly, discrepancies between planned and delivered dose could also lead to range uncertainties. An uncertainty in tissue density affects the proton penetration and position of the Bragg peak while it only minimally affects the photon depth-dose profile (see Figure 5.2) [67, 119]. Thus, this uncertainty can lead to underdosage in the target volume or overdosage at an OAR during proton therapy delivery. The two main sources of range uncertainties will each be further discussed.

### 5.3.1.1. Range calculation in the treatment planning system

Uncertainties in the range calculation in the treatment planning can be further categorized into inaccuracies due to CT and inaccuracies due to the dose algorithm (see the left branch of Figure 5.1). A CT-scanner measures the attenuation of X-rays during the passage through the body at many different angles around the patient. Reconstruction algorithms transform linear attenuation coefficient measurements into voxelized samples of Hounsfield Units (HU), which is a quantitative scale used for describing the measured density of the body [121]. With HU, the CT-images used for treatment planning of proton therapy can be generated. As a consequence, errors in the HU or CT-images have an impact on the treatment planning. Firstly, the CT-reconstruction might be a source of errors. Reconstruction algorithms are based on modeling and statistics, resulting in uncertainties in HU and therefore the CT-image [122]. A second significant cause of errors is the HU to stopping power conversion. Treatment planning systems for proton therapy require a CT calibration curve relating HU to proton stopping powers. The stoichiometric calibration of CT-scanners is used most widely and is known to be reliable for photon dose calculation. However, the physics of X-ray and of proton interactions in matter are fundamentally different and the mapping is therefore not strictly one-to-one [123, 124]. This is an important issue for future research. Thirdly, errors in HU can be caused by CT-artifacts, including noise and beam hardening, due to very dense targets. Inaccuracies due to the dose algorithm affect the range calculation in proton treatment plans. The dose algorithm currently used in HollandPTC is the Monte Carlo model, which is believed to be the most accurate algorithm currently available. This model

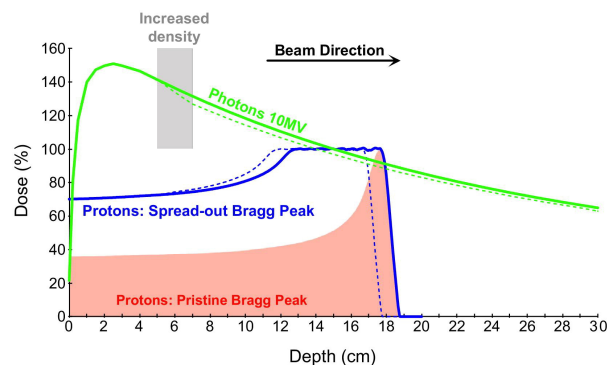


Figure 5.2: Depth-dose curves of photons and protons without (solid line) and with (dashed line) an increased density variation in the beam entrance region. Adjusted from Engelsman et al. [67]



utilizes probability distributions and is therefore associated with uncertainties in range prediction. In HollandPTC, calculation accuracy of 1% is used clinically.

### 5.3.1.2. Discrepancies between planned and delivered dose

The first source of discrepancies between the planned and delivered dose is the relative biological effectiveness (RBE) [66]. This value defines the ratio of the photon (reference) dose and the proton dose necessary to cause the same level of biological response [125]. For proton beams, an RBE of 1.1 is applied in current clinical practice. However, the RBE should vary throughout the beam path because the characteristics of the particles are different depending on their location in the beam [125]. As a result, an underdosage to the target or underestimation of the toxicity might occur when using a constant value for RBE.

Secondly, since the stopping power of protons depends to a large extent on the properties of all range absorbing materials in the beam's path, density heterogeneities in the beam path can lead to large dose differences to a target or OAR [65]. Density heterogeneities include a cavity that fills with air or liquid or density changes within the tumor.

Lastly, similar to density heterogeneities, setup differences and organ motion can cause significant variations in the extent and location of the distal falloff region [66]. These geometric changes include interfraction motion (i.e. between each fraction) and intrafraction motion (i.e. during the treatment delivery). Setup uncertainties are defined as errors in reproducing a patient's position which influences the position of the whole treatment field. The magnitude of setup uncertainties can be decreased by using immobilization devices (knee support) and image guidance (with a pretreatment CBCT or setting up to lasers). Next, the complexity of organ motion depends on the characteristics of the organ. Intrafraction motion can include unpredictable anatomical changes such as bowel movements or more constant motion such as respiration. Interfraction motion mostly includes shrinkage of the tumor and changes in filling of the stomach, small bowel, bladder, etc.

### 5.3.2. Strategies to address uncertainties in proton therapy

Several articles have addressed uncertainties for proton therapy and studied correction methods. Effectively dealing with uncertainties in treatment planning and treatment delivery is the biggest challenge in realizing the potential of proton therapy and in defining its ultimate role in radiotherapy [67]. In Table 5.1, an overview of treatment strategies to account for uncertainties in LACC-radiotherapy is provided. With exception of the plan library strategy, which has been explained in section 2.1.1.2 and 2.1.3, the applicability of each of these treatment strategies will be further discussed.

#### 5.3.2.1. Margins

The majority of studies evaluating uncertainties in photon therapy use the planning target volume (PTV) concept. A 3D safety margin is assigned to the CTV to ensure that the CTV will receive the prescribed dose in the face of treatment setup and anatomy variations [118]. The PTV-concept is currently applied in LACC photon therapy treatment as discussed in section 2.1.1.2. Except for situations when margins might become too large due to extensive uncertainties (i.e. anatomical variations), this strategy is considered to be simple and not resource-intensive. However, margins are less suitable for proton therapy because of the combined uncertainties of both positioning and proton range [121]. The current PTV-concept is based on the assumption that the dose distribution is shape invariant with respect to geometrical uncertainties, which is not the case for proton beams [67]. The proton range uncertainty could be addressed by adding an extra margin to the proximal and distal part of the CTV in the beam path (see Figure 5.3) [127]. Beam-specific distal and proximal margins give rise to the concept of the beam-specific PTV and density changes leading to an underdosage of the target volume could

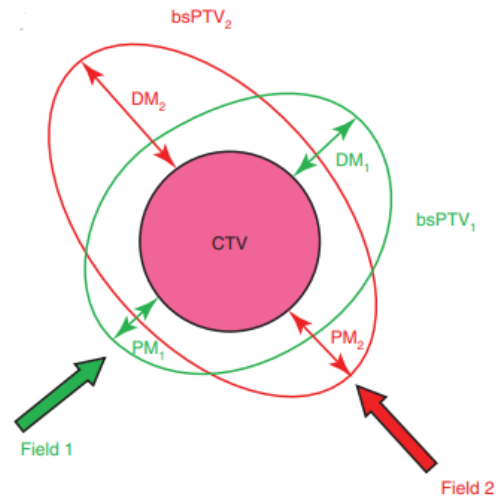


Figure 5.3: Beam-specific distal margins (DM) and proximal margins (PM) make up a beam-specific planning target volume (bsPTV) for each field. Adjusted from Zeng et al. [120]

Table 5.1: Overview of treatment strategies in locally advanced cervical cancer radiotherapy to correct for uncertainties [67, 126] OAR = organ at risk, CTV = clinical target volume

Technique	Characteristics	Advantages	Disadvantages
Margins	A 3D safety margin is assigned to the contour such that target coverage is assured	<ul style="list-style-type: none"> <li>• Simple</li> <li>• Not resource-intensive</li> <li>• No impact on treatment on set</li> </ul>	<ul style="list-style-type: none"> <li>• May increase target volume and reduce sparing of OARs</li> <li>• Not applicable to range uncertainty of protons</li> </ul>
Robust planning	Account for uncertainties in the optimization cost function	<ul style="list-style-type: none"> <li>• Applicable to proton therapy</li> <li>• Improved target coverage and OAR-sparing when compared to margins</li> </ul>	<ul style="list-style-type: none"> <li>• Calculation of a large number of scenarios</li> </ul>
Plan library	Create multiple potential treatment plans for each patient, representing different 'likely anatomies'	<ul style="list-style-type: none"> <li>• Significant reduction in OAR-dose</li> <li>• Possible increase in target coverage</li> </ul>	<ul style="list-style-type: none"> <li>• Adequate training needed</li> <li>• Time-consuming on set if difficult</li> <li>• Need to consider intrafraction filling and monitor treatment times</li> <li>• Might not account for all scenarios</li> </ul>
Plan adaptation	Rescan and replan at set time points throughout treatment	<ul style="list-style-type: none"> <li>• Reduce OAR dose while maintaining CTV coverage</li> <li>• Compensate for reduction in tumor volume</li> </ul>	<ul style="list-style-type: none"> <li>• Time and resource-consuming</li> </ul>
Daily re-optimization	Create new treatment plans online while the patient is on the treatment couch	<ul style="list-style-type: none"> <li>• Potential reduction of doses to OARs</li> <li>• Highly personalized treatment</li> </ul>	<ul style="list-style-type: none"> <li>• Adequate training needed</li> <li>• Resource-intensive</li> <li>• Specialized systems or treatment platforms required</li> </ul>
Online tracking	Utilize fiducial markers/transponders for real-time tumor tracking to account for intra-fraction target motion	<ul style="list-style-type: none"> <li>• Certainty regarding target position</li> <li>• Allows very small margin around target</li> <li>• Tracks intra-fraction motion</li> </ul>	<ul style="list-style-type: none"> <li>• Complex</li> <li>• Additional procedure needed</li> </ul>

be decreased [120]. However, this method does not apply to delivery techniques using non-uniform beam doses, including IMPT, as such anatomical variations could lead to hot or cold spots within the CTV itself and not just at the periphery of the target volume.

### 5.3.2.2. Robust planning

A more advanced strategy is to minimize the impact of anatomical variations by explicitly including those as error scenarios in the optimization of the treatment unit settings [67]. This is called robust treatment planning. An often used strategy to incorporate range uncertainties and setup errors into the cost function and constraints is 'minimax optimization' [128]. Minimax optimization requires a number of planning scenarios. For each planning scenario, the dose distribution of a treatment plan with a different combination of setup robustness (SR [mm]) and relative range robustness (RR, [%]) is calculated. SR is simulated with shifts of the beam isocenters and RR is related to stopping-power prediction and simulated by scaling the proton beam energy or HU of the CT. Then, the dose distributions are evaluated and the worst scenario is optimized by minimizing the corresponding worst objective function value. In other words, the possible loss for a worst-case scenario is minimized. After robust optimization, the plan should be evaluated on coverage criteria under the specified uncertainty conditions, which is called robustness evaluation. Optimized plans are evaluated by moving the beam isocenters, related to SR, scaling the mass density, related to RR, and re-computing the dose [128]. Korevaar et al. proposed a method to 'summarize' the resulting dose distributions into an evaluation dose distribution and to assess the robust plan quality [129]. The voxel-wise minimum and voxel-wise maximum dose compose of respectively the lowest dose and highest dose per voxel in all scenarios. The voxel-wise minimum dose is most similar to the traditional PTV-concept for evaluating the CTV-coverage and underdosage [129]. The voxel-wise maximum dose shows possible hot spots in the target and hot dose regions near density heterogeneities like the spinal cord and vertebrae. Acceptance criteria used in the PTV-concept, for instance  $D_{\max} < 107\%$ , might need adjustments to be applicable as acceptance criteria for voxel-wise dose composites. Both the robust treatment planning and evaluation method discussed in this section are currently applied in HollandPTC for other cancer sites.

### 5.3.2.3. Plan adaptation, daily re-optimization, online tracking

Three more complex procedures include plan adaptation, daily re-optimization, and online tracking. Plan adaptation includes re-scanning and re-planning at set time points throughout the treatment course. It might permit a small PTV-margin while it accommodates shape and position changes of the target and OARs, for instance due to tumor shrinkage over the treatment course [130]. However, when applying plan adaptation as the only treatment strategy, intra and interfraction motion of the uterus are respectively not or partly taken into account and larger margins are still required. The EMBRACE-protocol does not include re-planning at set time points, but advises monitoring of the uterus movement with a daily CBCT to decide if re-planning would be necessary when a PotD-approach is not used [27]. In Erasmus MC, re-planning is considered when the backup plan is chosen more than three times during the whole treatment course (see section 2.1.2).

The daily re-optimization technique allows for generating daily treatment plans, based on images acquired just prior to each treatment fraction. Ideally, daily generated treatment plans would replace the need for a plan library. In this way, robustness settings and margins could be reduced to obtain better OAR-sparing while maintaining the target coverage. However, online planning requires future research on adequate automatic delineation, dose planning, and quality analysis (QA) before clinical implementation. Speed is thereby essential as cervix-uterus motion during re-optimization time may offset the advantage of online planning. Efforts are made to automatize delineation, using deformable image registration [131], and near real-time adaptation of IMPT-plans [132]. An alternative approach was investigated by Jagt et al. [133]. In their study, an automated prior-plan adaptation method for aIMPT of LACC was used to account for large day-to-day anatomical variations in this patient group. Selecting a plan from a plan library and adjusting it to the daily anatomy resulted in clinically acceptable treatment plans, which demonstrated the feasibility of the used adaptation method.

For online tracking, radio-opaque markers implanted around or within the tumor can be used for target tracking during treatment delivery. In this way, beam delivery can be synchronized with intrafraction motion. Studies evaluated the applicability of online tracking during EBRT as an alternative to the brachytherapy boost, but the technique is currently not applied in LACC-treatment [134, 135]. As intrafraction motion in LACC is less pronounced than interfraction motion, tumor tracking is less relevant [136]. In Erasmus MC, polymer markers are used for localization of the target volume during the daily CBCT and aid in plan selection, as discussed in section 2.1.2. Additionally, the protocol requirements of EMBRACE do not include real-time tumor tracking [27].

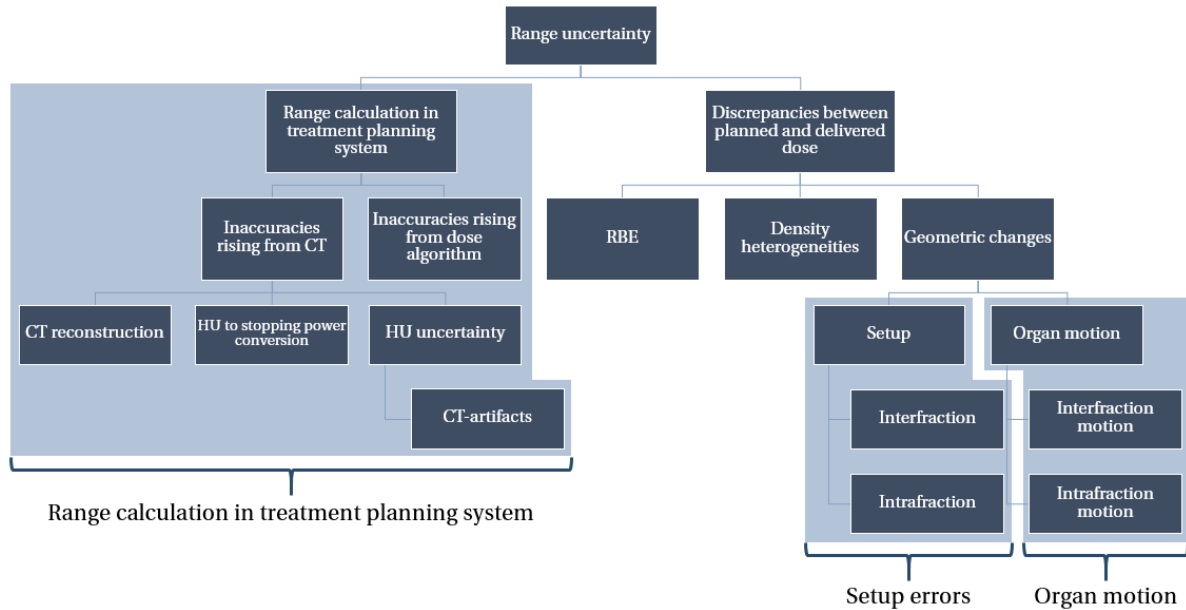


Figure 5.4: Uncertainties for LACC aIMPT-treatment summarized in three subjects. Adjusted from McGowan et al.[69] CT = computed tomography, HU = Hounsfield Unit, RBE = relative biological effectiveness

In summary, plan adaptation should be evaluated to complement the treatment planning strategy proposed in this thesis. Daily re-optimization and online tracking are respectively not yet clinically available or less relevant for LACC-treatment. These three techniques will therefore not be considered in the strategy to address uncertainties in the implementation as proposed in this thesis.

## 5.4. Proposed strategy for aIMPT of LACC

The uncertainties that will be considered for LACC aIMPT-treatment in HollandPTC can be summarized in three sources: range calculation in the treatment planning system, setup uncertainties, and organ motion (see Figure 5.4). Clinically applicable strategies to address these errors will be proposed in the following sections.

### 5.4.1. Range calculation in the treatment planning system

3% is accepted as RR in robust optimization planning and applied in planning studies on cervical cancer [53, 54, 74] and in clinical practice for other cancer sites, including head-and-neck cancer, at HollandPTC. For LACC, uncertainties arising from range calculation in the treatment planning system are expected to be similar to those of other cancer sites treated at HollandPTC. Firstly, the same CT reconstruction methods and dose algorithms are used for the other cancer sites. Secondly, CT artifacts due to very dense targets are not likely to occur as there is a lack of bones in the beam path. Therefore, an RR of 3% will be introduced for aIMPT-treatment of LACC.

### 5.4.2. Setup uncertainties

Setup uncertainties have a random and systematic component [66]. Random uncertainties are uncertainties in patient setup that differ from fraction to fraction. By using immobilization devices and setup protocols, setup accuracy can be increased but it is not possible to set up the patient in exactly the same position every time [66, 137]. Systematic uncertainties result from a systematic misalignment with respect to the planning CT-scan. As a result, there will be a measurable deviation of the location of reference points in the planning CT-scan from those of the imaging during treatment. Generally, a much smaller dose effect of random errors than of systematic errors is expected, as the random component has a chance to be compensated for by another fraction [137]. However, a clinically applicable method to determine the total magnitude of these uncertainties with proton therapy is not yet available in HollandPTC. Van Herk et al. have developed a set of formulas, which is defined as a margin recipe, to generate CTV to PTV-margins for photon therapy [138]. The simplified margin recipe ( $2.5\Sigma + 0.7\sigma$ ) assumes that the minimum dose to the CTV is 95% for 90% of patients.

In this equation,  $\Sigma$  is the quadratic sum of the standard deviations of all systematic uncertainties and  $\sigma$  is the quadratic sum of the standard deviations of all random uncertainties. The margin recipe by Van Herk et al. will be used in this thesis to quantify the errors for LACC-treatment and determine the amount of correction required.

Because there are multiple target volumes that move differently, the setup errors per target volume are expected to be different. The clinical target volume of LACC-patients consists of two anatomical locations: the CTV-LR, including the cervix-uterus, and the CTV-E, including the elective lymph nodes. The CTV-LR is at the level of the pelvic bones, whereas the CTV-E extends towards the vertebrae, especially for large pelvic + para-aortic region EBRT (as discussed in section 2.1.1.2).

#### 5.4.2.1. CTV-E

Interfraction setup errors of the CTV-E can be caused by non-rigid differences in the positioning of the patient. Nervous patients might have difficulties relaxing the pelvic muscles. As a result, the pelvic bones are rotated with respect to the vertebral column, i.e. the CTV-LR is rotated with respect to the CTV-E. Bony alignment, using the pretreatment CBCT, is based on the pelvic bones and rotational setup variations of the vertebrae may thus occur. This error is both systematic and random, as it might arise during the acquisition of both the planning CT-scan and pretreatment CBCT. Ahmad et al. calculated the setup errors after a translational and rotational correction (+- 3 degrees) at the vertebrae was applied for fifteen prone-treated LACC-patients [139]. Residual errors are shown in Table 5.2. LACC-patients in HollandPTC will be treated in supine position, which resulted in a lower number of treatment fractions with a displacement of >5 mm when compared to the study by Ahmad et al. [140]. Therefore, the values proposed in Table 5.2 might be too conservative.

Secondly, the allowed threshold before table rotation needs correction is 0.6 degrees at the isocenter, which is generally positioned nearby the CTV-LR. While this rotation uncertainty will only result in a small setup error for the CTV-LR, the estimated distance of 20 cm between the isocenter and the tip of CTV-E will lead to a 2 mm inaccuracy at the tip of the CTV-E. Since this is the maximum inaccuracy that can occur, the corresponding standard deviation can be calculated by multiplying 2 mm with 68% to get a random error of 1.4 mm [141].

Lastly, an error in positioning of the CTV-E can also arise during the fraction. Patient positioning might change during the planning CT-scan or treatment delivery, resulting in respectively systematic or random intrafraction setup uncertainties. Heijkoop et al. assessed these positioning errors in prone-treated LACC-patients by comparing pre and post-fraction CBCTs using the pelvic bony anatomy [142]. The mean time between the CBCTs, i.e. the treatment time, was 20.8 min. Since the expected treatment time in HollandPTC is expected to be 10 minutes, the resulting intrafraction changes in patient positioning were divided by the square root of 2. The outcomes for both 20 and 10 minutes are shown in Table 5.3. Additionally, patients treated prone showed increased intrafraction displacement compared to supine positioning [143]. Therefore, the uncertainties as demonstrated by Heijkoop et al. may be too conservative for the treatment of LACC-patients in HollandPTC.

Table 5.3: Intrafractional patient setup errors of a prone-positioned locally advanced cervical cancer patient for 20 minutes and 10 minutes treatment time [142] LR = left right, SI = superior inferior, AP = anterior posterior

	20 min			10 min		
	LR [mm]	SI [mm]	AP [mm]	LR [mm]	SI [mm]	AP [mm]
M	-0.1	0.4	1.1	-0.1	0.3	0.8
$\Sigma$	1.3	0.4	0.6	0.9	0.3	0.4
$\sigma$	1.4	1.0	1.1	1.5	0.7	0.8

Table 5.4 provides an overview of the identified errors for CTV-E and the proposed margins in mm to correct for these uncertainties.

Table 5.4: Overview of identified setup uncertainties for CTV-E. The total error is quadratically summed and the corresponding margin is calculated with the margin recipe proposed by Van Herk et al. [138] LR = left right, SI = superior inferior, AP = anterior posterior

	LR		SI		AP	
	$\Sigma$	$\sigma$	$\Sigma$	$\sigma$	$\Sigma$	$\sigma$
Setup interfraction patient [mm]	0.6	0.3	1.3	1.5	2.2	2.4
Setup interfraction table [mm]	-	1.4	-	-	-	1.4
Setup intrafraction patient 10 min [mm]	0.9	1.0	0.3	0.7	0.4	0.8
Total error [mm]	1.1	1.7	1.3	1.7	2.2	2.9
<b>Required margin [mm]</b>		<b>4.0</b>		<b>7.6</b>		<b>4.5</b>

#### 5.4.2.2. CTV-LR

Interfraction setup errors of the CTV-LR are not similar to the errors of the CTV-E. CBCT-alignment with matching on the pelvic bony anatomy corrects for differences in positioning of the patient. Additionally, the proximity of the CTV-LR to the isocenter limits the effect of inaccuracies due to table rotation. The only similarity in setup errors between CTV-E and CTV-LR is the intrafraction patient setup differences, which cannot be corrected using the bony anatomy alignment. Therefore, the same setup intrafraction errors apply to the CTV-LR as to the CTV-E and the corresponding margins are presented in Table 5.5.

Table 5.5: Overview of identified setup uncertainties for CTV-LR. The total error is quadratically summed and the corresponding margin is calculated with the margin recipe proposed by Van Herk et al. [138] LR = left right, SI = superior inferior, AP = anterior posterior

	LR		SI		AP	
	$\Sigma$	$\sigma$	$\Sigma$	$\sigma$	$\Sigma$	$\sigma$
Setup intrafraction patient 10 min [mm]	0.9	1.5	0.3	0.7	0.4	0.8
Total error [mm]	0.9	1.5	0.3	0.7	0.4	0.8
<b>Required margin [mm]</b>		<b>3.0</b>		<b>1.6</b>		<b>1.2</b>

#### 5.4.2.3. Proposed margins for setup uncertainties

Ideally, setup uncertainties are included in the robustness optimization and corrected by using the setup robustness (SR) [mm] of both target volumes. However, the setup errors differ between the target volumes and it is technically not (yet) possible to incorporate different setup errors into the optimization functions of Raystation, which is the treatment planning system used in HollandPTC. An alternative is to correct for the uncertainties with a combination of margins and robust optimization. This will be discussed in section 5.4.4.2.

### 5.4.3. Organ motion

Inter and intrafraction variation is an issue in pelvic radiotherapy as bladder, bowel, and rectum filling can move the target volume or surrounding pelvic structures in or out of the treatment field [126]. Even though LACC-patients follow drinking instructions, bladder volumes are not consistent and reduce significantly during the course of treatment [40]. Additionally, daily variation in the rectal filling can lead to anterior and posterior shifts of the cervix-uterus [126]. Organ motion does not result in uncertainties for the CTV-E, but has a profound effect on the CTV-LR. The proposed strategy to manage the impact of organ motion uncertainties on the CTV-LR will concern a plan library in combination with margins.

#### 5.4.3.1. Interfraction motion

The internal target volumes (ITVs) as generated in Erasmus MC consist of a large range of possible cervix-uterus positions expanded with a margin, for instance a range from 0 to 50% of the bladder-filling when generating an empty-to-half-full ITV-T. Further tissue sparing could potentially be obtained by adapting the number of plans more specifically to the range of uterus motion. Therefore, an interpolation that contains one single position of the cervix-uterus, for instance at 50% of the bladder-filling, could be used. This interpolation method is included in the proposed PotD-approach for aIMPT of LACC, which will now be discussed. The process steps of this approach are also visualized in Figure 5.5. Firstly, the distance between



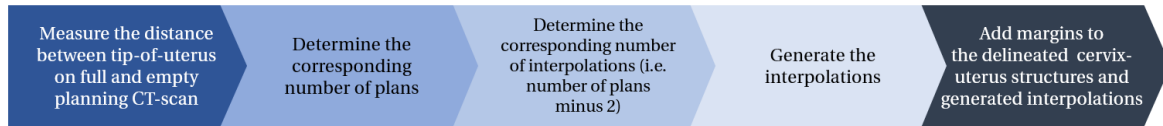


Figure 5.5: Process for generating the plan library. The distance between the tip-of-the-uterus on the full and empty bladder planning CT-scan correspond to the number of plans in Figure 5.6.

the tip of the uterus on the full and empty-bladder CT-scan has to be measured. The maximum distance between interpolations should approximate 10 mm, according to the method used by Visser et al., so the corresponding number of plans can be found in Figure 5.6 [144]. The number of required interpolations is the number of plans minus two, as the cervix-uterus delineated on the full and empty-bladder CT-scans is considered for respectively the full and empty treatment plans. In some cases, the distance between the tip of the uterus on the full and empty-bladder CT-scan, when 12 and 13 mm for instance, results in a distance between interpolations  $>10$  mm. An additional margin in the main cervix-uterus motion directions of 12 mm is therefore proposed. Since bladder-filling generally moves the CTV-LR in the superior direction, the applied margin will be divided into 9 mm for the superior direction and 3 mm for the inferior direction. Additionally, the CTV-LR moves towards anterior under influence of rectal filling, but towards posterior under influence of bladder filling. Therefore, a margin of 6 mm will be applied in both anterior and posterior direction. Lastly, literature suggested a 7 mm margin for lateral motion of the CTV-LR [41]. The currently applied margin in the left-right direction in Erasmus MC is 5 mm. Since the plan library approach can partly account for the lateral motion found in literature, a left-right margin of 6 mm will be applied for aIMPT-treatment of LACC.

#### 5.4.3.2. Intrafraction motion

The intrafraction motion of the uterus was quantified with the use of a formula and data set, which were available in Erasmus MC. Firstly, the formula was based on a total of 632 daily pre- or post-CBCTs for sixteen LACC-patients with a large tip-of-uterus displacement from a study by Heijkoop et al. [142]. The formula relates the bladder inflow rate to the volume of the bladder at the start of a treatment fraction and is illustrated in Figure 5.7a. Every 100 ml extra bladder volume at the start of the treatment increased the inflow rate by approximately 1 ml/min. Secondly, the data set included CBCTs of ten LACC-patients, categorized as movers. Per patient, five CBCTs with the corresponding bladder volume [cc] and position of the tip of the uterus [x,y]

Distance between uterus on full-bladder and empty-bladder CT-scan [mm]	Number of plans			
	2	3	4	5
5	5.0	2.5	1.7	1.3
6	6.0	3.0	2.0	1.5
7	7.0	3.5	2.3	1.8
8	8.0	4.0	2.7	2.0
9	9.0	4.5	3.0	2.3
10	10.0	5.0	3.3	2.5
11	11.0	5.5	3.7	2.8
12	12.0	6.0	4.0	3.0
13	13.0	6.5	4.3	3.3
14	14.0	7.0	4.7	3.5
15	15.0	7.5	5.0	3.8
16	16.0	8.0	5.3	4.0
17	17.0	8.5	5.7	4.3
18	18.0	9.0	6.0	4.5
19	19.0	9.5	6.3	4.8
20	20.0	10.0	6.7	5.0
21	21.0	10.5	7.0	5.3
22	22.0	11.0	7.3	5.5
23	23.0	11.5	7.7	5.8
24	24.0	12.0	8.0	6.0
25	25.0	12.5	8.3	6.3
26	26.0	13.0	8.7	6.5
27	27.0	13.5	9.0	6.8
28	28.0	14.0	9.3	7.0
29	29.0	14.5	9.7	7.3
30	30.0	15.0	10.0	7.5
31	31.0	15.5	10.3	7.8
32	32.0	16.0	10.7	8.0
33	33.0	16.5	11.0	8.3
34	34.0	17.0	11.3	8.5
35	35.0	17.5	11.7	8.8
36	36.0	18.0	12.0	9.0
37	37.0	18.5	12.3	9.3
38	38.0	19.0	12.7	9.5
39	39.0	19.5	13.0	9.8
40	40.0	20.0	13.3	10.0

Figure 5.6: In the proposed treatment planning strategy, the number of plans in the plan library depends on the distance between the uterus on the full-bladder and empty-bladder CT-scan [mm]. The distance between the interpolations [mm] (highlighted in blue) should always approximate 10 mm. For instance, a measured distance between the uterus on the planning CT-scans of 15 mm corresponds to a distance of 7.5 mm between the interpolations and the need for three treatment plans. The number of interpolations is the number of plans minus two. *CT = computed tomography*

were available. The first and fifth CBCT contained respectively the bladder with the least and most filling. Analysis of this data set provided insight into the correlation between the average bladder volume during a treatment and uterus motion. The correlation is shown in Figure 5.7b. The formula and data set were used to predict the intrafraction motion of the uterus due to bladder filling.

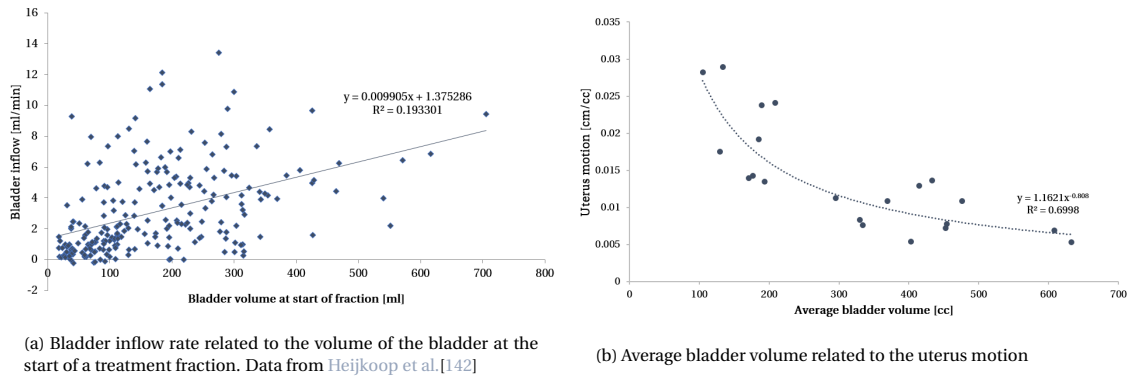


Figure 5.7: Formula (Figure 5.7a) and data set (Figure 5.7b) about intrafraction motion of the uterus in patients with locally advanced cervical cancer

An example calculation of the intrafraction motion for one patient is provided in Figure 5.8. To start with, the formula by Heijkoop et al. was applied to correlate the measured bladder volumes of the CBCTs to the inflow in [ml/min] per patient in the data set. Then, the total inflow was calculated for a treatment time of five, ten (example outcome shown in Figure 5.8), and fifteen minutes. The average bladder volume per treatment time is  $\frac{\text{measured bladder volume}}{\text{measured bladder volume} + \text{the inflow during treatment time}}$ . The correlation between the average bladder volume during treatment and uterus motion was used to determine the amount of uterus motion per cc bladder filling. With the knowledge of the total inflow for the treatment time, the uterus motion could be calculated and expressed as a percentage of the maximum uterus motion, which was defined as the distance between the tip of the uterus on the first and fifth CBCT. The intrafraction motion as a percentage of the total uterus motion per treatment time is visualized in Figure 5.9. The latter provides insight into the margin required to correct intrafraction motion. Since the treatment time in HollandPTC is expected to be 10 minutes, Figure 5.9 demonstrates that a margin of 14% of the total uterus motion would ensure a coverage of 95% of the intrafraction motion. However, this might be too conservative as it is assumed that the CTV-LR is located on the edge of the selected interpolation before the treatment fraction and will therefore move out of the radiation field during treatment. Additionally, the data was based on patients with a large tip-of-uterus displacement. A margin of 10% in the direction of the uterus motion due to bladder filling is therefore sufficient to account for the intrafraction motion with a treatment time of 10 minutes.

CBCT	Formula by Heijkoop et al		Inflow in 10 min [cc/10min]	Correlation between average bladder volume and uterus motion			
	Bladder volume [cc]	Inflow [ml/min]		Average bladder volume [cc]	Uterus motion per cc [cm/cc]	Motion in 10 minutes [cm]	% motion of total distance
1	127	2.63	26.3	140	0.0214	0.564	10.8%
2	251	3.86	38.6	270	0.0126	0.486	9.28%
3	409	5.43	54.3	436	0.0086	0.464	8.86%
4	543	6.75	67.5	577	0.0068	0.461	8.80%
5	723	8.54	85.4	766	0.0054	0.464	8.85%

Figure 5.8: Example calculation of uterus motion during a treatment time of 10 minutes for one patient in the dataset. CBCT = cone beam computed tomography



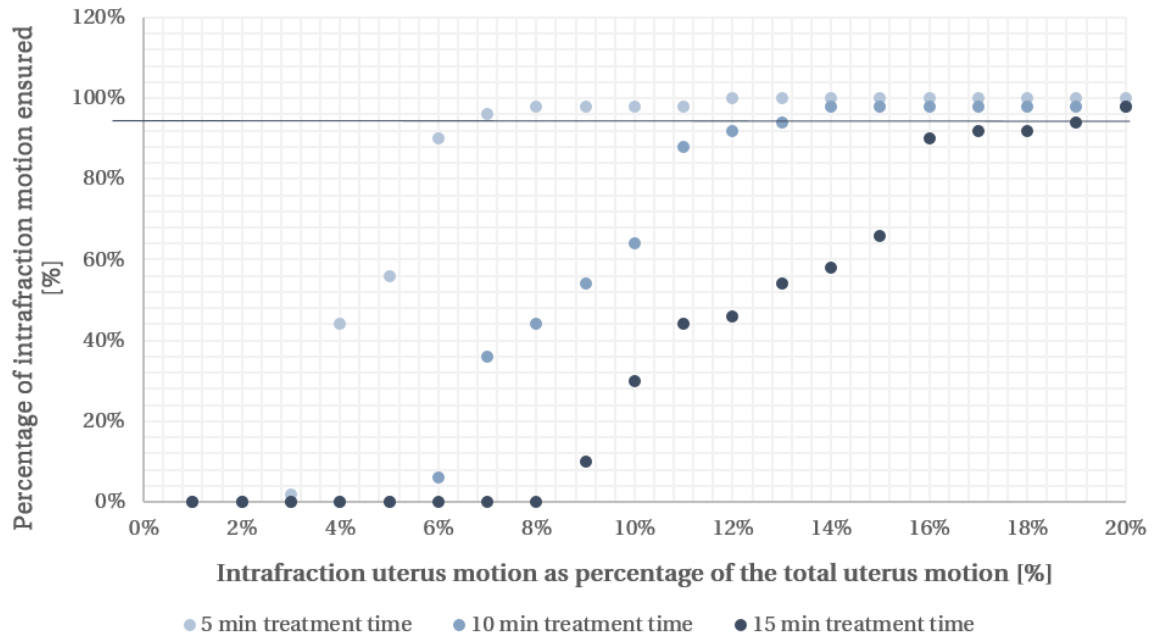


Figure 5.9: Intrafraction motion of the uterus (as percentage of the total uterus motion) related to the occurrence of the intrafraction motion in analyzed CBCTs. The blue line corresponds to coverage of 95% of the intrafraction motion during treatment time.

#### 5.4.4. Clinical implementation of aIMPT

The process for treatment planning is proposed in Figure 5.10. A summary of the proposed aIMPT-strategy is provided in Figure 5.11. The clinical implementation of each correction method, i.e. RR, SR, and the plan library with margins, will be discussed further into detail.

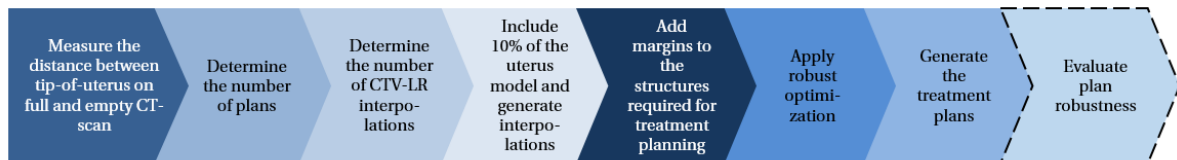


Figure 5.10: Proposed process for generating the plan library and applying robustness. The distance between the tip-of-the-uterus on the full and empty bladder planning CT-scan correspond to the number of plans in Figure 5.6. The strategy for plan evaluation was not yet established in this thesis. *CT* = computed tomography, *CTV-LR* = low-risk clinical target volume

##### 5.4.4.1. Plan library and margins

The ITVs applied in Erasmus MC are created with the in-house application *Erasmus RTStudio*, which uses a nonrigid registration algorithm to derive a patient-specific cervix-uterus shape model as described in section 2.1.1.2 [46]. However, HollandPTC prefers the whole workflow to be implemented in the treatment planning system Raystation. Raystation provides a scripting environment for automatizing treatment planning workflows, customizing interaction between Raystation and other systems, creating new capabilities which are not available in the user interface, or making research tools. Most importantly, scripting enables the implementation of an interpolation tool.

Academic Medical Center (AMC) in Amsterdam has already developed a script in Raystation for generating interpolations between structures. This script was used for the study by Visser et al. [144]. They also implemented this tool clinically for the PotD-strategy for bladder and cervical cancer and agreed to share their script with Erasmus MC. The script requires a matched full and empty bladder CT-scan and a structure set on the full-bladder CT-scan consisting of the delineated CTV-LR and bladder for both scans. Additionally, the location of the desired interpolations has to be filled in, for instance at 33% and 67% for a patient requiring four plans in the plan library.

The script starts with checking whether the required input is available and correct. The CTV-LR and bladder delineated on the full and empty CT-scan are defined as controlling structures, ROIs. Overlap between the bladder and CTV-LR is removed for both scans. A mesh of the controlling ROIs serves as input for the biomechanical deformable image registration algorithm. The result of this deformable image registration is a deformation vector field that describes the correspondence between the two CT-scans. The deformation vector field is applied to the vertices of the CTV-LR and bladder on the full bladder scan. The measured distance between two vertices is the vector difference and can be scaled to obtain an interpolation.

This script is made available in Raystation for HollandPTC as part of this master thesis and works in research setting.

#### 5.4.4.2. Robust optimization (RR and SR)

The overview in Figure 5.11 shows that the required setup robustness (SR) differs between the two target volumes. CTV-E requires a larger SR for all directions. However, treatment planning system Raystation is not (yet) able to robustly optimize by applying different optimization settings per target volume. Therefore, the robustness settings for both CTV-LR and CTV-E have to be the same in clinical practice. A simple solution could be to apply the same SR to both CTV-LR and CTV-E and equalize the absolute difference with margins. For instance, 5 mm SR is used for CTV-LR and CTV-E in all directions. The required SR in the left-right direction of CTV-LR has to be 3.0 mm (see Figure 5.11), so the SR would be too robust by 2 mm (5 mm applied minus 3 mm required). Additionally, a 5 mm margin was required to account for the limitations in the plan library. 2 mm could be subtracted from the 5 mm margin resulting in a margin to correct for the plan library of 3 mm in the left-right direction of the CTV-LR when applying 5 mm SR. However, the correlation between margins and robustness is not that simple. *van Dijk et al.* compared the robustness of minimax-based IMPT-plans, using a 3% RR and a 3.5 mm SR, with PTV-based IMPT-plans, applying a 5 mm PTV-margin, for ten head-and-neck cancer patients [145]. In contrast to minimax optimization, the PTV-concept for IMPT showed poor robustness performance. Despite the fact that the compared IMPT-plans had a larger PTV-margin than SR, the PTV-concept was demonstrated to be insufficient as errors occurred in the center of the CTV and at the border of the target volume. These findings suggest that robustness settings are not linearly correlated to margins. Nevertheless, studies quantifying the relationship between PTV-margins and robustness are lacking.

		CTV-LR			CTV-E		
		LR	SI	AP	LR	SI	AP
RR [%]	Range calculation in TPS	3%			3%		
SR [mm]	Setup interfraction patient						
	Setup interfraction table						
	Setup intrafraction patient						
	Total	3.0	1.2	1.6	4.0	4.5	7.6
Plan library and margins [mm]	Interfraction organ motion	Per 10 mm uterus motion an additional plan					
	Limitation plan library	5	9 & 3	6			
	Intrafraction organ motion	+ 10% of the uterus motion model					

Figure 5.11: Proposed plan library and robustness strategy for the low-risk clinical target volume (CTV-LR), including the uterus and cervix, and elective clinical target volume (CTV-E), including the nodes. *LR* = left right, *SI* = superior inferior, *AP* = anterior posterior, *RR* = range robustness, *SR* = setup robustness, *TPS* = treatment planning system

## 5.5. Discussion

In this chapter, an aIMPT-strategy for LACC-patients in HollandPTC is proposed. Proton therapy is less tolerant to uncertainties in both treatment planning and delivery when compared to photon therapy, mainly due to the range uncertainty of protons. Therefore, the current PTV-concept using margins is less suitable for proton therapy. The main sources of range uncertainty for LACC proton therapy were identified in literature and data available in Erasmus MC. Next, the uncertainties were quantified and categorized in three main sources, which were range calculation in the treatment planning system, setup uncertainties, and organ motion. For each of the three sources, a correction method was evaluated and combined into a final aIMPT-strategy. This aIMPT-strategy consists of a PotD-approach with margins and robust planning and can be clinically implemented in Raystation. In this discussion section, the proposed treatment planning strategy is compared with those applied in earlier studies and future work is discussed, followed by the conclusion.

Several studies implemented an aIMPT-strategy different from the proposed method in this thesis. An earlier planning study by [Gort et al.](#) evaluated two and four field proton therapy for twelve LACC-patients [54]. No plan library was used and the CTV-LR was expanded with an anisotropic margin of 5 mm in the left-right and 10 mm in the anterior, posterior, and superior direction for proton therapy. Additionally, robust optimization parameters were 3% RR and 5 mm SR in all orthogonal directions. Plan evaluation, using 5 mm setup uncertainty with isocenter shifts in 14 directions and an RR of 3%, showed that the target coverage was robust to inter- and intrafraction motion. In contrast to the margin strategy proposed in this thesis, it was unclear what studies the selection of robustness settings and margins was based on and which uncertainties were taken into account. Additionally, no difference was made between margins for the lymph nodes and CTV-LR, possibly leading to an overconservative margin strategy for the CTV-E. Lastly, while [Gort et al.](#) did not use a PotD-strategy, applied margins and SR are larger when compared to the margins proposed in this thesis, which could result in a reduced OAR-sparing. [van de Schoot et al.](#) explored differences between IMPT and VMAT-plans for thirteen LACC-patients [53]. Three, one, or two ITVs were generated for a uterus displacement above 20 mm, below 10 mm, or in between, respectively. No margins were applied. Both IMPT and VMAT-plans were robustly optimized with 8 mm SR in six directions and for the IMPT-plans an RR of 3% was included. Robustness evaluation consisted of fourteen scenarios of 8 mm isocenter shifts and demonstrated an inadequate CTV-coverage for 10.7% of the simulated fractions for both IMPT and VMAT. The remaining fractions had an adequate target coverage while IMPT reduced OAR-dose significantly. The correction strategy of [van de Schoot et al.](#) has smaller margins than proposed in this thesis but was not sufficient enough to ensure ITV-robustness. Considering both publications, the treatment planning strategy proposed in this thesis is in line with the existing exploratory studies.

Identifying and correcting for uncertainties arising from proton therapy is a complex field to explore. In general, studies focus specifically on one source of the uncertainties. Summing all these errors might lead to an overestimation, while not all uncertainties appear at the same time and with their maximum magnitude. An overconservative correction method will improve the target coverage but decrease the sparing of OARs. As a result, the beneficial aspects of proton therapy when compared to photon therapy will be eliminated. A balance has to be found between addressing all uncertainties and OAR-sparing. Further studies, which quantify all these uncertainties together, will need to be undertaken to further improve the aIMPT-strategy. This chapter provides a basis for determining the most optimal correction strategy. The main sources of uncertainties were identified and the corresponding correction method was determined per source. As a result, the final correction strategy can be proposed.

Currently, the implementation of daily re-optimization as a correction strategy for uncertainties in aIMPT for LACC is too complex even though this technique is promising. There are some limitations to overcome before daily re-optimization can be considered as an appropriate alternative for the proposed treatment planning strategy. Firstly, the in-room CT-scanner in HollandPTC could be used to easily acquire new planning CT-scans right before or after a treatment fraction but is not yet clinically available. Additionally, treatment planning is time-consuming due to manual contouring and long calculation times and should be accelerated to enable fast re-planning or daily re-optimization. The continuous developments made in this field are promising for future implementation of the re-optimization strategy.

Figure 5.4 illustrates that not all uncertainties identified in the literature were considered in the proposed aIMPT-strategy in this thesis. Uncertainties arising from RBE were not taken into account. Since literature does not provide clinically implementable corrections yet, a constant RBE is used in current clinical practice. Additionally, [Berger et al.](#) demonstrated that density heterogeneities, including bowel gas cavities and outline variations induced by weight changes, had a minor impact on accumulated dose in target volumes and OARs of IMPT for seven LACC-patients [146]. However, the volume of gas and magnitude of weight variation

might lead to a larger dosimetric impact. Different beam configurations might reduce the impact of density changes, as the beam directions determine which organs are crossed by the proton's path [146, 147]. Another possibility for diminishing the influence of the rectal gas cavities is by introducing rectal balloons filled with water [147]. More research is needed to quantify the impact of density heterogeneities on dose distributions and to assess clinically applicable correction methods.

Besides focusing on correcting uncertainties, further studies could also focus on reducing identified uncertainties, especially those arising from range calculation in the treatment planning system. For instance, studies are investigating proton computed tomography (pCT) to reduce or even eliminate range uncertainties with respect to HU to stopping power conversion [148].

Further work is needed to improve the script acquired from the AMC in Amsterdam. Currently, extrapolation of the cervix-uterus and bladder (i.e. 110%) is not yet possible. The generated interpolations have to be validated on accuracy and compared with the interpolations as currently generated by ErasmusRTStudio. The script should also be specified for HollandPTC by making it more user-friendly with an interface, clear notification of errors, and an instruction manual.

Additionally, the optimal balance of robustness settings and margins still has to be validated. This could be done by evaluating the robustness of treatment plans with different combinations of margins and setup robustness. However, robust optimization and evaluation are computationally expensive so this would require some computational time [129]. An alternative is to generate plans with an SR of 5 mm and an RR of 3% and evaluate the robustness of the CTV-LR for 2 or 3 mm isocenter shifts. In this way, insight is provided in the surplus as the SR is larger than required for the CTV-LR. This surplus could be subtracted from the margins with respect to the limitation of the plan library. Next, the strategy for a backup plan, as currently applied in the plan library of Erasmus MC, is not yet established. The most suitable PTV-BU-T should be determined before the treatment planning strategy can be implemented in HollandPTC. The strategy for robust evaluation of plans and the re-planning strategy should also be investigated. Before clinical implementation in HollandPTC, the treatment planning strategy have to be validated for its clinical applicability and the plans have to be evaluated on the target coverage and robustness. A retrospective study using available weekly CT-scans or CBCTs would therefore be recommended.

In conclusion, the development and implementation of the aIMPT-planning strategy for LACC-patients in HollandPTC were proposed. Proton therapy is less tolerant to uncertainties in both treatment planning and delivery when compared to photon therapy, mainly due to the range uncertainty of protons. The main sources of range uncertainty in LACC-treatment are errors due to range calculation in the treatment planning system, setup errors, and organ motion. Uncertainties due to the range calculation in the treatment planning system can be considered with an RR of 3%. Setup errors are different for the CTV-LR and CTV-E and will be partially included in 5 mm SR. Inter- and intrafraction motion of the target volume under influence of bladder and rectal filling will be taken into account with a plan library and additional margins. Recommendations for further work in Holland PTC include establishing the balance between robustness settings and margins and optimizing the clinical implementation of the plan library.

# 6

## Translating the current workflow for LACC-patients in Erasmus MC into the HollandPTC environment

### 6.1. Introduction

Erasmus MC has almost ten years of experience with the plan-of-the-day-strategy (PotD) for the treatment of LACC-patients. PROTECT's clinical pilot study requires the workflow and PotD-strategy in Erasmus MC to be implemented in HollandPTC to facilitate aIMPT. Since HollandPTC is an independent center with its own resources, information systems, and procedures, the workflow has to be tailored to its environment.

In this chapter, the workflow for LACC-patients in HollandPTC is proposed. Firstly, the current workflow in Erasmus MC is mapped. Then, requirements for the workflow in HollandPTC are generated. At the end of this chapter, a clinical workflow is proposed and the implementation in HollandPTC is investigated.

### 6.2. Map the current workflow in Erasmus MC

#### 6.2.1. Methods

Process mapping of the PotD-process in Erasmus MC aids in the understanding of the process steps in the radiotherapy department. Information was gathered through (informal) meetings with radiation therapists, radiation oncologists, and medical physicists, evaluation of the protocols used, and observations during the treatment of cervical cancer patients in Erasmus MC. An overview of the workflow was validated by a radiation therapist.

#### 6.2.2. Results

The workflow for PotD includes two main categories: 1) Generating a plan library and 2) Selecting the most suitable plan from this plan library before each fraction. These subcategories can be subdivided into a total of seven phases (see Figure 6.1) and each phase will be explained.

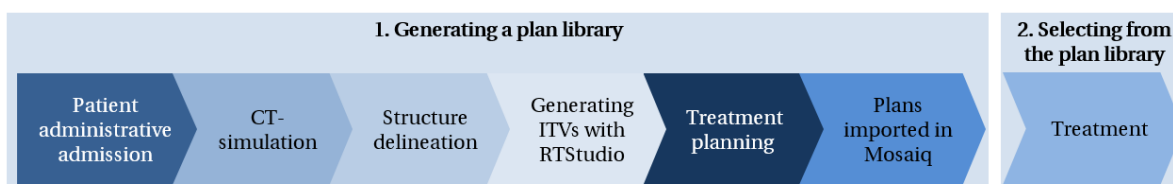


Figure 6.1: The current workflow in the radiotherapy department of Erasmus MC for locally advanced cervical cancer treatment consists of two general steps and seven substeps. *CT* = computed tomography, *ITV* = internal target volume

#### **6.2.2.1. Patient administrative admission**

The patient planners (PPR) of the radiotherapy department register the patient in the electronic health record used in Erasmus MC, HiX. Appointments are made for the CT-simulation, a diagnostic MRI-scan, the initial consultation with the radiation oncologist, treatment fractions, follow-up, and more. Additionally, the PPR sends patient information to a patient's home. During the first consultation, the radiation oncologist informs the patient about the treatment and performs a physical examination. Then, the radiation oncologist places the polymer-based markers used for localization of the cervix during the treatment and gives the patient preparation instructions for the planning CT-scans.

#### **6.2.2.2. CT-simulation**

The planning CT-scans are acquired in one of the two CT-scanners at the radiotherapy department. The patient is expected to have a full bladder, after following the drinking instructions, and is placed in treatment position. A pilot CT-scan is made to determine the scanning field of view. Then, intravenous contrast fluid is administered by intravenous infusion, followed by a planning CT-scan acquisition with a full bladder. The radiation therapist marks reference points for laser alignment with a tiny tattoo before the patient is asked to go to the toilet to empty her bladder. Next, the empty bladder CT-scan is acquired. The data is sent to the picture archiving and communication system of the radiotherapy department (RT-PACS). Lastly, the radiation therapist starts an automatic contouring tool, named ABAS, for the full bladder CT-scan that delineates the bladder, body outline, and some bony structures.

#### **6.2.2.3. Structure delineation**

The radiation therapist imports the image data and automatically generated structure set in MIM-software, which is used for contouring. The quality of the structure set is examined and it is determined whether the bladder filling was sufficient. The radiation therapist then delineates the bladder for the empty bladder CT-scan and aligns both planning CT-scans. All jobs are checked by a second radiation therapist. The radiation oncologist delineates the target volume on both CT-scans and the remaining OARs, including the bowel, rectum, and sigmoid, on the full bladder CT-scan. Remarks for the treatment planning are noted in HiX. After approval of the delineated structures during a meeting of the radiation oncologists in the gynecology workgroup, called the mono, the radiation therapist sends the scans and structure sets to RTStudio.

#### **6.2.2.4. Generating ITVs with Erasmus RTStudio**

The ITVs applied in Erasmus MC are created with the in-house application Erasmus RTStudio. The full and empty bladder CT-scans are imported into the software and aligned on the bony anatomy. The patient-specific cervix-uterus shape model and corresponding ITVs are then derived. The radiation therapist also creates the tubular structures around the implanted polymer markers position, which aid in position verification. Then, a medical physicist verifies the bony alignment and ITVs before importing the structure sets and CT-scans into the treatment planning system Monaco. Additionally, the medical physicist is responsible for expanding the ITV-T of the empty bladder CT-scan (named zITV) with a 5 mm margin, except for the caudal direction, to create an ITV-empty-T.

#### **6.2.2.5. Treatment planning**

The radiation therapist determines the setup reference point on the CT-scan. Then, the radiation therapist makes planning structures, used for constraints, and the final PTVs by summing the ITV-Ts and ITV-E and expanding these with margins. A second radiation therapist reviews these steps. Then, the first radiation therapist places the isocenter within a maximum distance of 11 cm to the most caudal located marker. The radiation therapist makes the treatment plans followed by a check of the dose distributions and constraints. The treatment plans are sent from Monaco to RTManager, which is also an in-house application, and checked by a second radiation therapist. The radiation oncologist reviews and approves the plans in Monaco before the radiation therapist can finalize these. The radiation therapist provides an overview of the treatment in HiX and exports the approved plan to RTManager and to Mosaik, which is the record and verify system. Lastly, the treatment plans are verified by a medical physicist in Monaco.

#### **6.2.2.6. Import plans in Mosaik**

Treatment delivery is prepared in Mosaik by checking if all plans and settings are correct. Then, two treatment calendars are added to plan the treatment and imaging sessions in respectively MasterRX and Imaging RadRX. These two tools track the amount of dose given during treatment and imaging. All these actions are monitored by a second radiation therapist.



### 6.2.2.7. Treatment

Just before treatment, the radiation therapist checks the settings and notes made on previous treatments. Patient positioning and plan selection take place according to the process discussed in section 2.1.2. After treatment delivery, the given dose is saved and added to the total dose as recorded in MasterRX. MasterRX provides a dose summary so that the amount of given dose can be tracked to prevent giving too much dose.

## 6.3. Generating requirements for the workflow

Before a PotD-workflow for HollandPTC can be developed, it is necessary to have more insight into what requirements this workflow has to fulfill. To obtain a complete and structured list of requirements, two steps were considered: the investigator thought of as many requirements as possible and a risk evaluation of the current workflow in Erasmus MC was executed with radiation therapists, medical physicists, and a radiation oncologist.

### 6.3.1. Input from the investigator

#### 6.3.1.1. Methods

The Pugh's checklist, developed for the assessment of a product, was followed to generate as many requirements as possible [149]. Different points of view were regarded, including the patient, radiation therapist, radiation oncologist, medical physics, and information technology (IT), when going through the checklist for the two categories in the workflow for PotD. One or two main objectives and corresponding requirements were thought of per Pugh's aspect. Lastly, each requirement was categorized as a hard (quantifiable) or soft requirement (a wish).

#### 6.3.1.2. Results

The Pugh's checklist consists of 24 checkpoints. One point was added to consider technical standards in the workflow. Ten points did not apply to the investigated process, so objectives and requirements for the remaining fifteen items were generated. An overview of the total checklist can be found in Appendix D. Figure 6.2 presents the applied checkpoints with the corresponding explanation per point. Additionally, one or multiple main objectives were identified per point. Appendix E presents the requirements. Each requirement corresponds to a point of view, is categorized as either a hard or soft requirement, and has a code to facilitate fast identification.

<b>Product liability</b> <i>Unintended consequences?</i> Hospital is ultimately responsible	<b>Target product costs</b> <i>What is the price?</i> In house development	<b>Manufacturing facilities</b> <i>What facilities?</i> Preferably designed in Raystation	<b>Safety</b> <i>Which safety facilities?</i> Limits human errors as much as possible	<b>Performance</b> <i>Which functions?</i> Accurate plans Fast plan generating Easy plan selection Trust that plan is optimal
<b>Quality and reliability</b> <i>Failure modes?</i> Errors can be solved by MP or IT department	<b>Quantity</b> <i>Size of run?</i> Should work on each PC with required software / radiotherapy machine in HollandPTC	<b>Standards</b> <i>Which standards apply?</i> Should follow data protection regulations	<b>Appearance</b> <i>Preferences of users?</i> Can be used intuitively	<b>Life in service</b> <i>How intensively used?</i> Applicable to each cervical cancer patient
<b>Testing</b> <i>Which quality tests?</i> Needs validation Needs continuous risk evaluation	<b>Ergonomics</b> <i>Understanding, using?</i> Easy applied by trained therapists	<b>Installation, operation</b> <i>Install and learn to use?</i> Installation by IT-department Training of users will be in house	<b>Technical standards</b> <i>Technical environment?</i> Adapted as much as possible to currently available software	<b>Maintenance</b> <i>Maintenance necessary?</i> Has to be operable after update of currently available software

Figure 6.2: Fifteen checkpoints applied for generating requirements to the plan-of-the-day-workflow. All checkpoints are drafted by Pugh with exception of *Technical standards* [149]. Per checkpoint, a short explanation is given followed by one or more main objectives.

### 6.3.2. Input from a risk evaluation of the current workflow

#### 6.3.2.1. Methods

The reduction of error through risk management becomes more and more important in the medical field. A risk analysis is a systematic methodology for identifying potential points of failure within a process, determining effects, and identifying actions to prevent these problems [150]. An often-used method is the Failure

Mode and Effect Analysis (FMEA). This method places the burden of error prevention on the designs of the systems in which users work with the input of team members during the process as the base [151]. In general, an FMEA consists of five steps [150]:

- Select the process to be studied
- Assemble a multidisciplinary team
- Collect and organize information on the process
- Conduct a hazard analysis
- Develop and implement actions and outcomes measures

The FMEA-steps were used during this risk evaluation. To start with, the process to be studied was the current PotD-workflow for LACC-patients in Erasmus MC. The multidisciplinary team consisted of two medical physicists, one radiation oncologist, and two experienced radiation therapists (one expert in creating ITVs, the other in generating the plan library). The seven phases in the current PotD-workflow, as reported in 6.2.2, were shared with the participants. The hazard analysis was performed with the use of RISKID. This is an online risk management tool focusing on collaboration and ease of use. It provides an online environment so that participants can do the majority of the risk analysis regardless of time or place. The risk evaluation with RISKID included the following procedure:

#### **6.3.2.2. Brainstorming phase**

Firstly, all participants identified possible risks online. The users were asked to provide as many risks as possible per phase, to describe causes and consequences, and categorize each risk in one of the four categories Technical, Organization, Human, or Other. Participants were not allowed to see each other's answers.

#### **6.3.2.3. Categorizing and deduplicating phase**

The investigator checked the identified risks on duplicates and the categorization.

#### **6.3.2.4. Grading phase**

Participants were then invited to grade the risks in the online environment. Each risk was scored on a scale from 0 to 5 on four items: its probability, the time needed to solve the event, the impact on quality, and the impact on patient safety. The accompanying legend in Table 6.1 was shared with the participants. Participants were allowed to neglect a risk when they had not enough knowledge on this part of the process. When all participants finished grading, RISKID calculated the grading results by using the modus calculation. The final score was based on majority voting. If two grades had an equal number of votes, the highest was selected. RISKID also calculated the risk score, which is the probability score multiplied by the summation of the score for time, quality, and patient safety. The investigator checked the calculated grading on inconsistencies and irregularities and ranked the risks based on their risk score. The thirty risks with a high risk score were highlighted and, based on a risk score cutoff value, the significant hazards requiring a measurement were selected.

#### **6.3.2.5. Determining measures**

Then, an interactive online session was organized using the communication platform Microsoft Teams. The aim of the meeting was to reach an agreement on the identified risks and think of measures for the most important risks. The participants received the online presentation with the identified risks and scores on forehand. During the session with all participants, the grading was evaluated per identified risk and per important risk, measures were thought of. The investigator listed the action points, assigned these to participants, and summarized the total procedure and outcomes in a report for the radiotherapy department. The identified hazards and measures from the risk analysis were translated into requirements for the workflow in HollandPTC.



Table 6.1: Scoring legend for grading of risks during risk evaluation for the plan-of-the-day-strategy for cervical cancer in Erasmus MC

Item	Definition of score						
	0	1	2	3	4	5	
Chance	None	Less than once per year	Every year	Monthly	Weekly	Daily	
Impact on time	None	Very low (very easy solvable)	Low (easy solvable)	Average (jeopardized planning)	High (delayed planning)	Very high (postponed treatment)	
Impact on quality	None	Very low	Low	Average	High	Very high	
Impact on patient safety	None	Minimal health reduction	Low health reduction	Average health reduction	Chronic health reduction	Death of patient	

### 6.3.3. Results

During the brainstorming phase, 74 risks were identified (see Table 6.2). After categorizing and deduplicating, 60 risks were left for grading. Each risk was scored four times (probability, time needed to solve the event, the impact on quality, and the impact on patient safety) and therefore each participant had to score 240 items. In Appendix F, the identified risks and corresponding scores are shown. The modulus calculation method used by RISKID for calculating the final score per item led to some counterintuitive outcomes. An example is provided in Figure 6.3. Therefore, eleven items were adjusted based on the interpretation of the researcher and presented to the participants. The average risk score was 13.8 (SD 8.6). As can be seen in Table 6.3, 30 risks had a risk score greater than 13 and 11 risks had a risk score greater than 21. The latter were therefore considered to be the significant risks requiring measures. During the interactive session, measures were discussed for eleven important risks and two additional risks. One of the participants was absent during the meeting but shared remarks and input before the session. An overview of the measures is provided in Table 6.4. After the session, a summary was sent to all participants. A follow-up session was planned with the head of the radiation therapists to discuss a relevant selection of the action points. The determined measures were used as requirements to the HollandPTC workflow. The remaining risks with a score greater than 15 were also considered in the implementation of the workflow, but no measures were determined.

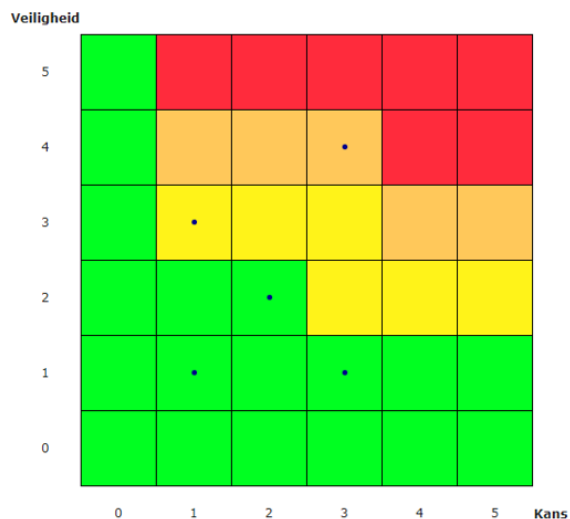


Figure 6.3: An example of a probability (X-axis) and safety score (Y-axis) for the requirement *The radiation oncologist selects a dose for the SIB-boost, but guidelines are lacking*. Modus calculation by RISKID would average the score for safety as 1. Since three participants scored safety >1, an average score of 1 would be inaccurate. Therefore, the investigator adjusted the score to 3.

## 6. Translating the current workflow for LACC-patients in Erasmus MC into the HollandPTC environment

Table 6.2: Number of risks identified during the brainstorming, categorizing, and deduplication phase in the risk evaluation for the plan-of-the-day-strategy for cervical cancer in Erasmus MC. *CT = computed tomography, ITV = internal target volume*

Phase	No of risks (brainstorming phase)	No of risks (after deduplication)
Register patient	3	3
Generate CT data	8	6
Delineate structures	7	6
Generate ITVs in RTStudio	14	12
Make treatment plans	15	11
Import treatment plans in Mosaiq	7	5
Patient treatment (per fraction)	20	17
<b>Total</b>	<b>74</b>	<b>60</b>

Table 6.3: 30 risks with the highest risk score (>13), including the first eleven risks with a risk score >21, identified for the plan-of-the-day-strategy for locally advanced cervical cancer in Erasmus MC. The risks were prioritized and numbered. *SIB = simultaneous integrated boost, CT = computed tomography, ITV = internal target volume, PTV = planning target volume, DVH = dose volume histogram, CBCT = cone beam CT, MP = medical physicist*

No	Risk	Score
1	Plan calculation is very time-consuming (with a minimum of four hours per plan)	35
2	The radiation oncologist selects a dose for the SIB-boost, but guidelines are lacking	30
3	The rectum-filling is not similar for empty/full CT-scans with inadequate interpolations as a result	30
4	The bladder is mainly empty during the mornings, but treatments cannot be planned in the afternoon	28
5	Incorrect CT is selected in the interpolation script	27
6	Number of processes does not correspond with number of treatment plans	24
7	Incorrect number of ITVs for a patient (a non-mover becomes a mover)	24
8	Single-user Monaco system is unavailable	24
9	zITV en ITV (+5 mm) for non-movers is missing	24
10	In general, the PTV of the nodes is evaluated with 95% in the DVH-statistics, but this is 90% for cervical cancer patients	24
11	Errors are made while selecting the planning template	24
12	Delineation of target volumes and the mono delay the process	21
13	Delineation of air and contrast is often forgotten	21
14	The uterus is located outside the isodose line	21
15	Low CBCT-quality	21
16	Treatment plans are named wrong	20
17	Radiation oncologists disapprove a treatment plan while it fulfills the prescribed requirements	18
18	The bony alignment is inaccurate (due to rotation of the pelvic bones, deformation, error in positioning of match box) resulting in an bad image registration	18
19	Incorrect structure is used for image registration	18
20	Radiation therapists forget to assess the maximum distance between the isocenter and the most caudal marker	18
21	Bladder is not full or empty in the corresponding CT-scans	18
22	Rectum or bladder filling is not sufficient for planning CT-scan	16
23	Linear interpolation is not representative for uterus rotation	16
24	Structures are assigned the incorrect names	16
25	MP check is not performed for all treatment plans	16
26	MasterRX consists of the wrong plans	16
27	Patients are given incorrect instructions	16
28	Lymph node is not visible on CBCT	15
29	The bladder and rectum filling is difficult to assess during planning CT-scans	15
30	Rotation of the pelvic bones is not similar for both planning CT-scans	14

Table 6.4: Overview of the measures for eleven important risks and two additional risks (marked with \*). *CT = computed tomography, SIB = simultaneous integrated boost, ITV = internal target volume, MP = medical physicist, PTV = planning target volume, DVH = dose volume histogram, PPR = patient planners*

Process step	No	Risk	Risk score	Measure	Status
Patient administrative admission	6	Number of processes does not correspond with number of treatment plans	24	Radiation oncologists already indicate whether the patient is a mover and non-mover in the start-form. Radiation oncologists should be notified during a general meeting.	In progress. Meeting has to be planned and prepared.
CT-simulation	2	The radiation oncologist selects a dose for the SIB, but guidelines are lacking	30	It is protocolized that radiation oncologists include the dose level in the structure name. Radiation oncologists should be notified during a general meeting.	In progress. Meeting has to be planned and prepared.
Structure delineation	12	Delineation of target volumes and the mono delay the process*	21	Medical specialists in training (AIOS) need extra time for delineation. A delineation <i>leerhuis</i> will be prepared and radiation oncologists should be notified during a general meeting.	In progress. <i>Leerhuis</i> has to be prepared and meeting has to be planned and prepared.
Generate ITVs in ErasmusRTStudio	7	Incorrect number of ITVs for a patient (a non-mover becomes a mover)	24	Radiation oncologists already have to indicate whether the patient is a mover and non-mover in the start-form. MP verifies this. Radiation oncologists should be notified during a general meeting.	In progress. Meeting has to be planned and prepared.
Generate ITVs in ErasmusRTStudio	5	Incorrect CT is selected in the interpolation script	27	Guidelines with respect to a maximum diameter for the rectum, similar to prostate treatment, during the planning CT-scan should be implemented.	Completed.
Generate ITVs in ErasmusRTStudio	3	The rectum-filling is not similar for empty/full CT-scans with inadequate interpolations as a result	30	The second radiation therapist and MP will detect these errors. No measure required.	Completed, no measure required.

Process step	No	Risk	Risk score	Measure	Status
Treatment planning	1	Plan calculation is very time-consuming (with a minimum of four hours per plan)	35	Feedback will be given to the FMT.	Completed.
Treatment planning	8	Single-user Monaco system is unavailable	24	Feedback will be given to the FMT.	Completed.
Treatment planning	9	zITV en ITV (+5 mm) for non-movers is missing	24	An additional item should be included in the checklist for MP.	Completed.
Treatment planning	10	In general, the PTV of the nodes is evaluated with 95% in the DVH-statistics, but this is 90% for cervical cancer patients	24	Radiation oncologists and radiation therapists should be notified during a general meeting.	In progress. Meeting has to be planned and prepared.
Treatment planning	11	Errors are made while selecting the planning template	24	Improvements on templates and iCycle will be discussed with Buddi, one of the iCycle specialists.	In progress while the required improvements are difficult to make.
Import plan in Mosaiq	25	MP check is not performed for all treatment plans*	16	Currently, there is a separate check point for each plan so further measures are not required.	Completed, no measure required.
Treatment	4	The bladder is mainly empty during the mornings, but treatments cannot be planned in the afternoon	28	The PPR could be asked whether fractions for patients without chemotherapy or hyperthermia on the day of treatment could be scheduled in the mornings.	In progress, proposal is sent to the PPR.

## 6.4. Implement the workflow in HollandPTC

### 6.4.1. Introduction

Knowledge of the current workflow in Erasmus MC can be combined with the generated requirements to design the workflow in HollandPTC. Since each institution has its own protocols, electronic patient record system, and logistics, a workflow cannot be copied directly from one center to another center. As stated before, Erasmus MC uses three treatment planning software applications (MIM, RTStudio, and Monaco), one record and verify system (Mosaic), and one information system (HiX(-RT)) clinically. In general, HollandPTC uses only one software application for the total treatment planning process (Raystation), one information system for the patient record (NeoZis), and one system for both workflow management and recording and verifying (ARIA). NeoZis is the electronic patient management system in HollandPTC. Patient data, including consults with doctors, diagnoses, an overview of the medication, letters, insurance, is saved in this system. Workflows are not managed with NeoZis, but with ARIA. HollandPTC has implemented the ARIA Oncology Information System to manage schedules of staff, resources, and finances in one system. It is designed to oversee all aspects of oncology care, but in HollandPTC it is mostly used for treatment preparation, monitoring treatment planning, appointment scheduling, and as a record and verify system. Therefore, each workflow has to be implemented in ARIA. The difference in software use between Erasmus MC and HollandPTC is illustrated in Figure 6.4.

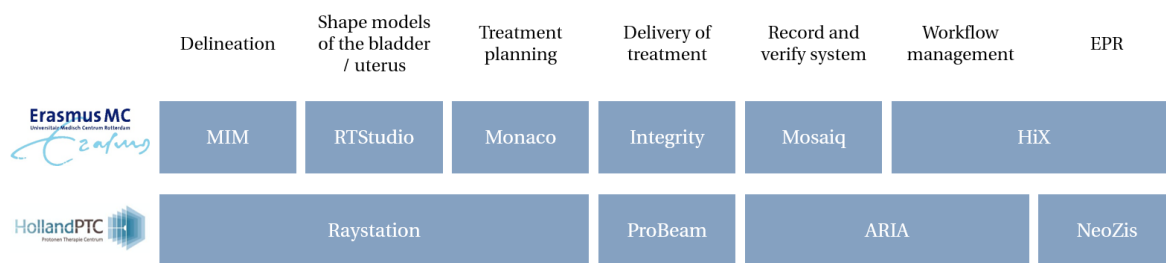


Figure 6.4: Differences in software between Erasmus MC and HollandPTC. *EPR = electronic patient record*

Implementing the workflow in ARIA includes implementation of the Care Path and the Treatment Management. Care Paths can be created for a variety of clinical, operational, or financial workflows and capture workflows, ensure tasks are completed, and auto-escalate overdue tasks for completion. For each clinical process in HollandPTC, including treatment of specific types of cancer, plan adaptation, or follow-up, Care Paths are created. A Care Path consists of a timeline with scheduled activities, which are categorized as administration, consultation, discussion, imaging, delineation, dose planning, medical physics (MP), or treatment. The first aim of this section is to implement a Care Path for LACC-treatment.

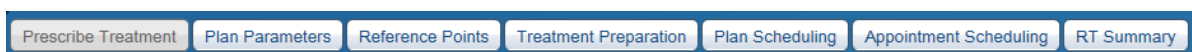


Figure 6.5: Treatment Management process in ARIA

Treatment Management tracks the process before treatment delivery (see Figure 6.5). This process has to be developed for LACC-treatment. In Prescribe Treatment, the radiation oncologist enters the RT-prescription. This is linked to the imported treatment plan(s). The Plan Parameters module has all beam and plan properties listed. In general, only one treatment plan is imported, but LACC-treatment requires multiple plans for the PotD-strategy, which makes the process more complex. For instance, the location of the reference point, defined as the beam dose specification point (DSP), is imported from the treatment plan into the module Reference Points. The dose limits to the reference point serve as safety limits for dose delivery. If the amount of monitor units (MU) delivered to a reference point leads to violation of the dose limit, the dose limit is overridden. An override always requires special authorization and treatment can only continue if the override is signed off by an authorized user. All overrides are stored as separate events in the ARIA database to be checked during or after treatment. Secondly, a breakpoint can be assigned to the reference point. If the total dose at a reference point passes the breakpoint, this is flagged and will require signing off to continue treatment. However, with a PotD-strategy, multiple plans are imported and each fraction the most suitable plan is selected. The safety limits for dose delivery should also apply to the PotD-strategy. The Treatment

Preparation module includes the setup and table settings followed by scheduling of the treatment fractions in Plan Scheduling. The daily setup imaging (CBCT) has to be scheduled as well and the PotD-strategy might introduce some scheduling challenges. In the same module, the plans and total treatment are approved by a medical physicist. With Appointment Scheduling, patient appointments can be arranged. RT Summary provides a summary of the whole treatment and should be adapted to the PotD-strategy. Dose limit overrides can also be found in RT Summary. The second aim of this section is to explore the feasibility of the clinical workflow with Reference Points, Plan Scheduling, and RT Summary in the Treatment Management process for LACC-treatment.

### 6.4.2. Methods

The implementation of a Care Path for LACC-treatment started with a design of the general workflow for LACC-treatment in HollandPTC. The corresponding requirements generated in section 6.3, notes, and further work were determined per phase in the workflow. Meetings with a senior radiation therapist and Care Paths for other cancers provided more information on the logistic process in HollandPTC. This was used to update the general workflow and to translate it into a Care Path.

Protocols from the Verbeeten institute, which is a center for radiotherapy and nuclear medicine in the Netherlands, and the AZ Groeninge hospital served as an example for the Treatment Management components Reference Points, Plan Scheduling, and RT Summary. These protocols were tested in ARIA's simulation environment. A planning CT-scan of an anthropomorphic phantom, made with the HollandPTC CT-scanner, was used for testing.

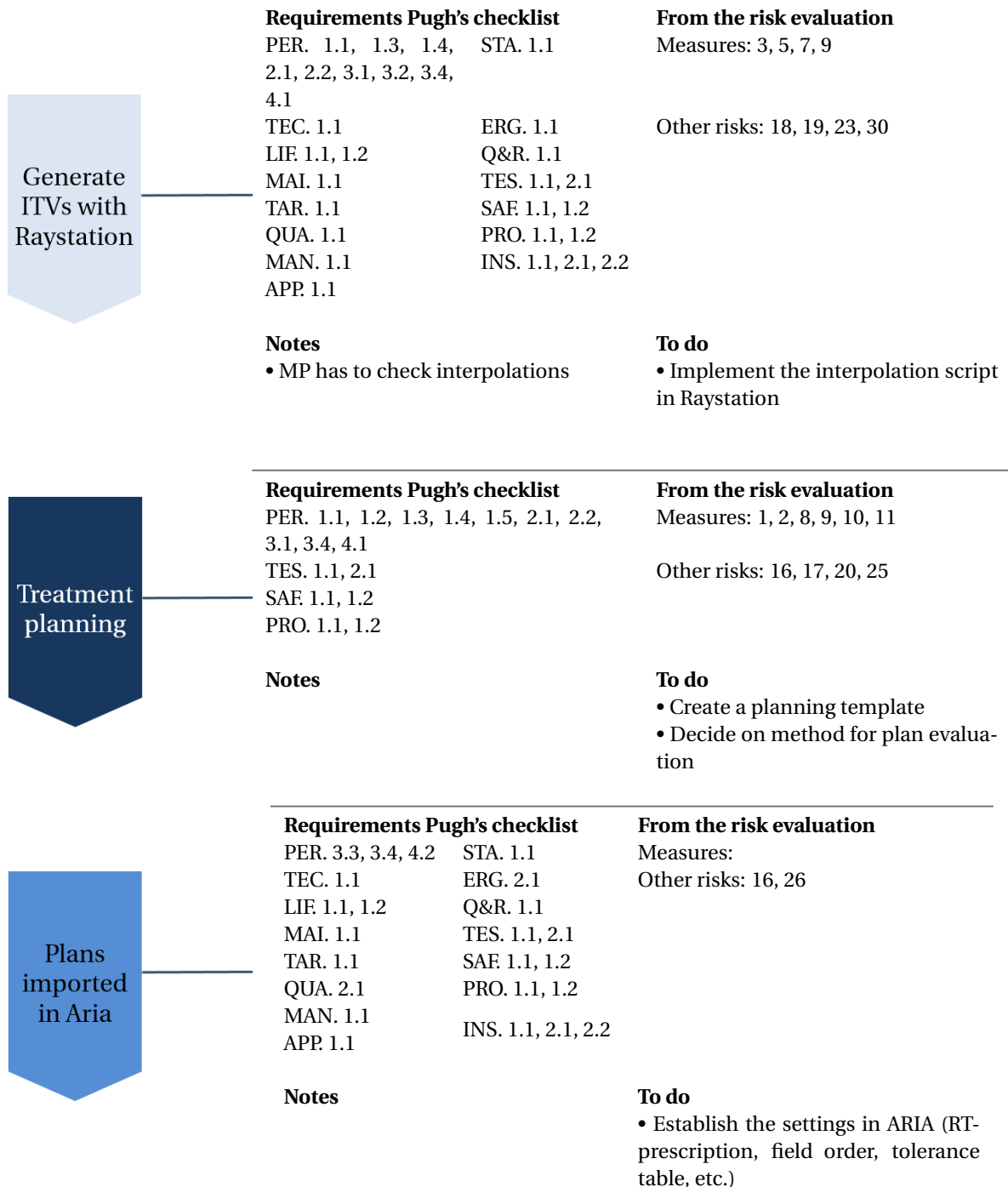
### 6.4.3. Results

#### 6.4.3.1. Care Path

Figure 6.6 provides the general workflow for LACC-treatment in HollandPTC with corresponding requirements, notes, and further work. The requirements from the Pugh's checklist, measures from the risk evaluation, and other risks from the risk evaluation are numbered and correspond to those listed in respectively Appendix D, Table 6.4, and Table 6.3. Figure 6.6 shows that for the phases Generate ITVs with Raystation, Plans imported in ARIA, and Treatment multiple requirements from the Pugh's checklist have to be considered. The requirements arising from the risk evaluation focus on the steps Generating ITVs with Raystation and Treatment planning. In general, notes and to-do-items concern logistic challenges due to the collaboration between HollandPTC and Erasmus MC and LUMC.

The next step was to translate the general workflow from Figure 6.6 into a Care Path in ARIA. Figure 6.7 visualizes the resulting Care Path, which contains the seven steps of the general workflow for HollandPTC specifically. Before the activity Tel co care coach, the patient is referred to HollandPTC through telephone, mail, or the referring system. The care coach schedules the care path and sends patient information. Consequently, the care coach informs the patient about the treatment and HollandPTC, after which the first consultation with the radiation oncologist takes place. Then, the radiation oncologist opens a Diagnosis Treatment Combination (DBC), which is used by the insurer to insure the entire care path. The care coach verifies this care path while the radiation oncologist discusses the patient positioning with radiation therapists. This will be used during the planning MR- and CT-acquisition. These images are processed, OARs are contoured, and the radiation oncologist delineates the target volume and additional OARs. Next, the radiation oncologist determines the image-guided proton therapy (IGPT) policy, including whether the patient is a mover or non-mover, and, if applicable, SIBs and other dose prescriptions. The delineations are checked by a second radiation oncologist. The next step is generating ITVs and treatment planning. Dose planning (DPL) includes creating the ITVs, a second radiation therapist and MP validating these ITVs, and making the treatment plans. The subsequent steps are the same for all cancers treated in HollandPTC. The plans have to be checked by a second radiation therapist and approved by the radiation oncologist. Additionally, the radiation oncologist reviews the plans with colleagues and any remarks on the plan or treatment specifications are noted. Then, the radiation therapist processes the treatment plan, which is also examined afterward, and a medical physicist validates the plans followed by a quality analysis (QA) process. Lastly, the treatment can be initiated. The treatment process will be discussed later in this section.

<p>Patient administrative admission</p>	<p><b>Requirements Pugh's checklist</b> PER.1.4, 3.2, 4.3</p> <p><b>Notes</b></p> <ul style="list-style-type: none"> <li>• The care coach schedules appointments</li> <li>• There is no gynaecology room in HollandPTC</li> <li>• Brachytherapy in Erasmus MC should be planned as soon as possible</li> <li>• The overall treatment time should not be more than seven weeks</li> </ul>	<p><b>From the risk evaluation</b> Measures: 4 Other risks: 27</p> <p><b>To do</b></p> <ul style="list-style-type: none"> <li>• Decide on location of appointments, especially chemotherapy and consultations</li> <li>• Add checklists to the Care Path in ARIA</li> <li>• Discuss DBCs</li> <li>• Decide whether marker implantation is necessary</li> </ul>
<p>CT-simulation</p>	<p><b>Requirements Pugh's checklist</b> PER. 1.1, 1.3, 1.4, 2.2, 3.1, 3.5, 4.3 SAF 1.1, 1.2 PRO. 1.1, 1.2</p> <p><b>Notes</b></p> <ul style="list-style-type: none"> <li>• A planning MRI-scan is preferred for each patient in HollandPTC</li> <li>• IMPT is sensitive to densities which is problematic for contrast fluid. A balance should be found between accurate delineation of blood vessels and lymph nodes. Two alternatives might be:             <ol style="list-style-type: none"> <li>1. MRI + full bladder CT w/o contrast + empty bladder CT with contrast</li> <li>2. MRI + full bladder CT without contrast + full bladder CT with contrast + empty bladder CT with delayed contrast</li> </ol> </li> <li>• Both CT-scans have a large FoV</li> <li>• Vessels are delineated in the empty bladder CT</li> <li>• Full bladder CT-scan has a large, empty bladder CT-scan has a small FoV</li> <li>• Vessels are delineated in the full bladder CT with contrast</li> </ul>	<p><b>From the risk evaluation</b> Measures: 3 Other risks: 21, 22, 29, 30</p> <p><b>To do</b></p> <ul style="list-style-type: none"> <li>• Implement a scan protocol for full and empty bladder CT-scan</li> <li>• Implement Dixon-sequence on MR-scanner</li> </ul>
<p>Structure delineation</p>	<p><b>Requirements Pugh's checklist</b> PER. 1.1, 1.4, 1.6, 2.2, 3.1 SAF 1.1, 1.2 PRO. 1.1, 1.2</p> <p><b>Notes</b></p>	<p><b>From the risk evaluation</b> Measures: 2, 6, 12 Other risks: 13, 24</p> <p><b>To do</b></p> <ul style="list-style-type: none"> <li>• Identify an automatic delineation tool like ABAS in Erasmus MC</li> <li>• Make a delineation template for radiation oncologists</li> <li>• Make a form for IGPT-settings</li> </ul>





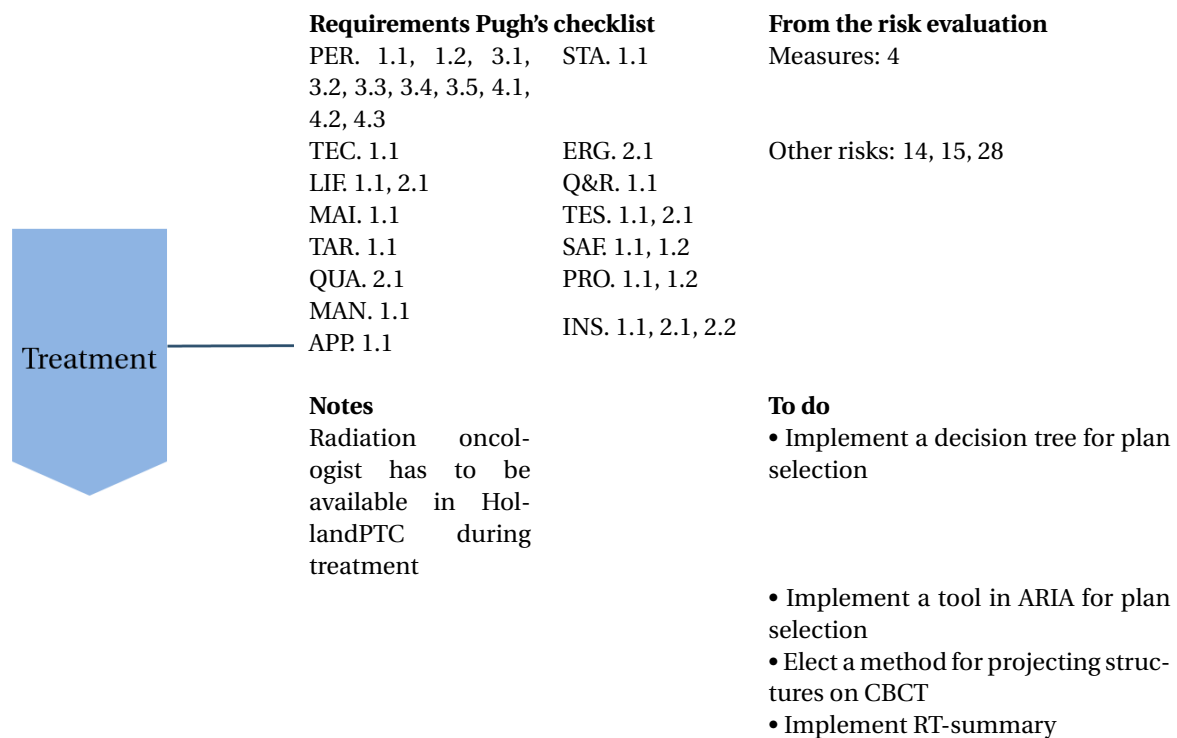


Figure 6.6: General workflow for locally advanced cervical cancer treatment in HollandPTC. Each of the seven steps includes the corresponding requirements from the Pugh's checklist, which can be found in Appendix E, and measures and other risks from the risk evaluation, which are listed in Table 6.4 and 6.3. Additionally, important notes and a to-do-list were added. *DBC*s = *diagnosis treatment combinations*, *CT* = *computed tomography*, *IMPT* = *intensity modulated proton therapy*, *MRI* = *magnetic resonance imaging*, *FoV* = *Field of View*, *ABAS* = *atlas-based automated segmentation*, *IGPT* = *image guided proton therapy*, *MP* = *medical physics*, *CBCT* = *cone beam CT*

However, the Care Path from Figure 6.7 does not include the total LACC-treatment workflow. Activities are located in Erasmus MC or LUMC as well because patients are referred from these hospitals. Brachytherapy, for instance, will be given at the academic hospitals since HollandPTC does not have the required facilities. Additionally, the presence of specialized nurses is warranted due to the possible side effects of cisplatin. Therefore, an updated workflow including activities located at the referring hospitals is proposed in Figure 6.8. Patient administrative admission is necessary for the referring hospital before referral. Additionally, the gynecology department of the referring hospital will stay in contact with the patient. It has to be decided whether marker implantation is necessary for aIMPT. If so, the first consultation with the radiation oncologist, including the marker implantation, will also take place in the referring hospital, since HollandPTC lacks the required facilities. The first consultation with the internist and the oncology nurse is likely to take place in the referring hospital as well. Figure 6.9 visualizes the treatment workflow for both HollandPTC and the referring hospital. When compared to the treatment preparation process, the treatment workflow has more uncertainties about locations due to the chemotherapy, including the contact with the nurses from internal medicine, and patient's appointments with the radiation oncologist.

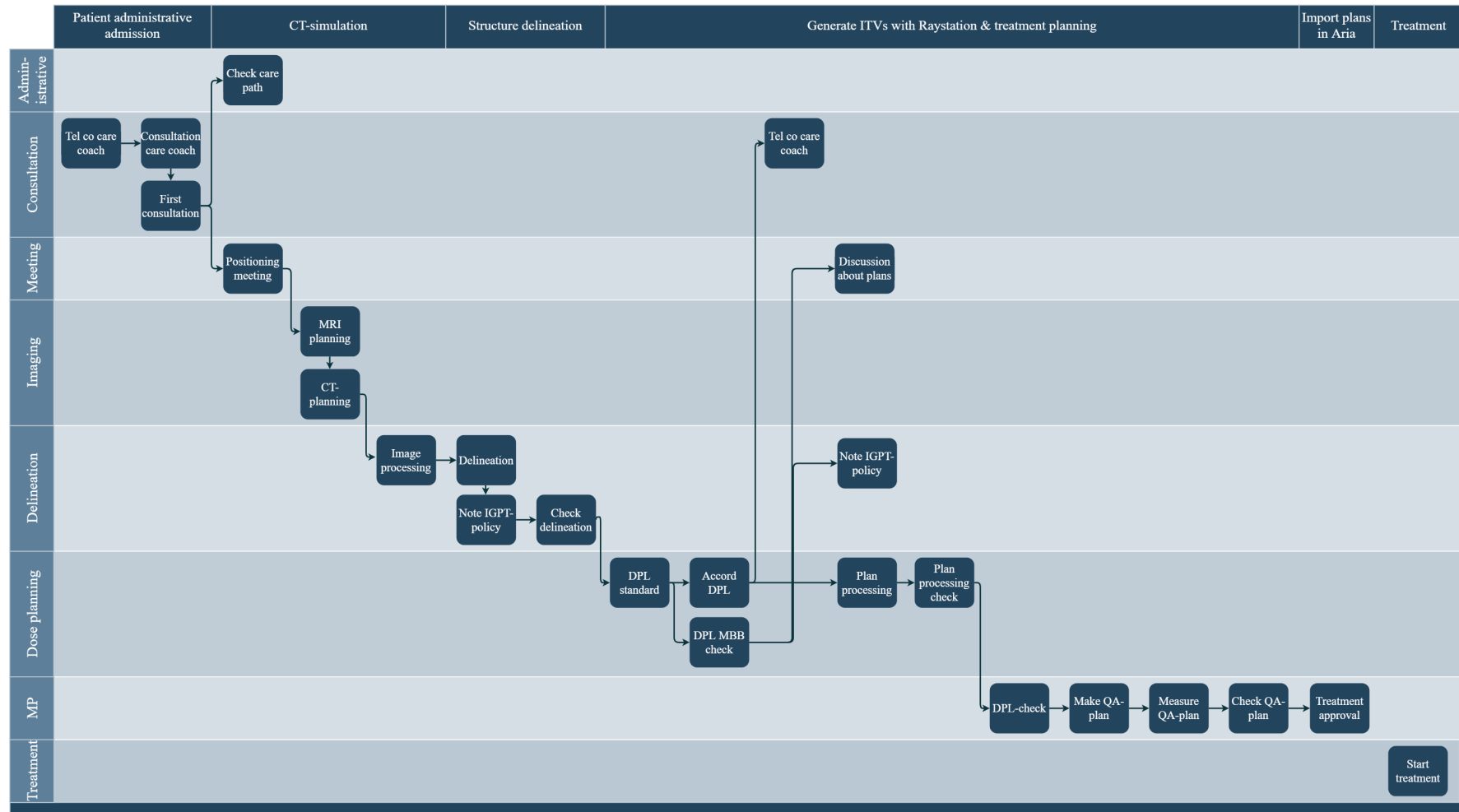


Figure 6.7: Workflow in HollandPTC until treatment, implemented in ARIA. The seven general steps are listed above the workflow. *MP* = medical physics, *Tel co* = consultation by phone, *MRI* = magnetic resonance imaging, *CT* = computed tomography, *IGPT* = image guided proton therapy, *DPL* = dose planning, *MBB* = radiation therapist, *QA* = quality analysis

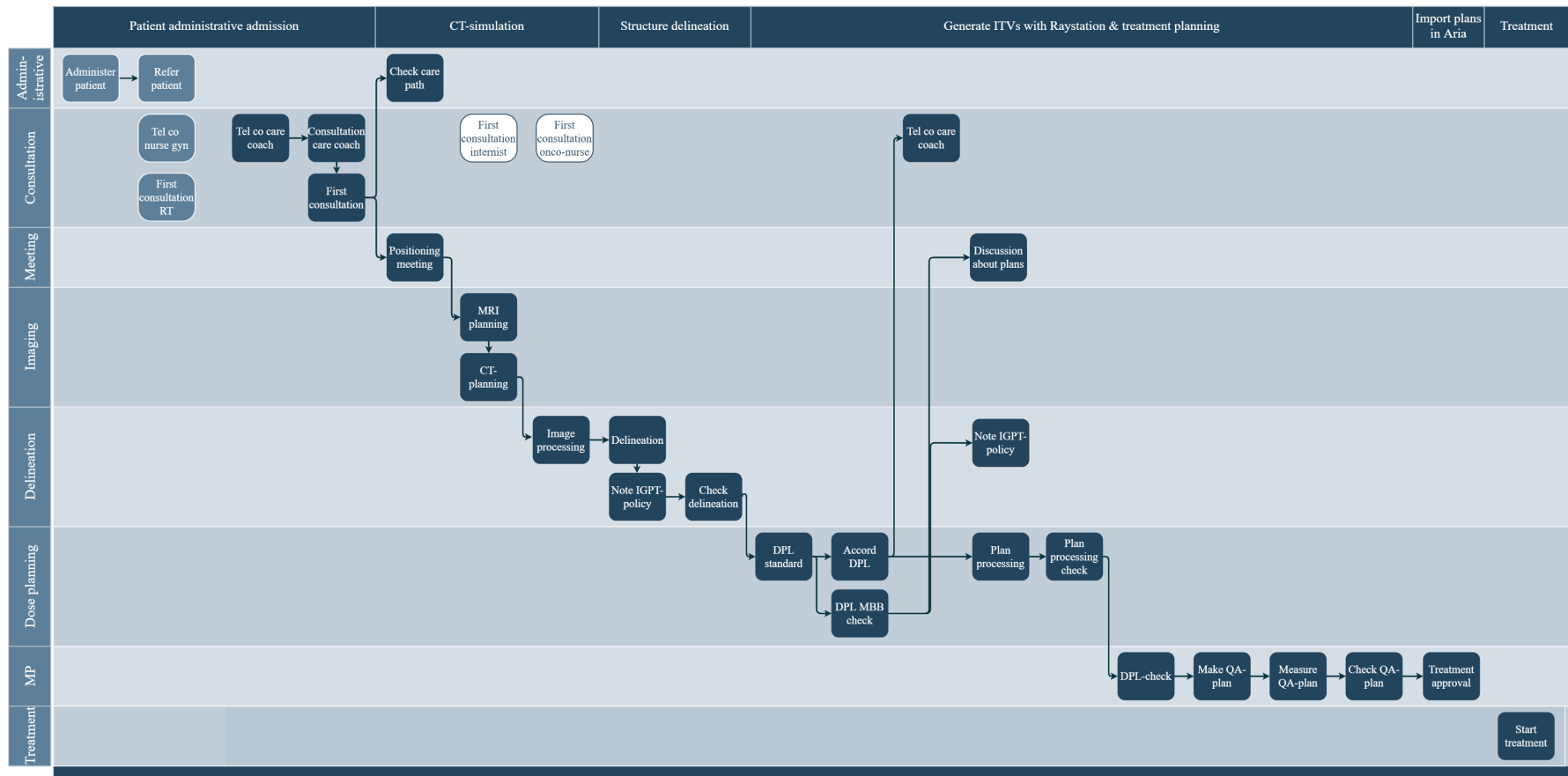


Figure 6.8: Workflow of HollandPTC until treatment, partly implemented in ARIA, including activities located at the referring hospitals. The seven general steps are listed above the workflow. Activities either take place in HollandPTC (dark blue), referring hospital (lighter blue), or yet unknown (white). *MP* = medical physics, *Tel co* = consultation by phone, *MRI* = magnetic resonance imaging, *CT* = computed tomography, *IGPT* = image guided proton therapy, *DPL* = dose planning, *MBB* = radiation therapist, *QA* = quality analysis

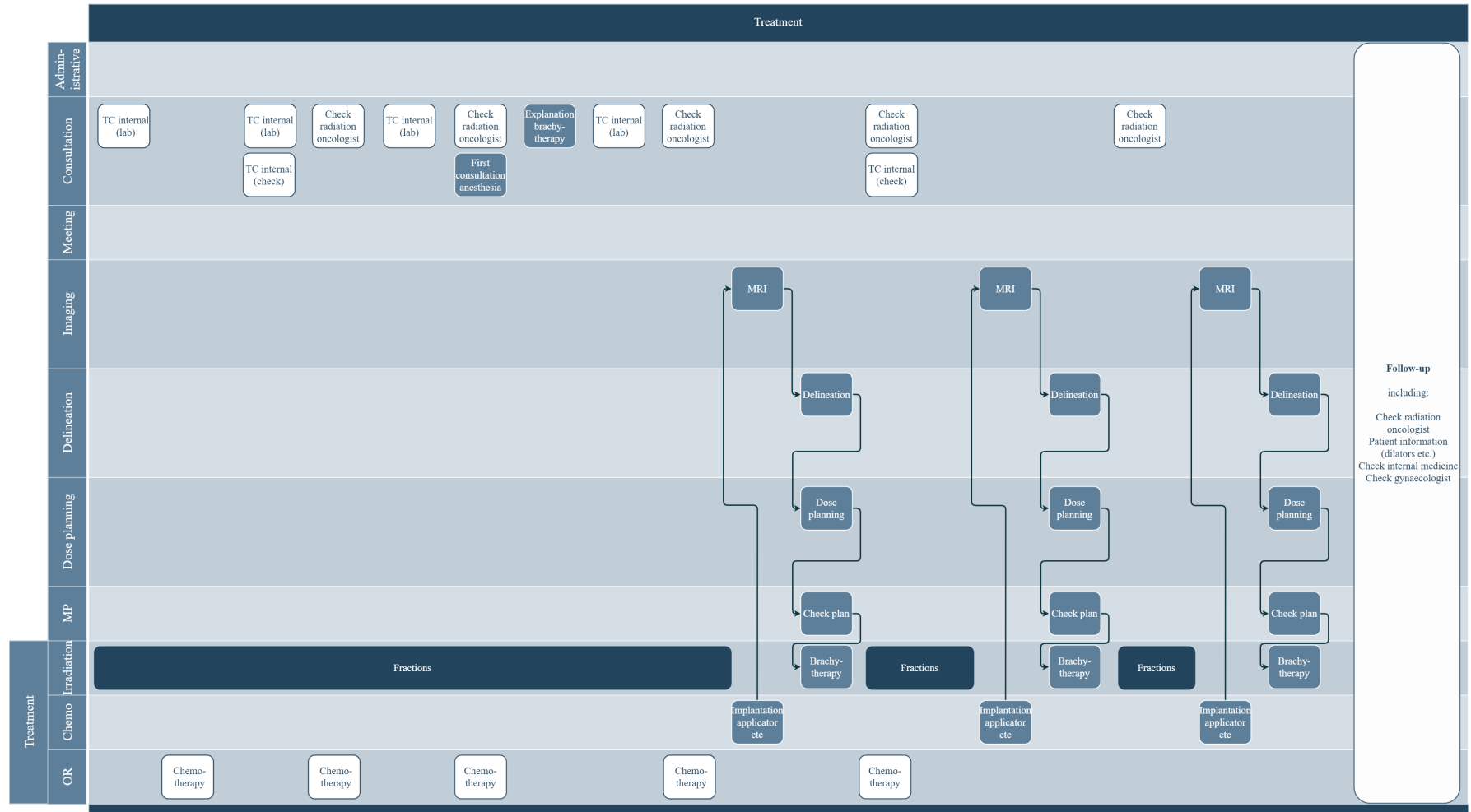


Figure 6.9: Treatment workflow of HollandPTC and referring hospitals. Activities either take place in HollandPTC (dark blue), referring hospital (lighter blue), or yet unknown (white). *MP* = medical physics, *Tel co* = consultation by phone, *MRI* = magnetic resonance imaging

### 6.4.3.2. Treatment Management process

Protocols from two medical institutes were evaluated for the implementation of the Treatment Management process for the PotD-strategy.

In the Verbeeten institute, besides the regular treatment plans, one empty plan is generated and named NPI plan. All plans except for the NPI plan have the same reference point. The following dose limits are applied in Reference Points (see Figure 6.10a):

- Total Dose Limit: summarized dose of all plans
- Daily Dose Limit / Session Dose Limit: dose per fraction of the plan with the highest planned dose per fraction
- Breakpoint: total dose of the plan with the highest total dose + 1 cGy

Then, all plans are approved. In Plan Scheduling, the NPI plan and the corresponding daily setup imaging are scheduled. Additionally, the other treatment plans are scheduled before treatment approval. Then, the scheduled plans are removed with exception of the NPI plan. Before each fraction, the CBCT is acquired whereafter the most suitable plan is selected and scheduled. However, RT Summary expects the delivered dose to be the summarized dose of all plans, but this is less as only one treatment plan is selected (see Figure 6.10b). It was unclear how the Verbeeten institute corrected this discrepancy.

In AZ Groeninge, it is protocolized that each treatment plan should have the same primary reference point by selecting the same PTV for each plan as reference point. The following dose limits are used in Reference Points (see Figure 6.11):

- Total Dose Limit: total dose of one plan
- Daily Dose Limit / Session Dose Limit: dose per fraction of one plan

Then, all three plans are approved. In Plan Scheduling, the treatment plan that is expected to occur most frequently is scheduled with the corresponding daily setup imaging. Additionally, the two other plans are scheduled before treatment approval. Then, these two plans are removed. During each fraction, the CBCT is acquired and the corresponding plan is selected and scheduled. At the end of the last fraction, RT Summary demonstrates that the delivered dose is one-third (so only one plan) of the planned dose (which were three plans). This is solved with a plan revision of all three plans. As a result, the planned dose in RT Summary is accurate and it is still visible which plan is irradiated on which day. Advantages of this approach are that only the three treatment plans are required, the total dose limit corresponds to the actual total dose limit, and RT Summary is corrected easily.

Plan	Field	Monitor Unit [MU]	Beam Dose Point Field Dose[Gy]	
20210409_1	Beam1	1214.21	0.474	
	Beam2	1254.99	0.463	
	Beam3	1313.80	0.292	
	Beam4	1033.50	0.293	
	Beam5	873.93	0.228	
	Planned Dose Per Fraction		1.750	
	<b>Planned Dose</b>		<b>43.745</b>	
20210409_2	Beam1	1838.53	0.558	
	Beam2	1915.81	0.524	
	Beam3	1658.01	0.184	
	Beam4	1522.10	0.357	
	Beam5	902.26	0.144	
	Planned Dose Per Fraction		1.766	
	<b>Planned Dose</b>		<b>44.150</b>	
Dose Corrections			0.000	
Delivered Dose from other plans			0.000	
Sum			87.895	
<b>APPROVED DOSE SUMMARY</b>				
Total Dose Limit			87.895	
Daily Dose Limit			1.766	
Session Dose Limit			1.766	
Breakpoint			1.767	
<b>Delivered Dose in Course (incl. dose corr)</b>			0.000	
<b>Remaining Planned Dose in Course</b>			87.895	
<b>Dose to be Recorded in Course</b>			<b>87.895</b>	
Dose to be Recorded from other Courses (excl...)			0.000	
<b>Total</b>			<b>87.895</b>	

(a) Example of dose limits as applied by Verbeeten institute for the PotD-workflow in ARIA. Two plans (20210409\_1 and 20210409\_2) both have five beams and the Total, Daily, and Session Dose Limit are manually filled in together with the Breakpoint.



(b) Example of when the amount of delivered dose is lower than the planned dose in RT Summary.

Figure 6.10: Examples of dose limits and RT Summary for clinical protocol from the Verbeeten institute for the PotD-workflow in ARIA.

In this thesis, the approach of AZ Groeninge was preferred, since no additional empty plan is required. Multiple treatment plans were generated for the phantom CT-scan, all with the same isocenter, number and angles of the beams, and reference point. These were exported to ARIA. However, if the total dose of one plan was filled in as the Total Dose Limit, the plans could not be approved while the Total Dose to be Recorded exceeds the Total Dose Limit, as shown in Figure 6.11. Therefore, the dose limits as proposed by the Verbeeten institute were applied, including the breakpoint. In this way, all plans could be approved and scheduled. The CBCT was assigned to one of the plans before treatment approval. After treatment approval, the scheduled fractions of the plans without the CBCT were removed.

## 6.5. Discussion

In this chapter, the clinical workflow for LACC-patients was developed and the implementation in ARIA, the oncology information system of HollandPTC, was investigated. Firstly, the current workflow in Erasmus MC was used to generate requirements with input from both the investigator and a risk evaluation with the users. A general workflow with corresponding requirements, notes, and to-do items, was designed before it was translated into a LACC-workflow for HollandPTC specifically and implemented as a Care Path in ARIA. Additionally, a LACC-workflow also considering the referring hospitals was designed. Questions remain about the location of some clinical activities, including consultations and chemotherapy. Then, steps were taken to implement the PotD-strategy for LACC-patients in ARIA's Treatment Management components Reference Points, Plan Scheduling, and RT Summary. Protocols from two other medical institutes served as an example. Their methods were tested and combined to obtain a final proposal for the three components. In this discussion section, the strengths and limitations of the used methods and future work required are discussed, followed by the conclusion.

The first strength of the method used is the combination of the Pugh's checklist and the risk analysis to generate requirements for the workflow in HollandPTC. Firstly, the Pugh's checklist provided general checkpoints that are useful to identify objectives and corresponding requirements. For instance, the objective with respect to Appearance states that using the software should feel intuitive. This goal can be obtained by designing a user interface for the script in Raystation. The acquired objectives can be used for monitoring and validation of the workflow design and implementation. However, a limitation is that these requirements are dynamic. For instance, with regards to requirement PER.2.2, there are degrees of smoothness of the workflow and the desired level might be different for oncologists and therapists. Therefore, the main goal of these requirements is to provide guidance during the workflow development process.

Secondly, the risk analysis obtained more specific requirements when compared to the Pugh's checklist while it simultaneously focused on improving the PotD-workflow in Erasmus MC. Users were actively encouraged to think about the PotD-process and improvements. Some limitations to the risk evaluation can be noted. The likelihood that each failure will persist throughout the process without being detected and corrected, i.e. the detectability, was not determined. The detectability could be from influence on the risk scores and therefore improve the identification of issues of greatest concern [150]. A risk that is less likely to be detected might have a higher priority than a risk with a high likelihood. In future hazard analyses, the


Plan	Field	Monitor Unit [MU]	Beam Dose Point Field Dose[Gy]	
20210409_1	Beam1	1214.21	0.474	
	Beam2	1254.99	0.463	
	Beam3	1313.80	0.292	
	Beam4	1033.50	0.293	
	Beam5	873.93	0.228	
	Planned Dose Per Fraction		1.750	
	<b>Planned Dose</b>		<b>43.745</b>	
20210409_2	Beam1	1838.53	0.558	
	Beam2	1915.81	0.524	
	Beam3	1658.01	0.184	
	Beam4	1522.10	0.357	
	Beam5	902.26	0.144	
	Planned Dose Per Fraction		1.766	
	<b>Planned Dose</b>		<b>44.150</b>	
Dose Corrections			0.000	
Delivered Dose from other plans			0.000	
Sum			87.895	
<b>APPROVED DOSE SUMMARY</b>				
Total Dose Limit			<b>44.150</b>	
Daily Dose Limit			1.766	
Session Dose Limit			1.766	
Breakpoint			0.000	
Delivered Dose in Course (incl. dose corr)			0.000	
Remaining Planned Dose in Course			87.895	
<b>Dose to be Recorded in Course</b>			<b>87.895</b> 	
Dose to be Recorded from other Courses (excl...)			0.000	
<b>Total</b>			<b>87.895</b>	

Figure 6.11: Example of dose limits as applied by AZ Groeninge for the PotD-workflow in ARIA. Two plans (20210409\_1 and 20210409\_2) both have five beams and the Total, Daily, and Session Dose Limit are manually filled in. The Dose to be Recorded in Course gives a warning that the Total Dose Limit is exceeded.

detectability of potential failures should be estimated. Secondly, the scoring system used for impact on time could be interpreted in different manners. As a result, the given score might be inconsistent. A consensus on rating scales is difficult to achieve. Ideally, the scoring system is discussed with participants on forehand to come to an agreement and equate interpretations. Lastly, the RISKID-system was less user-friendly than expected. The online environment replaced long, offline meetings for brainstorming and scoring and was therefore advantageous to busy clinicians. However, some tools and functions were counterintuitive and remained unclear, despite the instructions from the manual. The investigator gave feedback to the developers in order to further improve the online environment.

Another strength of this chapter is that the method used makes the workflow flexible to future changes in HollandPTC's environment and resources. For instance, HollandPTC has an in-room CT-scanner available, which could be used for daily image guidance instead of the CBCT. However, the CT-scanner is not yet implemented due to technical issues. The proposed workflow might change when the CT-scanner is in clinical use. Additionally, not all aspects of the workflow were clarified. HollandPTC is currently conducting a trial to give a small group of patients chemotherapy in HollandPTC whereas this normally would take place in the referring hospital. Outcomes of this trial might influence the chemotherapy process as proposed in this thesis. Next, LACC-treatment with proton therapy is not yet reimbursed by the health insurer. Changes in the DBCs might lead to a different workflow as well. In summary, the LACC-workflow will be and has to be subject to change. Developing workflows is an iterative process that should be repeated at certain time points or when new information is available. The list of requirements and the Care Path in ARIA can, however, be adjusted easily to facilitate workflow updates.

A limitation of ARIA was that the Treatment Management processes as applied in AZ Groeninge and Verbeeten institute could not be copied directly to HollandPTC. For instance, the override error for the Total Dose to be Recorded does not occur at AZ Groeninge. This could be due to settings and limitations implemented in the software that differ between institutions. As a result, each institution requires its own workflow development and validation.

Multiple notes and to-do's were listed in Figure 6.6. These have to be considered before implementing the workflow. The most efficient way to discuss the notes and achieve the to-do points is by organizing a meeting with experienced radiation therapists, medical physicists, and radiation oncologists from the three involved centers. Each step in the workflow can then be discussed and further developed. Guidelines and protocols should be written to give an overview of the final design and to describe each step in the process. After implementation, tests that go through the total workflow, as well as a prospective risk evaluation, should be performed for validation.

Further work is also required for the Reference Points settings. Even though the isocenter, number and angles of the beams, and the reference point were set the same for all exported treatment plans, ARIA irregularly assumed that the reference points between plans differed. As a result, the dose limitations could not be realized. The cause of this problem has not been found yet but is important for the robustness of the process and should therefore be detected.

For some of the steps in the Treatment Management process, including Prescribe Treatment and Plan Parameters, the currently used protocols are similar for each cancer. Still, these have to be evaluated for specific application for LACC-treatment and corresponding protocols have to be developed in future work. For instance, for Prescribe Treatment, the RT Prescription for LACC has to be implemented. The most appropriate tolerance table has to be determined and the use of positioning devices has to be implemented for Treatment Preparation. Similar to the Care Paths, implementation of the Treatment Management process should be followed by a validation using a test with a phantom.

In conclusion, the LACC-workflow was designed and the implementation in HollandPTC was investigated. A general workflow with corresponding requirements, notes, and to-do items was designed and consisted of similar steps as the current workflow in Erasmus MC. This workflow was translated into a Care Path for treatment preparation in ARIA, specifically for HollandPTC, and both a treatment preparation and treatment workflow considering the referring hospitals as well. Additionally, during the Treatment Management Process, dose limits and breakpoints serve as safety limits for dose delivery. A method is proposed to schedule the treatment plans and correct RT Summary. Further work should focus on the listed notes, to-do points, and uncertainties regarding locations of clinical activities to finalize the design and implementation of the Care Path. For Treatment Management, other components should be adjusted to LACC-treatment as well. Before clinical usage of the LACC-workflow in HollandPTC, it should be validated by phantom tests and a prospective risk evaluation.





# 7

## Conclusion

The aim of this thesis was to investigate the clinical implementation of aIMPT for LACC in HollandPTC, which was achieved by performing three steps.

A systematic review about the relationship between bone marrow dose and HT in LACC-patients treated with primary chemoradiation demonstrated a scarcity of studies and clinically useful prediction models for this correlation. The majority of the studies defining bone marrow as the whole pelvic bone found significant associations between bone marrow and HT, in contrast to studies evaluating lower density marrow spaces or active bone marrow. Dosimetric cut-off values for whole pelvic bone contouring were proposed. These values might be applicable in clinical practice and future studies may use whole pelvic bone contouring to develop normal tissue complication probability models.

Treatment planning for LACC was developed for HollandPTC. Uncertainties in the proton's range raise a new challenge for proton therapy when compared to photon therapy. The proposed aIMPT-strategy consisted of two parts. Firstly, a plan-of-the-day-approach with margins was developed to correct for inter- and intrafraction motion of the uterus. Secondly, robust planning was selected to account for inter- and intrafraction setup errors and uncertainties due to range calculation in the treatment planning system. Since the target volumes have different uncertainties, the balance between robustness settings and margins has to be considered before clinical implementation. Besides, the interpolation script should be specified for HollandPTC and the treatment planning strategy should be validated with a retrospective study on weekly CT-scans.

Lastly, the clinical workflow for LACC-patients was developed and the implementation in the oncology information system of HollandPTC, ARIA, was investigated. A Care Path was implemented in ARIA and an additional workflow considering the referring hospitals was designed as well. Questions remain about the location of some clinical activities. Steps were also taken to implement the plan-of-the-day-approach in ARIA's Treatment Management environment. Then, a method was proposed to schedule the multiple treatment plans and to accurately summarize the final dose. Before clinical usage of the LACC-workflow in HollandPTC, it should be validated by phantom tests and a prospective risk evaluation.

In conclusion, this thesis provides a base for the clinical implementation of aIMPT for LACC in HollandPTC. Further work should focus on finalizing and validating this clinical implementation before the initiation of PROTECT's clinical pilot study.



# Bibliography

- [1] IKNL, “Nkr cijfers.” [Online]. Available: [https://www.iknl.nl/nkr-cijfers?fs|epidemiologie\\_id=9&fs|tumor\\_id=302&fs|periode\\_id=78,79,80,81,82,83,84,85,86,87,88,89,90,91,92,93,94,95,96,97,98,99,100,101,102,103,104,105,106,107&fs|geslacht\\_id=15&fs|leeftijdsgroep\\_id=67,36,37,38,39,40,41&fs|jaren\\_na\\_diagnose\\_id=16&fs|eenheid\\_id=2&cs|type=line&cs|xAxis=periode\\_id&cs|series=leeftijdsgroep\\_id&ts|rowDimensions=periode\\_id&ts|columnDimensions=leeftijdsgroep\\_id&lang|language=nl](https://www.iknl.nl/nkr-cijfers?fs|epidemiologie_id=9&fs|tumor_id=302&fs|periode_id=78,79,80,81,82,83,84,85,86,87,88,89,90,91,92,93,94,95,96,97,98,99,100,101,102,103,104,105,106,107&fs|geslacht_id=15&fs|leeftijdsgroep_id=67,36,37,38,39,40,41&fs|jaren_na_diagnose_id=16&fs|eenheid_id=2&cs|type=line&cs|xAxis=periode_id&cs|series=leeftijdsgroep_id&ts|rowDimensions=periode_id&ts|columnDimensions=leeftijdsgroep_id&lang|language=nl)
- [2] C. J. Meijer, P. J. Snijders, and A. Brule, “Screening for cervical cancer: should we test for infection with high-risk hpv?” *Cmaj*, vol. 163, no. 5, pp. 535–538, 2000.
- [3] F. X. Bosch, M. M. Manos, N. Muñoz, M. Sherman, A. M. Jansen, J. Peto, M. H. Schiffman, V. Moreno, R. Kurman, and K. V. Shan, “Prevalence of human papillomavirus in cervical cancer: a worldwide perspective,” *JNCI: Journal of the National Cancer Institute*, vol. 87, no. 11, pp. 796–802, 1995.
- [4] N. Munoz, X. Castellsagué, A. B. de González, and L. Gissmann, “Hpv in the etiology of human cancer,” *Vaccine*, vol. 24, pp. S1–S10, 2006.
- [5] N. Muñoz, F. X. Bosch, S. De Sanjosé, R. Herrero, X. Castellsagué, K. V. Shah, P. J. Snijders, and C. J. Meijer, “Epidemiologic classification of human papillomavirus types associated with cervical cancer,” *New England journal of medicine*, vol. 348, no. 6, pp. 518–527, 2003.
- [6] E. Roura, X. Castellsagué, M. Pawlita, N. Travier, T. Waterboer, N. Margall, F. X. Bosch, S. de Sanjosé, J. Dillner, I. T. Gram, A. Tjønneland, C. Munk, V. Pala, D. Palli, K.-T. Khaw, R. V. Barnabas, K. Overvad, F. Clavel-Chapelon, M.-C. Boutron-Ruault, G. Fagherazzi, R. Kaaks, A. Lukanova, A. Steffen, A. Trichopoulou, D. Trichopoulos, E. Klinaki, R. Tumino, C. Sacerdote, S. Panico, H. B. Bueno-de Mesquita, P. H. Peeters, E. Lund, E. Weiderpass, M. L. Redondo, M.-J. Sánchez, M.-J. Tormo, A. Barricarte, N. Larrañaga, J. Ekström, M. Hortalund, D. Lindquist, N. Wareham, R. C. Travis, S. Rinaldi, M. Tommasino, S. Franceschi, and E. Riboli, “Smoking as a major risk factor for cervical cancer and pre-cancer: Results from the epic cohort,” *International Journal of Cancer*, vol. 135, no. 2, pp. 453–466, 2014. [Online]. Available: <https://onlinelibrary.wiley.com/doi/abs/10.1002/ijc.28666>
- [7] E. Roura, N. Travier, T. Waterboer, S. de Sanjosé, F. X. Bosch, M. Pawlita, V. Pala, E. Weiderpass, N. Margall, J. Dillner *et al.*, “The influence of hormonal factors on the risk of developing cervical cancer and pre-cancer: results from the epic cohort,” *PLoS One*, vol. 11, no. 1, p. e0147029, 2016.
- [8] S. E. Waggoner, “Cervical cancer,” *The Lancet*, vol. 361, no. 9376, pp. 2217–2225, 2003.
- [9] C. Marth, F. Landoni, S. Mahner, M. McCormack, A. Gonzalez-Martin, N. Colombo, and E. G. Committee, “Cervical cancer: Esmo clinical practice guidelines for diagnosis, treatment and follow-up,” *Annals of Oncology*, vol. 28, no. suppl\_4, pp. iv72–iv83, 2017.
- [10] *Cervixcarcinoom, landelijke richtlijn*, Commissie Richtlijnen Gynaecologische Oncologie Std., Mar. 2012. [Online]. Available: [https://richtlijndatabase.nl/richtlijn/cervixcarcinoom/cervixcarcinoom\\_-\\_startpagina.html](https://richtlijndatabase.nl/richtlijn/cervixcarcinoom/cervixcarcinoom_-_startpagina.html)
- [11] Kanker.nl, “Informatie over de baarmoederhals,” 2020. [Online]. Available: <https://www.kanker.nl/kankersoorten/baarmoederhalskanker/algemeen/informatie-over-de-baarmoederhals>
- [12] D. Parkin, S. Whelan, J. Ferlay, L. Teppo, and D. Thomas, “Cancer incidence in five continents, vol. viii. Lyon: International agency for research in cancer; 2002,” *IARC Scient. Publ*, no. 155.
- [13] IKNL, “Cin, ais en vain - classificatie cin,” 2015. [Online]. Available: [https://richtlijndatabase.nl/richtlijn/cin\\_ais\\_en\\_vain/pathologie/classificatie\\_cin.html](https://richtlijndatabase.nl/richtlijn/cin_ais_en_vain/pathologie/classificatie_cin.html)

- [14] P. J. Snijders, R. D. Steenbergen, D. A. Heideman, and C. J. Meijer, "Hpv-mediated cervical carcinogenesis: concepts and clinical implications," *The Journal of Pathology: A Journal of the Pathological Society of Great Britain and Ireland*, vol. 208, no. 2, pp. 152–164, 2006.
- [15] N. H. Genootschap, "Nhg-praktijkhandleiding baarmoederhalskanker bevolkingsonderzoek en diagnostiek," *Nederlands Huisartsen Genootschap*, 2016.
- [16] F. X. Bosch, T. R. Broker, D. Forman, A.-B. Moscicki, M. L. Gillison, J. Doorbar, P. L. Stern, M. Stanley, M. Arbyn, M. Poljak *et al.*, "Comprehensive control of human papillomavirus infections and related diseases," *Vaccine*, vol. 31, pp. H1–H31, 2013.
- [17] V. M. Coupé, H. de Melker, P. J. Snijders, C. J. Meijer, and J. Berkhof, "How to screen for cervical cancer after hpv16/18 vaccination in the netherlands," *Vaccine*, vol. 27, no. 37, pp. 5111–5119, 2009.
- [18] Cervivor, "Hpv and cervical cancer."
- [19] G. Y. Ho, M. H. Einstein, S. L. Romney, A. S. Kadish, M. Abadi, M. Mikhail, J. Basu, B. Thyssen, L. Reimers, P. R. Palan *et al.*, "Risk factors for persistent cervical intraepithelial neoplasia grades 1 and 2 managed by watchful waiting," *Journal of lower genital tract disease*, vol. 15, no. 4, p. 268, 2011.
- [20] *Cervicale intra-epitheliale neoplasie (CIN), richtlijn*, Nederlandse Vereniging van Obstetrie en Gynaecologie Std., Nov. 2015. [Online]. Available: <https://www.oncoline.nl/cin-ais-en-vain>
- [21] K. L. Moore, A. M. Agur, A. F. Dalley *et al.*, "Essential clinical anatomy," 2015.
- [22] J. D. Brierley, M. K. Gospodarowicz, and C. Wittekind, *TNM classification of malignant tumours*. John Wiley & Sons, 2017.
- [23] N. Bhatla, J. Berek, M. Cuello, L. Denny, S. Grenman, K. Karunaratne *et al.*, "New revised figo staging of cervical cancer (2018). abstract s020. 2," in *FIGO XXII World Congress of Gynecology and Obstetrics. Rio de Janeiro, Brazil*, 2018, pp. 22–36.
- [24] I.-M. Jürgenliemk-Schulz, S. Beriwal, A. A. de Leeuw, J. C. Lindegaard, C. N. Nomden, R. Pötter, K. Tanderup, A. N. Viswanathan, and B. Erickson, "Management of nodal disease in advanced cervical cancer," in *Seminars in Radiation Oncology*, vol. 29, no. 2. Elsevier, 2019, pp. 158–165.
- [25] W. Small Jr, N. J. Tarbell, and M. Yao, *Clinical Radiation Oncology: Indications, Techniques, and Results*. John Wiley & Sons, 2017.
- [26] H. Kaur, P. M. Silverman, R. B. Iyer, C. F. Verschraegen, P. J. Eifel, and C. Charnsangavej, "Diagnosis, staging, and surveillance of cervical carcinoma," *American Journal of Roentgenology*, vol. 180, no. 6, pp. 1621–1631, 2003.
- [27] R. Pötter, K. Tanderup, C. Kirisits, A. de Leeuw, K. Kirchheiner, R. Nout, L. T. Tan, C. Haie-Meder, U. Mahantshetty, B. Segedin *et al.*, "The embrace ii study: The outcome and prospect of two decades of evolution within the gec-estro gyn working group and the embrace studies," *Clinical and translational radiation oncology*, vol. 9, pp. 48–60, 2018.
- [28] J. M. Straughn and C. Yashar, "Management of locally advanced cervical cancer," 2021. [Online]. Available: [https://www.uptodate.com/contents/management-of-locally-advanced-cervical-cancer?sectionName=DEFINITION%20OF%20LOCALLY%20ADVANCED-STAGE%20CERVICAL%20CANCER&topicRef=3244&anchor=H2&source=see\\_link#H2](https://www.uptodate.com/contents/management-of-locally-advanced-cervical-cancer?sectionName=DEFINITION%20OF%20LOCALLY%20ADVANCED-STAGE%20CERVICAL%20CANCER&topicRef=3244&anchor=H2&source=see_link#H2)
- [29] E. study, "Gec esto gyn working group and network." [Online]. Available: <https://www.embracestudy.dk/Public/Default.aspx?main=1&sub=5&embrace=embrace>
- [30] T. Girinsky, A. Rey, B. Roche, C. Haie, A. Gerbaulet, H. Randrianarivello, and D. Chassagne, "Overall treatment time in advanced cervical carcinomas: a critical parameter in treatment outcome," *International Journal of Radiation Oncology\* Biology\* Physics*, vol. 27, no. 5, pp. 1051–1056, 1993.
- [31] C. A. Perez, P. W. Grigsby, H. Castro-Vita, and M. A. Lockett, "Carcinoma of the uterine cervix. i. impact of prolongation of overall treatment time and timing of brachytherapy on outcome of radiation therapy," *International Journal of Radiation Oncology\* Biology\* Physics*, vol. 32, no. 5, pp. 1275–1288, 1995.

- [32] K. Tanderup, L. U. Fokdal, A. Sturdza, C. Haie-Meder, R. Mazon, E. Van Limbergen, I. Jürgenliemk-Schulz, P. Petric, P. Hoskin, W. Dörr *et al.*, “Effect of tumor dose, volume and overall treatment time on local control after radiochemotherapy including mri guided brachytherapy of locally advanced cervical cancer,” *Radiotherapy and oncology*, vol. 120, no. 3, pp. 441–446, 2016.
- [33] H. Lukka, H. Hirte, A. Fyles, G. Thomas, L. Elit, M. Johnston, M. F. K. Fung, and G. Browman, “Concurrent cisplatin-based chemotherapy plus radiotherapy for cervical cancer—a meta-analysis,” *Clinical Oncology*, vol. 14, no. 3, pp. 203–212, 2002.
- [34] “Cisplatine.” [Online]. Available: <https://www.farmacotherapeutischkompas.nl/bladeren/preparaatteksten/c/cisplatine#contra-indicaties>
- [35] E. Burchardt and A. Roszak, “Hyperthermia in cervical cancer—current status,” *Reports of Practical Oncology & Radiotherapy*, vol. 23, no. 6, pp. 595–603, 2018.
- [36] A. Szasz, N. Szasz, and O. Szasz, “Hyperthermia results and challenges,” in *Oncothermia: Principles and Practices*. Springer, 2010, pp. 17–88.
- [37] B. Hildebrandt, P. Wust, O. Ahlers, A. Dieing, G. Sreenivasa, T. Kerner, R. Felix, and H. Riess, “The cellular and molecular basis of hyperthermia,” *Critical reviews in oncology/hematology*, vol. 43, no. 1, pp. 33–56, 2002.
- [38] R. Baskar, K. A. Lee, R. Yeo, and K.-W. Yeoh, “Cancer and radiation therapy: current advances and future directions,” *International journal of medical sciences*, vol. 9, no. 3, p. 193, 2012.
- [39] M. C. Joiner and A. Van der Kogel, *Basic clinical radiobiology fourth edition*. CRC press, 2009.
- [40] R. Ahmad, M. S. Hoogeman, S. Quint, J. W. Mens, I. de Pree, and B. J. Heijmen, “Inter-fraction bladder filling variations and time trends for cervical cancer patients assessed with a portable 3-dimensional ultrasound bladder scanner,” *Radiotherapy and oncology*, vol. 89, no. 2, pp. 172–179, 2008.
- [41] A. Taylor and M. E. Powell, “An assessment of interfractional uterine and cervical motion: implications for radiotherapy target volume definition in gynaecological cancer,” *Radiotherapy and Oncology*, vol. 88, no. 2, pp. 250–257, 2008.
- [42] A. Buchali, S. Koswig, S. Dinges, P. Rosenthal, J. Salk, G. Lackner, D. BoÈhmer, L. Schlenger, and V. Budach, “Impact of the filling status of the bladder and rectum on their integral dose distribution and the movement of the uterus in the treatment planning of gynaecological cancer,” *Radiotherapy and oncology*, vol. 52, no. 1, pp. 29–34, 1999.
- [43] R. Ahmad, M. S. Hoogeman, M. Bondar, V. Dhawtal, S. Quint, I. De Pree, J. W. Mens, and B. J. Heijmen, “Increasing treatment accuracy for cervical cancer patients using correlations between bladder-filling change and cervix–uterus displacements: proof of principle,” *Radiotherapy and oncology*, vol. 98, no. 3, pp. 340–346, 2011.
- [44] L. Bondar, M. Hoogeman, J. W. Mens, G. Dhawtal, I. De Pree, R. Ahmad, S. Quint, and B. Heijmen, “Toward an individualized target motion management for imrt of cervical cancer based on model-predicted cervix–uterus shape and position,” *Radiotherapy and Oncology*, vol. 99, no. 2, pp. 240–245, 2011.
- [45] M. t. Kley and S. Sodjo, “Lab-gyn-ct scan- en intekenprotocol cervix potd patienten,” Jun. 2020.
- [46] L. Bondar, M. S. Hoogeman, E. M. Vásquez Osorio, and B. J. Heijmen, “A symmetric nonrigid registration method to handle large organ deformations in cervical cancer patients,” *Medical physics*, vol. 37, no. 7Part1, pp. 3760–3772, 2010.
- [47] S. T. Heijkoop, T. R. Langerak, S. Quint, L. Bondar, J. W. M. Mens, B. J. Heijmen, and M. S. Hoogeman, “Clinical implementation of an online adaptive plan-of-the-day protocol for nonrigid motion management in locally advanced cervical cancer imrt,” *International Journal of Radiation Oncology\* Biology\* Physics*, vol. 90, no. 3, pp. 673–679, 2014.

- [48] T. H. Kim, E. K. Chie, D. Y. Kim, S. Y. Park, K. H. Cho, K. H. Jung, Y. H. Kim, D. K. Sohn, S.-y. Jeong, and J.-G. Park, "Comparison of the belly board device method and the distended bladder method for reducing irradiated small bowel volumes in preoperative radiotherapy of rectal cancer patients," *International Journal of Radiation Oncology\* Biology\* Physics*, vol. 62, no. 3, pp. 769–775, 2005.
- [49] S. Quint, J. Penninkhof, and S. Sodjo, "Lab-alg-tst behandelng cervix/blaa potd," Oct. 2020.
- [50] O. Cho, M. Chun, S.-J. Chang, Y.-T. Oh, and O. K. Noh, "Prognostic value of severe lymphopenia during pelvic concurrent chemoradiotherapy in cervical cancer," *Anticancer research*, vol. 36, no. 7, pp. 3541–3547, 2016.
- [51] K. Otto, "Volumetric modulated arc therapy: Imrt in a single gantry arc," *Medical physics*, vol. 35, no. 1, pp. 310–317, 2008.
- [52] M. Bondar, M. Hoogeman, J. Mens, S. Quint, R. Ahmad, G. Dhawtal, and B. Heijmen, "Individualized nonadaptive and online-adaptive intensity-modulated radiotherapy treatment strategies for cervical cancer patients based on pretreatment acquired variable bladder filling computed tomography scans," *International Journal of Radiation Oncology\* Biology\* Physics*, vol. 83, no. 5, pp. 1617–1623, 2012.
- [53] A. J. van de Schoot, P. de Boer, K. F. Crama, J. Visser, L. J. Stalpers, C. R. Rasch, and A. Bel, "Dosimetric advantages of proton therapy compared with photon therapy using an adaptive strategy in cervical cancer," *Acta Oncologica*, vol. 55, no. 7, pp. 892–899, 2016.
- [54] E. M. Gort, J. C. Beukema, W. Matysiak, N. M. Sijtsema, S. Aluwini, J. A. Langendijk, S. Both, and C. L. Brouwer, "Inter-fraction motion robustness and organ sparing potential of proton therapy for cervical cancer," *Radiotherapy and Oncology*, vol. 154, pp. 194–200, 2020.
- [55] M. D. Hasselle, B. S. Rose, J. D. Kochanski, S. K. Nath, R. Bafana, C. M. Yashar, Y. Hasan, J. C. Roeske, A. J. Mundt, and L. K. Mell, "Clinical outcomes of intensity-modulated pelvic radiation therapy for carcinoma of the cervix," *International Journal of Radiation Oncology\* Biology\* Physics*, vol. 80, no. 5, pp. 1436–1445, 2011.
- [56] N. Horeweg, C. L. Creutzberg, E. C. Rijkmans, M. S. Laman, L. A. Velema, V. L. Coen, T. C. Stam, E. M. Kerkhof, J. R. Kroep, C. D. de Kroon *et al.*, "Efficacy and toxicity of chemoradiation with image-guided adaptive brachytherapy for locally advanced cervical cancer," *International Journal of Gynecologic Cancer*, vol. 29, no. 2, 2019.
- [57] S. Heijkoop, R. Nout, S. Quint, J. Mens, B. Heijmen, and M. Hoogeman, "Dynamics of patient reported quality of life and symptoms in the acute phase of online adaptive external beam radiation therapy for locally advanced cervical cancer," *Gynecologic oncology*, vol. 147, no. 2, pp. 439–449, 2017.
- [58] K. Kirchheiner, R. A. Nout, A. Czajka-Pepl, E. Ponocny-Seliger, A. E. Sturdza, J. C. Dimopoulos, W. Dörr, and R. Pötter, "Health related quality of life and patient reported symptoms before and during definitive radio (chemo) therapy using image-guided adaptive brachytherapy for locally advanced cervical cancer and early recovery—a mono-institutional prospective study," *Gynecologic oncology*, vol. 136, no. 3, pp. 415–423, 2015.
- [59] J. Huang, F. Gu, T. Ji, J. Zhao, and G. Li, "Pelvic bone marrow sparing intensity modulated radiotherapy reduces the incidence of the hematologic toxicity of patients with cervical cancer receiving concurrent chemoradiotherapy: a single-center prospective randomized controlled trial," *Radiat Oncol*, vol. 15, no. 1, 2020. [Online]. Available: <https://www.embase.com/search/results?subaction=viewrecord&id=L632504388&from=export>
- [60] N. R. Abu-Rustum, S. Lee, A. Correa, and L. S. Massad, "Compliance with and acute hematologic toxic effects of chemoradiation in indigent women with cervical cancer," *Gynecologic oncology*, vol. 81, no. 1, pp. 88–91, 2001.
- [61] A. Dueñas-González, L. Cetina-Perez, C. Lopez-Graniel, A. Gonzalez-Enciso, E. Gómez-Gonzalez, L. Rivera-Rubi, G. Montalvo-Esquivel, D. Muñoz-Gonzalez, J. Robles-Flores, E. Vazquez-Govea *et al.*, "Pathologic response and toxicity assessment of chemoradiotherapy with cisplatin versus cisplatin plus gemcitabine in cervical cancer: a randomized phase ii study," *International Journal of Radiation Oncology\* Biology\* Physics*, vol. 61, no. 3, pp. 817–823, 2005.

- [62] W. F. Boron and E. L. Boulpaep, *Medical Physiology, 2e Updated Edition E-Book*. Elsevier health sciences, 2012.
- [63] L. K. Mell, J. D. Kochanski, J. C. Roeske, J. J. Haslam, N. Mehta, S. D. Yamada, J. A. Hurteau, Y. C. Collins, E. Lengyel, and A. J. Mundt, "Dosimetric predictors of acute hematologic toxicity in cervical cancer patients treated with concurrent cisplatin and intensity-modulated pelvic radiotherapy," *International Journal of Radiation Oncology\* Biology\* Physics*, vol. 66, no. 5, pp. 1356–1365, 2006.
- [64] "Heavy charged particles for cancer radiation therapy." [Online]. Available: <https://player.slideplayer.com/16/5078166/#>
- [65] W. D. Newhauser and R. Zhang, "The physics of proton therapy," *Physics in Medicine & Biology*, vol. 60, no. 8, p. R155, 2015.
- [66] T. Pawlicki, D. J. Scanderbeg, and G. Starkschall, *Hendee's radiation therapy physics*. John Wiley & Sons, 2016.
- [67] M. Engelsman, M. Schwarz, and L. Dong, "Physics controversies in proton therapy," in *Seminars in radiation oncology*, vol. 23, no. 2. Elsevier, 2013, pp. 88–96.
- [68] M. A. Vyfhuis, N. Onyeuku, T. Diwanji, S. Mossahebi, N. P. Amin, S. N. Badiyan, P. Mohindra, and C. B. Simone, "Advances in proton therapy in lung cancer," *Therapeutic advances in respiratory disease*, vol. 12, p. 1753466618783878, 2018.
- [69] S. McGowan, N. Burnet, and A. Lomax, "Treatment planning optimisation in proton therapy," *The British journal of radiology*, vol. 86, no. 1021, pp. 20 120 288–20 120 288, 2013.
- [70] H. Kooy and C. Grassberger, "Intensity modulated proton therapy," *The British journal of radiology*, vol. 88, no. 1051, p. 20150195, 2015.
- [71] F. M. Khan, J. P. Gibbons, and P. W. Sperduto, *Khan's treatment planning in radiation oncology*. Lippincott Williams & Wilkins, 2016.
- [72] E. Rijkmans, R. Nout, I. Rutten, M. Ketelaars, K. Neelis, M. Laman, V. Coen, K. Gaarenstroom, J. Kroep, and C. Creutzberg, "Improved survival of patients with cervical cancer treated with image-guided brachytherapy compared with conventional brachytherapy," *Gynecologic oncology*, vol. 135, no. 2, pp. 231–238, 2014.
- [73] C. N. Nomden, A. A. de Leeuw, M. A. Moerland, J. M. Roesink, R. J. Tersteeg, and I. M. Jürgenliemk-Schulz, "Clinical use of the utrecht applicator for combined intracavitary/interstitial brachytherapy treatment in locally advanced cervical cancer," *International Journal of Radiation Oncology\* Biology\* Physics*, vol. 82, no. 4, pp. 1424–1430, 2012.
- [74] E. Dinges, N. Felderman, S. McGuire, B. Gross, S. Bhatia, S. Mott, J. Buatti, and D. Wang, "Bone marrow sparing in intensity modulated proton therapy for cervical cancer: efficacy and robustness under range and setup uncertainties," *Radiotherapy and Oncology*, vol. 115, no. 3, pp. 373–378, 2015.
- [75] W. Y. Song, S. N. Huh, Y. Liang, G. White, R. C. Nichols, W. T. Watkins, A. J. Mundt, and L. K. Mell, "Dosimetric comparison study between intensity modulated radiation therapy and three-dimensional conformal proton therapy for pelvic bone marrow sparing in the treatment of cervical cancer," *Journal of applied clinical medical physics*, vol. 11, no. 4, pp. 83–92, 2010.
- [76] S. G. Moore and K. L. Dawson, "Red and yellow marrow in the femur: age-related changes in appearance at mr imaging," *Radiology*, vol. 175, no. 1, pp. 219–223, 1990.
- [77] M. Cristy, "Active bone marrow distribution as a function of age in humans," *Physics in Medicine & Biology*, vol. 26, no. 3, p. 389, 1981.
- [78] L. Shao, Y. Luo, and D. Zhou, "Hematopoietic stem cell injury induced by ionizing radiation," *Antioxidants & redox signaling*, vol. 20, no. 9, pp. 1447–1462, 2014.



- [79] J. M. Kirwan, P. Symonds, J. A. Green, J. Tierney, M. Collingwood, and C. J. Williams, "A systematic review of acute and late toxicity of concomitant chemoradiation for cervical cancer," *Radiotherapy and Oncology*, vol. 68, no. 3, pp. 217–226, 2003.
- [80] C. Lei, S. Ma, J. A. Manni Huang, B. Liang, J. Dai, and L. Wu, "Long-term survival and late toxicity associated with pelvic intensity modulated radiation therapy (imrt) for cervical cancer involving ct-based positive lymph nodes," *Frontiers in oncology*, vol. 9, 2019.
- [81] H. Van Meir, R. Nout, M. Welters, N. Loof, M. De Kam, J. Van Ham, S. Samuels, G. Kenter, A. Cohen, C. Melief *et al.*, "Impact of (chemo) radiotherapy on immune cell composition and function in cervical cancer patients," *Oncoimmunology*, vol. 6, no. 2, p. e1267095, 2017.
- [82] S. M. McGuire, S. K. Bhatia, W. Sun, G. M. Jacobson, Y. Menda, L. L. Ponto, B. J. Smith, B. A. Gross, J. E. Bayouth, J. J. Sunderland *et al.*, "Using [18f] fluorothymidine imaged with positron emission tomography to quantify and reduce hematologic toxicity due to chemoradiation therapy for pelvic cancer patients," *International Journal of Radiation Oncology\* Biology\* Physics*, vol. 96, no. 1, pp. 228–239, 2016.
- [83] S. G. Ellsworth, "Field size effects on the risk and severity of treatment-induced lymphopenia in patients undergoing radiation therapy for solid tumors," *Advances in radiation oncology*, vol. 3, no. 4, pp. 512–519, 2018.
- [84] A. H. Klopp, J. Moughan, L. Portelance, B. E. Miller, M. R. Salehpour, E. Hildebrandt, J. Nuanjing, D. D'Souza, L. Souhami, W. Small Jr, R. Gaur, and A. Jhingran, "Hematologic toxicity in rtog 0418: A phase 2 study of postoperative imrt for gynecologic cancer," *Int J Radiat Oncol Biol Phys*, vol. 86, no. 1, pp. 83–90, 2013. [Online]. Available: <https://www.embase.com/search/results?subaction=viewrecord&id=L368700339&from=export>
- [85] Y. Cheng, Y. Ma, J. Zheng, H. Deng, X. Wang, Y. Li, X. Pang, H. Chen, F. He, L. Wang *et al.*, "Impact of chemotherapy regimens on normal tissue complication probability models of acute hematologic toxicity in rectal cancer patients receiving intensity modulated radiation therapy with concurrent chemotherapy from a prospective phase iii clinical trial," *Frontiers in oncology*, vol. 9, p. 244, 2019.
- [86] S. S. Noticewala, N. Li, C. W. Williamson, C. K. Hoh, H. Shen, M. T. McHale, C. C. Saenz, J. Einck, S. Plaxe, F. Vaida *et al.*, "Longitudinal changes in active bone marrow for cervical cancer patients treated with concurrent chemoradiation therapy," *International Journal of Radiation Oncology\* Biology\* Physics*, vol. 97, no. 4, pp. 797–805, 2017.
- [87] J. G. Bazan, G. Luxton, M. M. Kozak, E. M. Anderson, S. L. Hancock, D. S. Kapp, E. A. Kidd, A. C. Koong, and D. T. Chang, "Impact of chemotherapy on normal tissue complication probability models of acute hematologic toxicity in patients receiving pelvic intensity modulated radiation therapy," *International Journal of Radiation Oncology\* Biology\* Physics*, vol. 87, no. 5, pp. 983–991, 2013.
- [88] D. Cibula, R. Pötter, F. Planchamp, E. Avall-Lundqvist, D. Fischerova, C. Haie-Meder, C. Köhler, F. Landoni, S. Lax, J. C. Lindegaard *et al.*, "The european society of gynaecological oncology/european society for radiotherapy and oncology/european society of pathology guidelines for the management of patients with cervical cancer," *Virchows Archiv*, vol. 472, no. 6, pp. 919–936, 2018.
- [89] O. Elicin, S. Callaway, J. O. Prior, J. Bourhis, M. Ozsahin, and F. G. Herrera, "[18f]fdg-pet standard uptake value as a metabolic predictor of bone marrow response to radiation: Impact on acute and late hematological toxicity in cervical cancer patients treated with chemoradiation therapy," *Int J Radiat Oncol Biol Phys*, vol. 90, no. 5, pp. 1099–1107, 2014. [Online]. Available: <https://www.embase.com/search/results?subaction=viewrecord&id=L600299969&from=export>
- [90] E. Dinges, N. Felderman, S. McGuire, B. Gross, S. Bhatia, S. Mott, J. Buatti, and D. Wang, "Bone marrow sparing in intensity modulated proton therapy for cervical cancer: Efficacy and robustness under range and setup uncertainties," *Radiother Oncol*, vol. 115, no. 3, pp. 373–378, 2015. [Online]. Available: <https://www.embase.com/search/results?subaction=viewrecord&id=L604349888&from=export>

- [91] W. Y. Song, S. N. Huh, Y. Liang, G. White, R. C. Nichols, W. T. Watkins, A. J. Mundt, and L. K. Mell, "Dosimetric comparison study between intensity modulated radiation therapy and three-dimensional conformal proton therapy for pelvic bone marrow sparing in the treatment of cervical cancer," *J Appl Clin Med Phys*, vol. 11, no. 4, p. 3255, 2010. [Online]. Available: <https://www.embase.com/search/results?subaction=viewrecord&id=L360274673&from=export>
- [92] E. M. Gort, J. C. Beukema, W. Matysiak, N. M. Sijtsema, S. Aluwini, J. A. Langendijk, S. Both, and C. L. Brouwer, "Inter-fraction motion robustness and organ sparing potential of proton therapy for cervical cancer," *Radiotherapy and Oncology*, vol. 154, pp. 194–200, 2021.
- [93] Y. Liang, K. Messer, B. S. Rose, J. H. Lewis, S. B. Jiang, C. M. Yashar, A. J. Mundt, and L. K. Mell, "Impact of bone marrow radiation dose on acute hematologic toxicity in cervical cancer: Principal component analysis on high dimensional data," *Int J Radiat Oncol Biol Phys*, vol. 78, no. 3, pp. 912–919, 2010. [Online]. Available: <https://www.embase.com/search/results?subaction=viewrecord&id=L50911864&from=export>
- [94] G. S. Collins, J. B. Reitsma, D. G. Altman, and K. G. Moons, "Transparent reporting of a multivariable prediction model for individual prognosis or diagnosis (tripod) the tripod statement," *Circulation*, vol. 131, no. 2, pp. 211–219, 2015.
- [95] N. P. Brodin, R. Kabarriti, M. K. Garg, C. Guha, and W. A. Tomé, "Systematic review of normal tissue complication models relevant to standard fractionation radiation therapy of the head and neck region published after the quantec reports," *International Journal of Radiation Oncology\* Biology\* Physics*, vol. 100, no. 2, pp. 391–407, 2018.
- [96] B. S. Rose, B. Aydogan, Y. Liang, M. Yeginer, M. D. Hasselle, V. Dandekar, R. Bafana, C. M. Yashar, A. J. Mundt, J. C. Roeske, and L. K. Mell, "Normal tissue complication probability modeling of acute hematologic toxicity in cervical cancer patients treated with chemoradiotherapy," *Int J Radiat Oncol Biol Phys*, vol. 79, no. 3, pp. 800–807, 2011. [Online]. Available: <https://www.embase.com/search/results?subaction=viewrecord&id=L50876345&from=export>
- [97] H. Zhu, K. Zakeri, F. Vaida, R. Carmona, K. K. Dadachanji, R. Bair, B. Aydogan, Y. Hasan, C. M. Yashar, and L. K. Mell, "Longitudinal study of acute haematologic toxicity in cervical cancer patients treated with chemoradiotherapy," *J Med Imaging Radiat Oncol*, vol. 59, no. 3, pp. 386–393, 2015. [Online]. Available: <https://www.embase.com/search/results?subaction=viewrecord&id=L603512524&from=export>
- [98] S. Lewis, S. Chopra, P. Naga, S. Pant, E. Dandpani, N. Bharadwaj, U. Mahantshetty, R. Engineer, J. Swamidas, J. Ghosh *et al.*, "Acute hematological toxicity during post-operative bowel sparing image-guided intensity modulated radiation with concurrent cisplatin," *The British Journal of Radiology*, vol. 91, no. 1092, p. 20180005, 2018.
- [99] T. Kumar, A. Schernberg, F. Busato, M. Laurans, I. Fumagalli, I. Dumas, E. Deutsch, C. Haie-Meder, and C. Chargari, "Correlation between pelvic bone marrow radiation dose and acute hematological toxicity in cervical cancer patients treated with concurrent chemoradiation," *Cancer Manage Res*, vol. 11, pp. 6285–6297, 2019. [Online]. Available: <https://www.embase.com/search/results?subaction=viewrecord&id=L2002278911&from=export>
- [100] U. Mahantshetty, R. Krishnatry, S. Chaudhari, A. Kanaujia, R. Engineer, S. Chopra, and S. Shrivastava, "Comparison of 2 contouring methods of bone marrow on ct and correlation with hematological toxicities in non-bone marrow-sparing pelvic intensity-modulated radiotherapy with concurrent cisplatin for cervical cancer," *Int J Gynecol Cancer*, vol. 22, no. 8, pp. 1427–1434, 2012. [Online]. Available: <https://www.embase.com/search/results?subaction=viewrecord&id=L365805854&from=export>
- [101] M. Page, J. McKenzie, P. Bossuyt, I. Boutron, T. Hoffmann, C. Mulrow *et al.*, "The prisma 2020 statement: an updated guideline for reporting systematic reviews. metaarxiv. 2020," 2020.
- [102] Y. Chang, Z. Y. Yang, G. L. Li, Q. Li, Q. Yang, J. Q. Fan, Y. C. Zhao, Y. Q. Song, and G. Wu, "Correlations between radiation dose in bone marrow and hematological toxicity in patients with cervical cancer: A comparison of 3dcr, imrt, and rapidarc," *Int J Gynecol Cancer*, vol. 26, no. 4, pp. 770–776, 2016. [Online]. Available: <https://www.embase.com/search/results?subaction=viewrecord&id=L610286512&from=export>

- [103] K. Albuquerque, D. Giangreco, C. Morrison, M. Siddiqui, J. Sinacore, R. Potkul, and J. Roeske, "Radiation-related predictors of hematologic toxicity after concurrent chemoradiation for cervical cancer and implications for bone marrow-sparing pelvic imrt," *Int J Radiat Oncol Biol Phys*, vol. 79, no. 4, pp. 1043–1047, 2011. [Online]. Available: <https://www.embase.com/search/results?subaction=viewrecord&id=L50908574&from=export>
- [104] N. Gupta, C. Prakash, K. Chakrabarty, U. Giri, A. Patel, and S. Choudhary, "Potential advantages of bone marrow sparing imrt in cancer cervix: A dosimetric evaluation," *J Clin Diagn Res*, vol. 13, no. 4, pp. XC01–XC05, 2019. [Online]. Available: <https://www.embase.com/search/results?subaction=viewrecord&id=L2001894796&from=export>
- [105] K. Yan, E. Ramirez, X. J. Xie, X. Gu, Y. Xi, and K. Albuquerque, "Predicting severe hematologic toxicity from extended-field chemoradiation of para-aortic nodal metastases from cervical cancer," *Pract Radiat Oncol*, vol. 8, no. 1, pp. 13–19, 2018. [Online]. Available: <https://www.embase.com/search/results?subaction=viewrecord&id=L618068771&from=export>
- [106] Y. M. Zhou, C. Freese, T. Meier, D. Go, K. Khullar, M. Sudhoff, M. Lamba, and J. Kharofa, "The absolute volume of pet-defined, active bone marrow spared predicts for high grade hematologic toxicity in cervical cancer patients undergoing chemoradiation," *Clin Transl Oncol*, vol. 20, no. 6, pp. 713–718, 2018. [Online]. Available: <https://www.embase.com/search/results?subaction=viewrecord&id=L618990741&from=export>
- [107] B. S. Rose, Y. Liang, S. K. Lau, L. G. Jensen, C. M. Yashar, C. K. Hoh, and L. K. Mell, "Correlation between radiation dose to 18f-fdg-pet defined active bone marrow subregions and acute hematologic toxicity in cervical cancer patients treated with chemoradiotherapy," *International Journal of Radiation Oncology\* Biology\* Physics*, vol. 83, no. 4, pp. 1185–1191, 2012.
- [108] K. Khullar, M. Sudhoff, J. Elson, T. Herzog, A. Jackson, C. Billingsley, M. Lamba, and J. Kharofa, "A comparison of dosimetric parameters in pet-based active bone marrow volume and total bone volume in prediction of hematologic toxicity in cervical cancer patients treated with chemoradiation," *J Radiat Oncol*, vol. 6, no. 2, pp. 161–165, 2017. [Online]. Available: <https://www.embase.com/search/results?subaction=viewrecord&id=L624002724&from=export>
- [109] S.-B. Wang, J.-P. Liu, K.-J. Lei, Y.-M. Jia, Y. Xu, J.-F. Rong, and C.-X. Wang, "The volume of 99mTc sulfur colloid spet-defined active bone marrow can predict grade 3 or higher acute hematologic toxicity in locally advanced cervical cancer patients who receive chemoradiotherapy," *Cancer Medicine*, vol. 8, no. 17, pp. 7219–7226, 2019.
- [110] C. S. Platta, A. Bayliss, D. McHaffie, W. A. Tomé, M. R. Straub, and K. A. Bradley, "A dosimetric analysis of tomotherapy based intensity modulated radiation therapy with and without bone marrow sparing in gynecologic malignancies," *Technol Cancer Res Treat*, vol. 12, no. 1, pp. 19–29, 2013. [Online]. Available: <https://www.embase.com/search/results?subaction=viewrecord&id=L368331051&from=export><http://www.tcr.org/download/17998>
- [111] L. K. Mell, I. Sirák, L. Wei, R. Tarnawski, U. Mahantshetty, C. M. Yashar, M. T. McHale, R. Xu, G. Honerkamp-Smith, R. Carmona, M. Wright, C. W. Williamson, L. Kasaová, N. Li, S. Kry, J. Michalski, W. Bosch, W. Straube, J. Schwarz, J. Lowenstein, S. B. Jiang, C. C. Saenz, S. Plaxe, J. Einck, C. Khorprasert, P. Koonings, T. Harrison, M. Shi, and A. J. Mundt, "Bone marrow-sparing intensity modulated radiation therapy with concurrent cisplatin for stage ib-iva cervical cancer: An international multicenter phase ii clinical trial (interTECC-2)," *Int J Radiat Oncol Biol Phys*, vol. 97, no. 3, pp. 536–545, 2017. [Online]. Available: <https://www.embase.com/search/results?subaction=viewrecord&id=L614160244&from=export>
- [112] A. Jodda, B. Urbański, T. Piotrowski, and J. Malicki, "Relations between doses cumulated in bone marrow and dose delivery techniques during radiation therapy of cervical and endometrial cancer," *Phys Med*, vol. 36, pp. 54–59, 2017. [Online]. Available: <https://www.embase.com/search/results?subaction=viewrecord&id=L615404859&from=export>
- [113] S. M. McGuire, S. K. Bhatia, W. Sun, G. M. Jacobson, Y. Menda, L. L. Ponto, B. J. Smith, B. A. Gross, J. E. Bayouth, J. J. Sunderland, M. M. Graham, and J. M. Buatti, "Using [18f]fluorothymidine

- imaged with positron emission tomography to quantify and reduce hematologic toxicity due to chemoradiation therapy for pelvic cancer patients," *Int J Radiat Oncol Biol Phys*, vol. 96, no. 1, pp. 228–239, 2016. [Online]. Available: <https://www.embase.com/search/results?subaction=viewrecord&id=L612646955&from=export>
- [114] P. J. Bolan, L. Arentsen, T. Sueblinvong, Y. Zhang, S. Moeller, J. S. Carter, L. S. Downs, R. Ghebre, D. Yee, J. Froelich *et al.*, "Water-fat mri for assessing changes in bone marrow composition due to radiation and chemotherapy in gynecologic cancer patients," *Journal of Magnetic Resonance Imaging*, vol. 38, no. 6, pp. 1578–1584, 2013.
- [115] R. Carmona, J. Pritz, M. Bydder, S. Gulaya, H. Zhu, C. W. Williamson, C. S. Welch, F. Vaida, G. Bydder, and L. K. Mell, "Fat composition changes in bone marrow during chemotherapy and radiation therapy," *International Journal of Radiation Oncology\* Biology\* Physics*, vol. 90, no. 1, pp. 155–163, 2014.
- [116] N. Li, S. S. Noticewala, C. W. Williamson, H. Shen, I. Sirak, R. Tarnawski, U. Mahantshetty, C. K. Hoh, K. L. Moore, and L. K. Mell, "Feasibility of atlas-based active bone marrow sparing intensity modulated radiation therapy for cervical cancer," *Radiotherapy and Oncology*, vol. 123, no. 2, pp. 325–330, 2017.
- [117] T. Yusufaly, A. Miller, A. Medina-Palomo, C. W. Williamson, H. Nguyen, J. Lowenstein, C. A. Leath III, Y. Xiao, K. L. Moore, K. M. Moxley *et al.*, "A multi-atlas approach for active bone marrow sparing radiation therapy: Implementation in the nrg-gy006 trial," *International Journal of Radiation Oncology\* Biology\* Physics*, 2020.
- [118] R. Mohan and D. Grosshans, "Proton therapy—present and future," *Advanced drug delivery reviews*, vol. 109, pp. 26–44, 2017.
- [119] A. Lomax, "Intensity modulated proton therapy and its sensitivity to treatment uncertainties 1: the potential effects of calculational uncertainties," *Physics in Medicine & Biology*, vol. 53, no. 4, p. 1027, 2008.
- [120] C. Zeng, R. A. Amos, B. Winey, C. Beltran, Z. Saleh, Z. Tochner, H. Kooy, and S. Both, *Proton Treatment Planning*. Cham: Springer International Publishing, 2018, pp. 45–105. [Online]. Available: [https://doi.org/10.1007/978-3-319-42478-1\\_3](https://doi.org/10.1007/978-3-319-42478-1_3)
- [121] E. J. Tryggestad, W. Liu, M. D. Pepin, C. L. Hallemeier, and T. T. Sio, "Managing treatment-related uncertainties in proton beam radiotherapy for gastrointestinal cancers," *Journal of Gastrointestinal Oncology*, vol. 11, no. 1, 2019. [Online]. Available: <https://jgo.amegroups.com/article/view/34259>
- [122] J. G. Fletcher, S. Leng, L. Yu, and C. H. McCollough, "Dealing with uncertainty in ct images," 2016.
- [123] R. Mohan, I. J. Das, and C. C. Ling, "Empowering intensity modulated proton therapy through physics and technology: an overview," *International Journal of Radiation Oncology\* Biology\* Physics*, vol. 99, no. 2, pp. 304–316, 2017.
- [124] C. G. Ainsley and C. M. Yeager, "Practical considerations in the calibration of ct scanners for proton therapy," *Journal of applied clinical medical physics*, vol. 15, no. 3, pp. 202–220, 2014.
- [125] H. Paganetti, A. Niemierko, M. Ancukiewicz, L. E. Gerweck, M. Goitein, J. S. Loeffler, and H. D. Suit, "Relative biological effectiveness (rbe) values for proton beam therapy," *International Journal of Radiation Oncology\* Biology\* Physics*, vol. 53, no. 2, pp. 407–421, 2002.
- [126] A. Webster, A. Appelt, and G. Eminowicz, "Image-guided radiotherapy for pelvic cancers: a review of current evidence and clinical utilisation," *Clinical Oncology*, 2020.
- [127] P. C. Park, X. R. Zhu, A. K. Lee, N. Sahoo, A. D. Melancon, L. Zhang, and L. Dong, "A beam-specific planning target volume (ptv) design for proton therapy to account for setup and range uncertainties," *International Journal of Radiation Oncology\* Biology\* Physics*, vol. 82, no. 2, pp. e329–e336, 2012.
- [128] A. Fredriksson, A. Forsgren, and B. Hårdemark, "Minimax optimization for handling range and setup uncertainties in proton therapy," *Medical physics*, vol. 38, no. 3, pp. 1672–1684, 2011.

- [129] E. W. Korevaar, S. J. Habraken, D. Scandurra, R. G. Kierkels, M. Unipan, M. G. Eenink, R. J. Steenbakkers, S. G. Peeters, J. D. Zindler, M. Hoogeman *et al.*, “Practical robustness evaluation in radiotherapy—a photon and proton-proof alternative to ptv-based plan evaluation,” *Radiotherapy and Oncology*, vol. 141, pp. 267–274, 2019.
- [130] J. Stewart, K. Lim, V. Kelly, J. Xie, K. K. Brock, J. Moseley, Y.-B. Cho, A. Fyles, A. Lundin, H. Rehbinder *et al.*, “Automated weekly replanning for intensity-modulated radiotherapy of cervix cancer,” *International Journal of Radiation Oncology\* Biology\* Physics*, vol. 78, no. 2, pp. 350–358, 2010.
- [131] Y. Qiao, T. Jagt, M. Hoogeman, B. P. Lelieveldt, and M. Staring, “Evaluation of an open source registration package for automatic contour propagation in online adaptive intensity-modulated proton therapy of prostate cancer,” *Frontiers in oncology*, vol. 9, p. 1297, 2019.
- [132] T. Jagt, S. Breedveld, R. Van Haveren, B. Heijmen, and M. Hoogeman, “An automated planning strategy for near real-time adaptive proton therapy in prostate cancer,” *Physics in Medicine & Biology*, vol. 63, no. 13, p. 135017, 2018.
- [133] T. Z. Jagt, S. Breedveld, R. Van Haveren, R. A. Nout, E. Astreinidou, B. J. Heijmen, and M. S. Hoogeman, “Plan-library supported automated replanning for online-adaptive intensity-modulated proton therapy of cervical cancer,” *Acta Oncologica*, vol. 58, no. 10, pp. 1440–1445, 2019.
- [134] B. O’Donnell, J. C. Shiao, T. A. Pezzi, N. Waheed, S. Sharma, M. D. Bonnen, and M. S. Ludwig, “Stereotactic body radiation therapy, intensity-modulated radiation therapy, and brachytherapy boost modalities in invasive cervical cancer: a study of the national cancer data base,” *International Journal of Gynecologic Cancer*, vol. 28, no. 3, 2018.
- [135] C. Mantz, “Stereotactic body radiation therapy as a boost alternative for nonmetastatic cancer of the cervix and endometrium: disease control and quality of life outcomes from a phase 2 trial at 3 years’ minimum follow-up,” *International Journal of Radiation Oncology• Biology• Physics*, vol. 96, no. 2, p. E286, 2016.
- [136] R. Jadon, C. Pembroke, C. Hanna, N. Palaniappan, M. Evans, A. Cleves, and J. Staffurth, “A systematic review of organ motion and image-guided strategies in external beam radiotherapy for cervical cancer,” *Clinical oncology*, vol. 26, no. 4, pp. 185–196, 2014.
- [137] M. Van Herk, “Errors and margins in radiotherapy,” in *Seminars in radiation oncology*, vol. 14, no. 1. Elsevier, 2004, pp. 52–64.
- [138] M. Van Herk, P. Remeijer, C. Rasch, and J. V. Lebesque, “The probability of correct target dosage: dose-population histograms for deriving treatment margins in radiotherapy,” *International Journal of Radiation Oncology\* Biology\* Physics*, vol. 47, no. 4, pp. 1121–1135, 2000.
- [139] R. Ahmad, M. S. Hoogeman, S. Quint, J. W. Mens, E. M. V. Osorio, and B. J. Heijmen, “Residual setup errors caused by rotation and non-rigid motion in prone-treated cervical cancer patients after online cbct image-guidance,” *Radiotherapy and Oncology*, vol. 103, no. 3, pp. 322–326, 2012.
- [140] L. V. Laursen, U. V. Elstrøm, A. Vestergaard, L. P. Muren, J. B. Petersen, J. C. Lindegaard, C. Grau, and K. Tanderup, “Residual rotational set-up errors after daily cone-beam ct image guided radiotherapy of locally advanced cervical cancer,” *Radiotherapy and Oncology*, vol. 105, no. 2, pp. 220–225, 2012.
- [141] A. Hayes, “Empirical rule,” 2021.
- [142] S. T. Heijkoop, T. R. Langerak, S. Quint, J. W. M. Mens, A. G. Zolnay, B. J. Heijmen, and M. S. Hoogeman, “Quantification of intra-fraction changes during radiotherapy of cervical cancer assessed with pre-and post-fraction cone beam ct scans,” *Radiotherapy and Oncology*, vol. 117, no. 3, pp. 536–541, 2015.
- [143] J. R. Olsen, P. J. Parikh, M. Watts, C. E. Noel, K. W. Baker, L. Santanam, and J. M. Michalski, “Comparison of dose decrement from intrafraction motion for prone and supine prostate radiotherapy,” *Radiotherapy and Oncology*, vol. 104, no. 2, pp. 199–204, 2012.



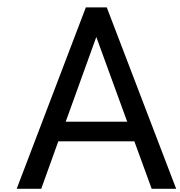
- [144] J. Visser, P. de Boer, K. F. Crama, Z. van Kesteren, C. R. Rasch, L. J. Stalpers, and A. Bel, "Dosimetric comparison of library of plans and online mri-guided radiotherapy of cervical cancer in the presence of intrafraction anatomical changes," *Radiation Oncology*, vol. 14, no. 1, pp. 1–13, 2019.
- [145] L. V. van Dijk, R. J. Steenbakkens, B. ten Haken, H. P. van der Laan, A. A. van 't Veld, J. A. Langendijk, and E. W. Korevaar, "Robust intensity modulated proton therapy (impt) increases estimated clinical benefit in head and neck cancer patients," *PLoS One*, vol. 11, no. 3, p. e0152477, 2016.
- [146] T. Berger, J. B. B. Petersen, J. C. Lindegaard, L. U. Fokdal, and K. Tanderup, "Impact of bowel gas and body outline variations on total accumulated dose with intensity-modulated proton therapy in locally advanced cervical cancer patients," *Acta Oncologica*, vol. 56, no. 11, pp. 1472–1478, 2017.
- [147] M. Soukup, M. Söhn, D. Yan, J. Liang, and M. Alber, "Study of robustness of impt and imrt for prostate cancer against organ movement," *International Journal of Radiation Oncology\* Biology\* Physics*, vol. 75, no. 3, pp. 941–949, 2009.
- [148] S. Meyer, J. Bortfeldt, P. Lämmer, F. S. Englbrecht, M. Pinto, K. Schnürle, M. Würfl, and K. Parodi, "Optimization and performance study of a proton ct system for pre-clinical small animal imaging," *Physics in Medicine & Biology*, vol. 65, no. 15, p. 155008, 2020.
- [149] S. Pugh, *Integrated methods for successful product engineering*. Addison-Wesley, 1990.
- [150] M. L. Chiozza and C. Ponzetti, "Fmea: a model for reducing medical errors," *Clinica chimica acta*, vol. 404, no. 1, pp. 75–78, 2009.
- [151] R. J. Mikulak, R. McDermott, and M. Beauregard, *The basics of FMEA*. CRC Press, 2017.





# **Appendices**





## Search term

### Embase

('pelvis tumor'/exp OR 'uterine cervix tumor'/exp OR 'genital tract tumor'/exp OR 'rectum cancer'/de OR 'anus cancer'/exp OR (((pelvis\* OR pelvic OR cervix\* OR cervical\* OR genital\* OR urogenital\* OR rectum OR rectal OR colorectal\* OR anal OR anus OR vulv\* OR ovarian\* OR endometr\* OR prostat\* OR gynecol\* OR gynaecol\*) NEAR/3 (tumor\* OR tumour\* OR neoplas\* OR malign\* OR cancer\* OR carcinom\* OR adenocarcin\*)):ab,ti,kw) AND ('radiotherapy'/exp OR (radiotherap\* OR ((radio\* OR radiation\* OR arc) NEAR/3 (therap\*)) OR EBRT OR IMRT OR ((external-beam\* OR intens\*-modul\*) NEAR/3 (radiation\* OR irradiation\* OR therap\*)) OR ((radiation\* OR radio\*) NEAR/3 (dose OR dosage\*)) OR proton\* OR VMAT\*):ab,ti,kw) AND (((('organs at risk'/de OR 'conservative treatment'/de OR 'radiation dose'/exp OR 'dosimetry'/de) AND 'bone marrow'/exp) OR (((marrow\*) NEAR/6 (sparing\* OR spare OR dose OR dosage\* OR dosimetr\* OR radiation\* OR irradiation\* OR conservativ\* OR organs-at-risk\*)):ab,ti,kw) NOT ([Conference Abstract]/lim)

### Medline

(exp Pelvic Neoplasms/ OR exp Uterine Cervical Neoplasms/ OR exp Urogenital Neoplasms/ OR exp Rectal Neoplasms/ OR (((pelvis\* OR pelvic OR cervix\* OR cervical\* OR genital\* OR urogenital\* OR rectum OR rectal OR colorectal\* OR anal OR anus OR vulv\* OR ovarian\* OR endometr\* OR prostat\* OR gynecol\* OR gynaecol\*) ADJ3 (tumor\* OR tumour\* OR neoplas\* OR malign\* OR cancer\* OR carcinom\* OR adenocarcin\*)):ab,ti,kf.) AND (exp Radiotherapy/ OR radiotherapy.fs. OR (radiotherap\* OR ((radio\* OR radiation\* OR arc) ADJ3 (therap\*)) OR EBRT OR IMRT OR ((external-beam\* OR intens\*-modul\*) ADJ3 (radiation\* OR irradiation\* OR therap\*)) OR ((radiation\* OR radio\*) ADJ3 (dose OR dosage\*)) OR proton\* OR VMAT\*):ab,ti,kf.) AND (((Organs at Risk/ OR Conservative Treatment/ OR exp Radiotherapy Dosage/ OR exp Radiation Dosage/) AND Bone Marrow/) OR (((marrow\*) ADJ3 (sparing\* OR spare OR dose OR dosage\* OR dosimetr\* OR radiation\* OR irradiation\* OR conservativ\* OR organs-at-risk\*)):ab,ti,kf.) NOT (news OR congress\* OR abstract\* OR book\* OR chapter\* OR dissertation abstract\*).pt.

### Web of Science]

TS=((((((pelvis\* OR pelvic OR cervix\* OR cervical\* OR genital\* OR urogenital\* OR rectum OR rectal OR colorectal\* OR anal OR anus OR vulv\* OR ovarian\* OR endometr\* OR prostat\* OR gynecol\* OR gynaecol\*) NEAR/2 (tumor\* OR tumour\* OR neoplas\* OR malign\* OR cancer\* OR carcinom\* OR adenocarcin\*))) AND ((radiotherap\* OR ((radio\* OR radiation\* OR arc) NEAR/2 (therap\*)) OR EBRT OR IMRT OR ((external-beam\* OR intens\*-modul\*) NEAR/2 (radiation\* OR irradiation\* OR therap\*)) OR ((radiation\* OR radio\*) NEAR/2 (dose OR dosage\*)) OR proton\* OR VMAT\*)) AND (((marrow\*) NEAR/2 (sparing\* OR spare OR dose OR dosage\* OR dosimetr\* OR radiation\* OR irradiation\* OR conservativ\* OR organs-at-risk\*))) AND DT=(Article OR Review OR Letter OR Early Access)



# B

## Selected items from TRIPOD-statement

An explanation for each item can be found in the TRIPOD-statement [94].

- 4ab Describe source data and specify study dates
- 5ac Specify study setting and provide treatment details
- 5b Describe eligibility criteria
- 6a Define predicted outcome including the time of assessment
- 7a Define predictor variables including time of measurement
- 9 Describe handling of missing data
- 10a Describe predictors handling in the analyses
- 10bi Specify statistical model
- 10bii Describe approach used for predictor selection before modeling
- 10biii Describe approach used for predictor selection during modeling
- 10biv Describe testing of interaction terms
- 10bvi Report internal validation
- 10c Describe prediction calculations in the validation setting
- 10di Describe measure for model discrimination
- 10dii Describe measures for model calibration
- 11 Creation of various risk groups
- 12 Identify differences between training and validation data
- 13a Describe sample size and number of events, preferably with temporal information
- 13bi-ii Describe patient characteristics
- 13biii-iv Describe participants with missing data
- 13c Show comparison of patient characteristics between training and validation data
- 14a Specify analyzed sample size and number of events
- 14b Report unadjusted associations between predictors and outcome

- 15a Present full prediction model
- 15b Explain how to use prediction model
- 16i-ii Report discrimination measure with confidence intervals
- 16iii Report calibration measures
- 16iv Report other model performance measures
- 17 Report results from model updating

# C

TRIPOD-score per included article



Table C.1: TRIPOD-score per included article with a maximum score of 29. V = fulfilled, NA = not applicable

	Type of TRIPOD study	4ab	5ac	5b	6a	7a	9	10a	10bi	10bii	10biii	10biv	10bvi	10c	10di	10dii	11	12	13a	13bi- 13biii-			13c	14a	14b	15a	15b	16i-ii	16iii	16iv	17	Total
																				ii	iv											
Rose, B.S. et al (2011)	IV	V	V	V	V		V	V	V	V	V		V	V	V			V	V	V	V	V	V	V		V	V					22
Huang J. et al	Ia	V	V	V	V			V	V	V	V				V				V	V	V		V	V	V			V				17
Chang, Y. et al	Ia	V	V	V	V				V	V	V								V	V			V	V	V	V	V					15
Klopp, A.H. et al	Ia	V	V	V	V	V		V	V	V	V								V	V			V	V								13
Kumar, T. et al	Ia	V	V	V	V	V			V	V	V								V	V			V	V								12
Rose, B.S. et al. (2012)	Ia	V	V	V	V	V		V	V		V								V	V			V							V		12
Wang, S.B. et al	Ia	V	V	V	V			V	V		V				V				V	V			V				V			V		12
Zhu, H. et al	Ia	V	V	V	V			V	V		V								V	V	V		V	V								12
Lewis, S. et al	Ia	V	V	V	V			V	V	V	V								V				V	V								11
Albuquerque, M.D. et al	Ia	V	V		V		V		V	V	V								V	V			V	V								11
Khullar K. et al	Ia	V	V	V	V				V		V				V				V	V			V				V					11
Elicin, O. et al.	Ia	V	V	V	V				V		V								V	V			V	V								10
Mell, L.K. et al	Ia	V	V	V	V			V	V		V								V	V			V									10
Yan, K. et al	Ia	V	V	V	V				V		V								V	V			V			V						10
Mahantshetty, U. et al	Ia	V	V	V	V				V		V								V	V			V									9
Zhou, Y.M. et al	Ia	V	V		V				V						V				V	V			V				V					9

# D

## Pugh's checklist

Product Life Span	Size and weight	Packaging	Transportation	Performance
Materials	Product policy	Environment	Appearance	Life in Service
Shell life and Storage	Social and political implications	Safety	Technical standards	Maintenance
Re-use, recycling	Installation, operation	Quality and reliability	Ergonomics	Testing
Manufacturing Facilities	Standards	Target Product Cost	Product Liability	Quantity

Pugh's checkpoint not specified for this workflow	Pugh's checkpoint	Added checkpoint
---------------------------------------------------	-------------------	------------------

Figure D.1: Pugh's checklist, applied for generating requirements for the plan-of-the-day-workflow for locally advanced cervical cancer patients with a corresponding legend [149]. One checkpoint was added (Technical standards) (dark blue) and not all checkpoints were used.



# E

## Requirements from the Pugh's checklist

Table E.1: Generated requirements with the use of the Pugh's checklist for generating a plan library and selecting from a plan library for LACC-patients

Pugh subject	Step	Objective	Code	Point of view	Hard or soft	
Performance	Generating a plan library	Accurate plans	PER.1.1	Oncologists, therapists	Hard	
			PER.1.2	Oncologists, therapists	Hard	
			PER.1.3	Patient, oncologists, therapists	Hard	
		PER.1.4	Therapists	Hard		
		PER.1.5	Oncologists, therapists	Hard		
		PER.1.6	Oncologists, therapists	Hard		
		Fast plan generating	PER.2.1	Therapists	Hard	
			PER.2.2	Patient, oncologists, therapists	Soft	
			PER.3.1	Oncologists, therapists	Hard	
	Selecting from a plan library	Easy plan selection	PER.3.2	Therapists	Hard	
			PER.3.3	Oncologists, therapists, MP	Hard	
			PER.3.4	Therapists, MP	Hard	
		Trust that a plan is optimal	PER.3.5	Patient, therapists	Soft	
			PER.4.1	Therapists	Soft	
			PER.4.2	Patient, therapists	Soft	
Technical standards	Both	Adapted as much as possible to currently available software	PER.4.3	Patient, therapists	Hard	
			TEC.1.1	IT, MP	Hard	
			LIF.1.1	IT, MP	Hard	
	Life in service	Both	Applicable to each cervical cancer patient	LIF.1.2	IT, MP	Hard
				MAI.1.1	IT, MP	Hard
	Maintenance	Both	Has to be operable after update of currently available software			
	Target product cost	Both	In house development	TAR.1.1	IT, MP	Soft
	Quantity	Generating a plan library	Should work on each PC with the required software	QUA.1.1	IT	Soft
		Selecting from a plan library	Should work on each radiotherapy machine in HPTC	QUA.2.1	IT	Soft
	Manufacturing Facilities	Both	In house development	MAN.1.1	IT	Soft
	Appearance	Both	Can be used intuitively	APP.1.1	Oncologists, therapists	Hard
	Standards	Both	Should follow data protection regulations	STA.1.1	MP, IT	Hard
	Ergonomics	Generating a plan library	Easily applied by trained therapists	ERG.1.1	Therapists	Hard

Table E.1: Generated requirements with the use of the Pugh's checklist for generating a plan library and selecting from a plan library for LACC-patients

Pugh subject	Step	Objective	Code	Point of view	Hard or soft
	Selecting from a plan library	Easily applied by trained therapists	ERG.2.1	Therapists	Hard
Quality and reliability	Both	Errors can be solved by own MP or IT department	Q&R.1.1	MP, IT	Hard
Testing	Both	Needs validation	TES.1.1	Oncologists, therapists, MP, IT	Hard
		Needs continuous risk evaluation	TES.2.1	Oncologists, therapists, MP, IT	Hard
Safety	Both	Limit human errors as much as possible	SAF.1.1	Oncologists, therapists, MP, IT	Soft
			SAF.1.2	Oncologists, therapists, MP	Hard
Product liability	Both	Hospital is ultimately responsible	PRO.1.1	Oncologists, therapists, MP	Hard
			PRO.1.2	Oncologists, therapists, MP, IT	Soft
Installation, operation	Both	Installation by own IT-department Training of users will be in house	INS.1.1	MP, IT	Hard
			INS.2.1	MP, IT	Hard
			INS.2.2	Oncologists, therapists, MP, IT	Hard





**F**

Identified risks

Table E1: Input of participants (in Dutch) during a risk evaluation of the plan-of-the-day-strategy for locally advanced cervical cancer in Erasmus MC. Risks were deduplicated, which is indicated by ↑ (= similar to risk above).

Processtap	Categorie	Risico	Oorzaak	Gevolg	Risico na categoriseren en ontubbelen	Kans	Tijd	Kwali- teit	Veilig- heid	Kans x Gevolg	
<b>Aanmelden patiënt</b>	Menselijk	Verkeerde instructies worden aan de patient meegegeven	* Afsprakenbureau stuurt verkeerde brief naar patient	* Patient heeft niet de juiste drinkinstructies/laxatie gevolgd	Verkeerde instructies worden aan de patient meegegeven	3	3	2	0	<b>15</b>	
	Menselijk	Patient heeft geen afspraak gekregen voor het plaatsen van de markers	* Afsprakenbureau/secretaresse heeft geen afspraak ingepland voor de patient	* Delay en patient moet alsnog markers geplaatst krijgen * Patiënt komt op CT zonder markers	Patient heeft geen afspraak gekregen voor het plaatsen van de markers	1	3	3	2	<b>8</b>	
	Menselijk	Aantal processen klopt niet met het aantal te maken plannen	* HIX aantal plannen verkeerd ingevuld, of wijziging wordt in het system niet goed doorgevoerd		Aantal processen klopt niet met het aantal te maken plannen	4	3	3	0	<b>24</b>	
<b>CT-data maken</b>	<b>aan-</b>	Organisatorisch	Arts kiest een dosis voor een SIB gebied, maar er zijn geen harde regels voor wanneer een gebied een lage sib dosis of hoge sib dosis moet krijgen	* Er zijn geen harde regels, het blijft gokken welke dosis het SIB gebied gaat krijgen met de brachytherapie. Het is een klein beetje arts afhankelijk welke dosis zij kiezen.	Planningslab kan eigenlijk nooit controleren of de juiste SIB dosis is gekozen * SIB gebied moet gewijzigd worden naar andere dosis	Arts kiest een dosis voor een SIB gebied, maar er zijn geen harde regels voor wanneer een gebied een lage sib dosis of hoge sib dosis moet krijgen	3	3	4	3	<b>30</b>

Table E1: Input of participants (in Dutch) during a risk evaluation of the plan-of-the-day-strategy for locally advanced cervical cancer in Erasmus MC. Risks were deduplicated, which is indicated by † (= similar to risk above).

Processtap	Categorie	Risico	Oorzaak	Gevolg	Risico na categoriseren en ontdebelen	Kans	Tijd	Kwali- teit	Veilig- heid	Kans x Gevolg
	Organisatorisch	De controle van de blaas en rectum vulling is lastig te beoordelen voor de CT laborant	* Rectum en blaasvulling is heel divers bij verschillende patienten, wij hebben geen harde 39 regels hiervoor	* Het rectum blijkt soms wel eens veel te vol te zijn, waardoor het doelgebied anders ligt en er vaak veldcontroles nodig zijn	De controle van de blaas en rectum vulling is lastig te beoordelen voor de CT laborant	3	1	2	2	15
	Menselijk	De loodkorreltjes zijn op de verkeerde CT geplaatst			De loodkorreltjes zijn op de verkeerde CT geplaatst	0	1	0	1	0
	Menselijk	Fout in dicom tags tijdens maken van CT (verkeerde patient naam, verkeerde serie description vol/leeg...)			Fout in dicom tags tijdens maken van CT (verkeerde patient naam, verkeerde serie description vol/leeg...)	1	1	3	3	7
	Menselijk	Scanlengte te klein (vooral ten opzichte van klierregio)		* Intekening van klieren is onmogelijk	Scanlengte te klein (vooral ten opzichte van klierregio)	1	5	2	1	8
	Overig	Ongewenst rectum/blaas vulling			Ongewenst rectum/blaas vulling	2	3	3	2	16

Table E1: Input of participants (in Dutch) during a risk evaluation of the plan-of-the-day-strategy for locally advanced cervical cancer in Erasmus MC. Risks were deduplicated, which is indicated by ↑ (= similar to risk above).

Processtap	Categorie	Risico	Oorzaak	Gevolg	Risico na categoriseren en ontdebelen	Kans	Tijd	Kwali- teit	Veilig- heid	Kans x Gevolg
	Overig	Laxatiepil is de avond van te voren niet gebruikt door de patiënt.	* Patient wil het niet of begrijpt het niet	* Darmen zitten te vol op de CT scan. Hier kan op dat moment niet altijd wat aan gedaan worden maar achteraf blijkt het wel een probleem te zijn voor het matchen op het bestralingsstoel.	↑	↑	↑	↑	↑	↑
	Overig	Drinkprotocol is niet juist uitgevoerd	* Patient heeft de brief niet gekregen of begrijpt de brief niet	* Patient moet van de CT tafel, moet opnieuw drinken en moet wachten in de wachtkamer. Het CT programma kan hierdoor ook flink uitlopen.	↑	↑	↑	↑	↑	↑

Table E1: Input of participants (in Dutch) during a risk evaluation of the plan-of-the-day-strategy for locally advanced cervical cancer in Erasmus MC. Risks were deduplicated, which is indicated by † (= similar to risk above).

Processtap	Categorie	Risico	Oorzaak	Gevolg	Risico na categoriseren en ontdebelen	Kans	Tijd	Kwali- teit	Veilig- heid	Kans x Gevolg
<b>Intekenen structuren</b>	Organisatorisch	Intekenen lucht en contrast (wat nodig is voor de dosisplanning) wordt vaak vergeten	* Er is hier geen checklist voor	* Wanneer het niet wordt gezien door de dosisplanningslaborant wordt het plan verkeerd berekend, wanneer het wel gezien wordt door de dosisplanningslaborant moet er een CT laborant zijn om dit alsnog in te tekenen (delay)	Intekenen lucht en contrast (wat nodig is voor de dosisplanning) wordt vaak vergeten	3	2	3	2	<b>21</b>
	Organisatorisch	Er is bij 17 patiënten geanalyseerd waar het proces vertraagd wordt. Dit blijkt bij het intekenen van het doelvolumen (bij 14 patiënten) en ook in de helft van de gevallen bij de MONO te zijn.	* Ook arts assistenten krijgen deze patiënten om in te tekenen. Het is een complexe intekening waardoor zij er langer de tijd voor nodig hebben	* Het komt te laat op de dosisplanning waardoor er vaak niet genoeg tijd is om deze plannen te maken. Patient moet uitgesteld worden.	Er is bij 17 patiënten geanalyseerd waar het proces vertraagd wordt. Dit blijkt bij het intekenen van het doelvolumen (bij 14 patiënten) en ook in de helft van de gevallen bij de MONO te zijn.	3	4	2	1	<b>21</b>

Table E1: Input of participants (in Dutch) during a risk evaluation of the plan-of-the-day-strategy for locally advanced cervical cancer in Erasmus MC. Risks were deduplicated, which is indicated by † (= similar to risk above).

Processtap	Categorie	Risico	Oorzaak	Gevolg	Risico na categoriseren en ontdebelen	Kans	Tijd	Kwali- teit	Veilig- heid	Kans x Gevolg
	Menselijk	Lege blaas CT is niet leeg of volle blaas is niet vol	laboranten hebben dit bij het maken van de scans niet opgemerkt * drinkinstructie niet gevolgd	*op toestel kan blijken dat een patient toch een "mover" is * niet-rigide bewegingsmodel is niet accuraat (intekenvariatie)	Lege blaas CT is niet leeg of volle blaas is niet vol	2	4	3	2	<b>18</b>
	Menselijk	Bekkenrotatie in lege en volle blaas niet gelijk		* moeilijke match of niet representatieve situatie voor op het toestel	Bekkenrotatie in lege en volle blaas niet gelijk	2	1	3	1	<b>10</b>
	Menselijk	Naam structuur niet volgens protocol (ex: in het nederlands, of typfout in het benaming van de structuren)			Naam structuur niet volgens protocol (ex: in het nederlands, of typfout in het benaming van de structuren)	1	1	1	1	<b>3</b>

Table F1: Input of participants (in Dutch) during a risk evaluation of the plan-of-the-day-strategy for locally advanced cervical cancer in Erasmus MC. Risks were deduplicated, which is indicated by † (= similar to risk above).

Processtap	Categorie	Risico	Oorzaak	Gevolg	Risico na categoriseren en ontdebellen	Kans	Tijd	Kwali- teit	Veilig- heid	Kans x Gevolg
	Overig	Intekening komt niet overeen met de anatomie op de scan	MR-data is gemaakt met een andere blaasvulling of ligging * Er wordt al geanticipeerd op een leger rectum of andere blaasvulling * MR-data is te lang geleden?	* Te groot doelvolumen in lege of volle blaas situatie, waardoor het te bestralen doelvolumen onnodig groot is * Biedt weinig houvast voor validatie van de anatomie bij imaging na positioneren tijdens de behandeling * de te genereren halfvolle blaasstructuur kan gaan overlappen met het doelgebied * patient kan onterecht als non-mover worden aangemerkt	Intekening komt niet overeen met de anatomie op de scan	2	2	1	1	<b>8</b>

Table E1: Input of participants (in Dutch) during a risk evaluation of the plan-of-the-day-strategy for locally advanced cervical cancer in Erasmus MC. Risks were deduplicated, which is indicated by ↑ (= similar to risk above).

Processtap	Categorie	Risico	Oorzaak	Gevolg	Risico na categoriseren en ontdebelen	Kans	Tijd	Kwali- teit	Veilig- heid	Kans x Gevolg
	Overig	Intekening van beide scans in niet consistent (blaas op een van de scans is bijvoorbeeld groter getekend dan de blaas op de andere scan)			↑	↑	↑	↑	↑	↑
<b>ITV aanmaken met RTStudio</b>	Technisch	ITV programma niet beschikbaar	* Database vol, of programma niet beschikbaar, of verkeerde versie programma		ITV programma niet beschikbaar	1	1	2	1	<b>4</b>
	Technisch	Lineaire interpolatie niet representatief voor de kanteling van het orgaan			Lineaire interpolatie niet representatief voor de kanteling van het orgaan	2	1	4	3	<b>16</b>
	Technisch	Vectoren zijn niet representatief voor de verplaatsing van de organen (mismatch tussen gekozen punten door het algoritme, kruizing van vector)			↑	↑	↑	↑	↑	↑



Table E1: Input of participants (in Dutch) during a risk evaluation of the plan-of-the-day-strategy for locally advanced cervical cancer in Erasmus MC. Risks were deduplicated, which is indicated by ↑ (= similar to risk above).

Processtap	Categorie	Risico	Oorzaak	Gevolg	Risico na categoriseren en ontdebelen	Kans	Tijd	Kwali- Veilig- heid	Kans x Gevolg	
	Menselijk	Positie van markers verwisseld tussen eerste scan en tweede scans			Positie van de markers niet juist aangegeven op een van de scan	2	2	3	2	<b>14</b>
	Menselijk	Positie van de markers niet juist aangegeven op een van de scan			↑	↑	↑	↑	↑	
	Menselijk	Marges van de makers verkeerd gekozen			Marges van de makers verkeerd gekozen	2	2	3	2	<b>14</b>
	Menselijk	Verkeerde metrix gebruikt bij het maken van de DIR (blaas ipv Uterus en vice-versa)			Verkeerde metrix gebruikt bij het maken van de DIR (blaas ipv Uterus en vice-versa)	3	2	2	2	<b>18</b>
	Menselijk	Verkeerde benaming van de structuren bij het opslaan van de RTstruct			Verkeerde benaming van de structuren bij het opslaan van de RTstruct	2	3	3	2	<b>16</b>
	Menselijk	Verkeerde R waarde bij het maken van de halfvolle blaas (R <>0.5)			Verkeerde R waarde bij het maken van de halfvolle blaas (R <>0.5)	0	2	4	4	<b>0</b>

Table E1: Input of participants (in Dutch) during a risk evaluation of the plan-of-the-day-strategy for locally advanced cervical cancer in Erasmus MC. Risks were deduplicated, which is indicated by † (= similar to risk above).

Processtap	Categorie	Risico	Oorzaak	Gevolg	Risico na categoriseren en ontdebelen	Kans	Tijd	Kwali- Veilig- heid	Kans x Gevolg	
	Menselijk	interpolatie script gebruikt ipv ITV script (of vice-versa)			interpolatie script gebruikt ipv ITV script (of vice-versa)	0	2	4	3	<b>0</b>
	Menselijk	CT vol/leeg verkeerd gekozen in de script (moving CT versus primary CT)			CT vol/leeg verkeerd gekozen in de script (moving CT versus primary CT)	3	2	4	3	<b>27</b>
	Overig	Rectum tussen leeg/vol niet gelijk, daardoor verkeerde interpolatie			Rectum tussen leeg/vol niet gelijk, daardoor verkeerde interpolatie	3	4	3	3	<b>30</b>
	Menselijk	De rigid match is verkeerd (rotatie bekken, vervorming, matchbox niet goed gezet...), en daardoor is de DIR ook niet juist			De rigid match is verkeerd (rotatie bekken, vervorming, matchbox niet goed gezet...), en daardoor is de DIR ook niet juist	2	2	4	3	<b>18</b>

Table E1: Input of participants (in Dutch) during a risk evaluation of the plan-of-the-day-strategy for locally advanced cervical cancer in Erasmus MC. Risks were deduplicated, which is indicated by † (= similar to risk above).

Processtap	Categorie	Risico	Oorzaak	Gevolg	Risico na categoriseren en ontdebellen	Kans	Tijd	Kwali- Veilig- heid	Kans x Gevolg		
101	Maken van plannen	Organisatorisch	Verkeerd aantal ITVs gemaakt bij een patiënt (non-mover wordt mover)	Er is geen stap in hix voor de arts hiervoor * Patiënt wordt standaard aangemeld als mover in systeem * Arts moet dit handmatig wijzigen	* Delay * Laborant moet achter de arts aan om te weten te komen of de patient een (non) mover is * Patiënt wordt opeens een mover * Extra rekentijd plannen	Verkeerd aantal ITVs gemaakt bij een patiënt (non-mover wordt mover)	3	3	3	2	24
		Menselijk	Bij het PTV van de nodes wordt vaak de 95% ingevuld in de DVH statistics. Maar bij het PTV van de nodes bij de cervix patiënten kijken we naar 90% van de dosis.	* Dit zijn we gewend want we kijken bij alle andere plannen naar het percentage wat 95% van de dosis ontvangt.	* Het plan wordt veel te heet	Bij het PTV van de nodes wordt vaak de 95% ingevuld in de DVH statistics. Maar bij het PTV van de nodes bij de cervix patiënten kijken we naar 90% van de dosis.	3	1	3	4	24
		Menselijk	Bij non movers is zITV en ITV (+5 mm) niet aanwezig.	* Fysica is vergeten een nieuw ITV aan te maken	* Wanneer de dosisplanningslaborant dit niet ziet, wordt er een verkeerd PTV gedraaid en wordt de patient verkeerd bestraald	Bij non movers is zITV en ITV (+5 mm) niet aanwezig.	3	2	4	2	24

Table E1: Input of participants (in Dutch) during a risk evaluation of the plan-of-the-day-strategy for locally advanced cervical cancer in Erasmus MC. Risks were deduplicated, which is indicated by † (= similar to risk above).

Processtap	Categorie	Risico	Oorzaak	Gevolg	Risico na categoriseren en ontdebelen	Kans	Tijd	Kwali- Veilig- heid	Kans x Gevolg	
	Organisatorisch	Artsen zijn het soms niet eens met het plan, terwijl het wel voldoet aan ons protocol.	* Arts heeft niet in de overdracht geschreven dat hij/zij van het protocol af wil wijken.	* Delay; plan moet opnieuw berekend worden en dit duurt erg lang	Artsen zijn het soms niet eens met het plan, terwijl het wel voldoet aan ons protocol.	3	4	2	0	<b>18</b>
	Menselijk	Er wordt vergeten om te kijken of de maximale afstand van het isocentrum naar de meest caudale clip maximaal 11 cm is.	* Extra stap wat bij andere plannen niet van toepassing is	* Het plan moet opnieuw gemaakt worden. Als dit niet gezien wordt, heeft het toestel namelijk een probleem want die kunnen de clips dan niet goed beoordelen.	Er wordt vergeten om te kijken of de maximale afstand van het isocentrum naar de meest caudale clip maximaal 11 cm is.	2	4	3	2	<b>18</b>
	Technisch	Geen single-user Monaco system beschikbaar			Geen single-user Monaco system beschikbaar	4	4	2	0	<b>24</b>
	Technisch	Het duurt heel erg lang voordat een plan berekend is (minimaal 4 uur per plan)	* Het is een complex plan en de Monaco servers zijn heel erg traag	* Plan van een Cervix POTD kan nooit binnen 1 dag klaar zijn. Dit betekent soms dat, wanneer de stap voor ons pas laat beschikbaar komt, de patient uitgesteld moet worden.	Het duurt heel erg lang voordat een plan berekend is (minimaal 4 uur per plan)	5	3	3	1	<b>35</b>

Table F1: Input of participants (in Dutch) during a risk evaluation of the plan-of-the-day-strategy for locally advanced cervical cancer in Erasmus MC. Risks were deduplicated, which is indicated by ↑ (= similar to risk above).

Processtap	Categorie	Risico	Oorzaak	Gevolg	Risico na categoriseren en ontdebellen	Kans	Tijd	Kwali- teit	Veilig- heid	Kans x Gevolg
	Technisch	lange tijd nodig voor dosisplanning door moeilijkheidsgraad en grootte van het doelgebied (en dan keer 2 of 3!)	* door gebruik van verschillende SIB doseringen moeilijk te automatiseren in iCycle. anders zou je de plannings 's avonds kunnen aanzetten en de volgende ochtend kunnen beoordelen.		↑	↑	↑	↑	↑	↑
	Menselijk	iCycle gebruikt voor SIB plan			iCycle gebruikt voor SIB plan	3	2	0	0	6
	Menselijk	Planning gemaakt op CT leeg			Planning gemaakt op CT leeg	1	4	3	2	9
	Menselijk	Naamgeving plan komt niet overeen met het juiste plan	* verkeerde structuur gebruikt in de optimalisatie	* verkeerde dosisafgifte op toetsel	Naamgeving plan komt niet overeen met het juiste plan	2	2	4	4	20
	Menselijk	Plan benaming volle/leeg is gewisseld			↑	↑	↑	↑	↑	↑
	Menselijk	Fout tijdens het instellen van de template			Fout tijdens het instellen van de template	3	3	3	2	24
	Menselijk	Verkeerde Monaco template gebruikt			↑	↑	↑	↑	↑	↑

Table E1: Input of participants (in Dutch) during a risk evaluation of the plan-of-the-day-strategy for locally advanced cervical cancer in Erasmus MC. Risks were deduplicated, which is indicated by ↑ (= similar to risk above).

Processtap	Categorie	Risico	Oorzaak	Gevolg	Risico na categoriseren en ontdebelen	Kans	Tijd	Kwali- teit	Veilig- heid	Kans x Gevolg
	Menselijk	Verkeerde dosisniveau voor klieren of een klier vergeten			Verkeerde dosisniveau voor klieren of een klier vergeten					
	Menselijk	SIB-klier vergeten (of 1 van de klieren)			↑	↑	↑	↑	↑	↑
<b>Importeer plannen in MOSAIQ</b>	Menselijk	De geïmporteerde plannen zijn niet goed geapproved, wat handmatig moet gebeuren door de laboranten	* Vroeger gebeurde dit automatisch; nu moet dit handmatig gebeuren. Ook bij een wijziging van volgorde vergeet de laborant opnieuw te approveen.	* Script werkt niet op het bestralingstoestel	De geïmporteerde plannen zijn niet goed geapproved, wat handmatig moet gebeuren door de laboranten	2	4	1	1	<b>12</b>
	Menselijk	Fysica controle niet gedaan op alle plannen			Fysica controle niet gedaan op alle plannen	2	2	3	3	<b>16</b>
	Menselijk	Sum dose plan (Master prescription) wordt niet aangemaakt			Sum dose plan (Master prescription) wordt niet aangemaakt	1	2	0	5	<b>7</b>
	Menselijk	Verkeerde structuren worden opgestuurd (bijv. van planning ipv herplanning)			Verkeerde structuren worden opgestuurd (bijv. van planning ipv herplanning)	1	3	4	3	<b>10</b>

Table E1: Input of participants (in Dutch) during a risk evaluation of the plan-of-the-day-strategy for locally advanced cervical cancer in Erasmus MC. Risks were deduplicated, which is indicated by ↑ (= similar to risk above).

Processtap	Categorie	Risico	Oorzaak	Gevolg	Risico na categoriseren en ontdebelen	Kans	Tijd	Kwali- teit	Veilig- heid	Kans x Gevolg
	Menselijk	Bij het maken van een lege kalender en het maken van de CBCT velden, worden deze niet op de juiste manier geïmporteerd en aangemaakt door de laborant (ondanks het protocol).	* De stappen zijn iets anders dan alle andere doelgebieden waardoor dit soms in de automatisme van de laborant gebeurt.	* Het script op het bestralingstoestel werkt niet	Bij het maken van een lege kalender en het maken van de CBCT velden, worden deze niet op de juiste manier geïmporteerd en aangemaakt door de laborant (ondanks het protocol).	2	2	2	1	<b>10</b>
	Menselijk	Maar 1 plan wordt in Mosaiq geïmporteerd (ipv 2-3)			↑	↑	↑	↑	↑	↑
	Menselijk	Plannen worden niet gekoppeld aan dezelfde dose prescription			↑	↑	↑	↑	↑	↑
<b>Bestraling</b>	Overig	Patient kan haar plas niet meer ophouden waardoor ze van tafel moet.			Patient kan haar plas niet meer ophouden waardoor ze van tafel moet.	1	2	0	0	<b>2</b>

Table F1: Input of participants (in Dutch) during a risk evaluation of the plan-of-the-day-strategy for locally advanced cervical cancer in Erasmus MC. Risks were deduplicated, which is indicated by † (= similar to risk above).

Processtap	Categorie	Risico	Oorzaak	Gevolg	Risico na categoriseren en ontdebelen	Kans	Tijd	Kwali- teit	Veilig- heid	Kans x Gevolg
	Overig	Patient ligt te veel geroteerd met de wervels waardoor ze opnieuw ingesteld moet worden	* Sommige patienten hebben een flexibele rug waardoor die makkelijk gerooteerd kan liggen. Een andere oorzaak kan zijn dat de patient tijdens de CT gespannen heeft gelegen (tijdens bestraling meer ontspannen) en dit niet opgemerkt is door de CT laborant.	* Patient moet opnieuw ingesteld worden en er moet opnieuw een CBCT gemaakt worden. Als dit een aantal keer gebeurd, loopt het toestel ook uit	Patient ligt te veel geroteerd met de wervels waardoor ze opnieuw ingesteld moet worden	4	1	0	0	4
	Technisch	XVI stopt er mee tijdens het maken van een CBCT	* dat weet niemand	* Weer een nieuwe CBCT toevoegen (met kans dat dit verkeerd gedaan wordt), terug draaien van het toestel, patient ligt langer op tafel en patient heeft extra CT straling ontvangen wat niet nodig was.	XVI stopt er mee tijdens het maken van een CBCT	2	1	1	1	6



Table E1: Input of participants (in Dutch) during a risk evaluation of the plan-of-the-day-strategy for locally advanced cervical cancer in Erasmus MC. Risks were deduplicated, which is indicated by † (= similar to risk above).

Processtap	Categorie	Risico	Oorzaak	Gevolg	Risico na categoriseren en ontdebelen	Kans	Tijd	Kwali- teit	Veilig- heid	Kans x Gevolg
	Menselijk	Plan selectiedi- aloog komt niet op in Mosaiq	* POTD ad- ministratie na veldcontrole niet goed uitgevoerd	* vertraging van de patientbehan- deling (system verhindert de dosisafgifte)	Plan selectiedi- aloog komt niet op in Mosaiq	1	1	0	0	1
	Menselijk	Verkeerde plan gestraald terwijl op beelden het juiste plan is bepaald	* Er is geen di- recte verbinding tussen gekozen plan in XVI en in Mosaiq - plankeuze moet altijd door de imaging labo- rant worden doorgegeven aan de labo- rant achter de knoppen	* bij mijn weten is dit niet voorgekomen, maar het is niet onmogelijk dat het wel gebeurd is	Verkeerde plan gestraald terwijl op beelden het juiste plan is bepaald	1	0	4	3	7

Table F1: Input of participants (in Dutch) during a risk evaluation of the plan-of-the-day-strategy for locally advanced cervical cancer in Erasmus MC. Risks were deduplicated, which is indicated by † (= similar to risk above).

Processtap	Categorie	Risico	Oorzaak	Gevolg	Risico na categoriseren en ontdebelen	Kans	Tijd	Kwali- teit	Veilig- heid	Kans x Gevolg
	Technisch	De CBCT kwaliteit is te slecht	* Artefacten	* Backup plan stralen terwijl de positionering misschien wel mooi is * Moeilijk te beoordelen * Uterustop is slecht te zien en niet zeker of dit binnen de 95% ligt * Darm wordt gezien als uterus	De CBCT kwaliteit is te slecht	3	1	3	3	<b>21</b>
	Organisatorisch	De blaas blijkt in de ochtenden vaak te leeg, maar middag-afspraken kunnen roostertech- nisch niet	* Urineproductie komt langzaam op gang	* Vaak stralen met lege blaas	De blaas blijkt in de ochtenden vaak te leeg, maar middag-afspraken kunnen roostertech- nisch niet	4	1	3	3	<b>28</b>
	Menselijk	Verkeerde plan staat in MasterRX	* Fysica is niet gebeld * Wordt niet automatisch aangepast als eerst verkeerde plan is gekozen	* Uiteindelijke optelling van doses en plannen klopt niet	Verkeerde plan staat in MasterRX	2	1	3	4	<b>16</b>

Table E1: Input of participants (in Dutch) during a risk evaluation of the plan-of-the-day-strategy for locally advanced cervical cancer in Erasmus MC. Risks were deduplicated, which is indicated by † (= similar to risk above).

Processtap	Categorie	Risico	Oorzaak	Gevolg	Risico na categoriseren en ontdebelen	Kans	Tijd	Kwali- Veilig- heid	Kans x Gevolg	
	Organisatorisch	Na herplanning, plan van oorspronkelijk planning wordt gekozen (ipv van de nieuwe plan na de herplanning)			Na herplanning, plan van oorspronkelijk planning wordt gekozen (ipv van de nieuwe plan na de herplanning)	1	0	3	3	6
	Overig	Klieren liggen buiten hoge regio SIB maar de uterus ligt wel in BU plan			Klieren liggen buiten hoge regio SIB maar de uterus ligt wel in BU plan	2	1	2	3	12
	Overig	Klier onzichtbaar op CBCT			Klier onzichtbaar op CBCT	4	0	2	2	16
	Organisatorisch	Automatic bot match levert verkeerde resultaten		* Plankeuze onjuist	Automatic bot match levert verkeerde resultaten	1	1	4	4	9
	Menselijk	Er wordt vergeten om de bevindingen op te schrijven in de IGRT log van de patiënt in Mosaiq	* Druk, vergeten	* Niet veel, alleen kunnen de laboranten de volgende dag niet teruglezen over de patiënt	Er wordt vergeten om de bevindingen op te schrijven in de IGRT log van de patiënt in Mosaiq	4	1	2	0	12
	Overig	Het doelvolumen verplaatst zich na de plankeuze	* Intrafractiebeweging	* Doelvolumen ligt tijdens bestralen buiten isodoselij	Het doelvolumen verplaatst zich na de plankeuze	1	0	2	1	3

Table E1: Input of participants (in Dutch) during a risk evaluation of the plan-of-the-day-strategy for locally advanced cervical cancer in Erasmus MC. Risks were deduplicated, which is indicated by † (= similar to risk above).

Processtap	Categorie	Risico	Oorzaak	Gevolg	Risico na categoriseren en ontdebelen	Kans	Tijd	Kwali- teit	Veilig- heid	Kans x Gevolg
	Menselijk	Rotatie van bekken wordt niet gecontroleerd		* Klier ligt buiten de hoge dosis van de SIB regio	Rotatie van bekken wordt niet gecontroleerd	1	0	4	5	<b>9</b>
	Menselijk	Wanneer CBCT opnieuw gemaakt moet worden bij een POTD patiënt, moet deze er op een andere manier ingezet worden dan bij andere patiënten. Dit gaat wel eens fout	* De laborant voegt het CBCT veld in zijn automatische toezicht, zoals het standaard hoort te gaan alleen dit is bij een POTD patiënt niet de juiste manier	* Kalender wordt rood * Patient onnodig lang op tafel * Laboranten weten niet hoe dit op te lossen	Wanneer CBCT opnieuw gemaakt moet worden bij een POTD patiënt, moet deze er op een andere manier ingezet worden dan bij andere patiënten. Dit gaat wel eens fout	1	2	0	0	<b>2</b>
	Overig	Uterus ligt buiten BU plan			Uterus ligt niet in het doelgebied	3	4	2	1	<b>21</b>

Table E1: Input of participants (in Dutch) during a risk evaluation of the plan-of-the-day-strategy for locally advanced cervical cancer in Erasmus MC. Risks were deduplicated, which is indicated by ↑ (= similar to risk above).

Processtap	Categorie	Risico	Oorzaak	Gevolg	Risico na categoriseren en ontdebellen	Kans	Tijd	Kwali- teit	Veilig- heid	Kans x Gevolg
	Overig	De cervix/uterus van de patient blijkt toch te bewegen, terwijl aan het begin de patient een non mover leek te zijn. Er zijn maar twee plannen beschikbaar voor deze patient en geen van de plannen kan nu gekozen worden omdat de uterus buiten 95% valt	* Wanneer de blaas bijvoorbeeld leeg is, kan de uterus ineens toch naar voren klappen. Of wanneer de darmen extreem vol zijn kan de cervix ook naar voren geduwd worden.	* Patient van tafel en naar het toilet sturen of juist laten drinken, kijken met een nieuwe CBCT of dit heeft geholpen. Er zijn ook patienten die adhv dit probleem een veldcontrole krijgen en veranderen van een non mover naar een mover proces.	↑		↑	↑	↑	↑
	Overig	Patient is heel erg veel afgevallen	* Patienten hebben minder eetlust en/of veel diarree waardoor ze afvallen	* Het kan zijn dat de dosisverdeling niet meer klopt in de patient, maar ook kan het van binnen (darmen, blaas, uterus, cervix) anders liggen waardoor er geen juist plan gekozen kan worden.	↑	↑	↑	↑	↑	↑

Table F1: Input of participants (in Dutch) during a risk evaluation of the plan-of-the-day-strategy for locally advanced cervical cancer in Erasmus MC. Risks were deduplicated, which is indicated by ↑ (= similar to risk above).

Processtap	Categorie	Risico	Oorzaak	Gevolg	Risico na categoriseren en ontdebelen	Kans	Tijd	Kwali- teit	Veilig- heid	Kans x Gevolg
	Overig	De uterus neemt in volume toe door ophoping van bloed en/of patient verliest veel bloed via het cavum	* Tumor cervix af	sluit * Backup plan nodig * Herplanning nodig	↑	↑	↑	↑	↑	↑

